

Design of Biomimetic Passive Control for
Optimisation of Oscillating Hydrofoils in
Tidal Energy Capture

By James Glynn

A Thesis for the degree of Master of Science

University of Strathclyde
Department of Mechanical Engineering
Energy Systems Research Unit
2006



ESRU

Energy Systems Research Unit



THE
**UNIVERSITY OF
STRATHCLYDE**
IN GLASGOW

**SUSTAINABLE
ENGINEERING**

Copyright

The copyright of this dissertation belongs to the author under the terms of
The United Kingdom Copyright Acts
as qualified by
University of Strathclyde Regulation 3.49
Due acknowledgement must always be made of the use of any material contained in, or
derived from, this dissertation.

Please feel free to contact the author on;

 james.glynn@gmail.com

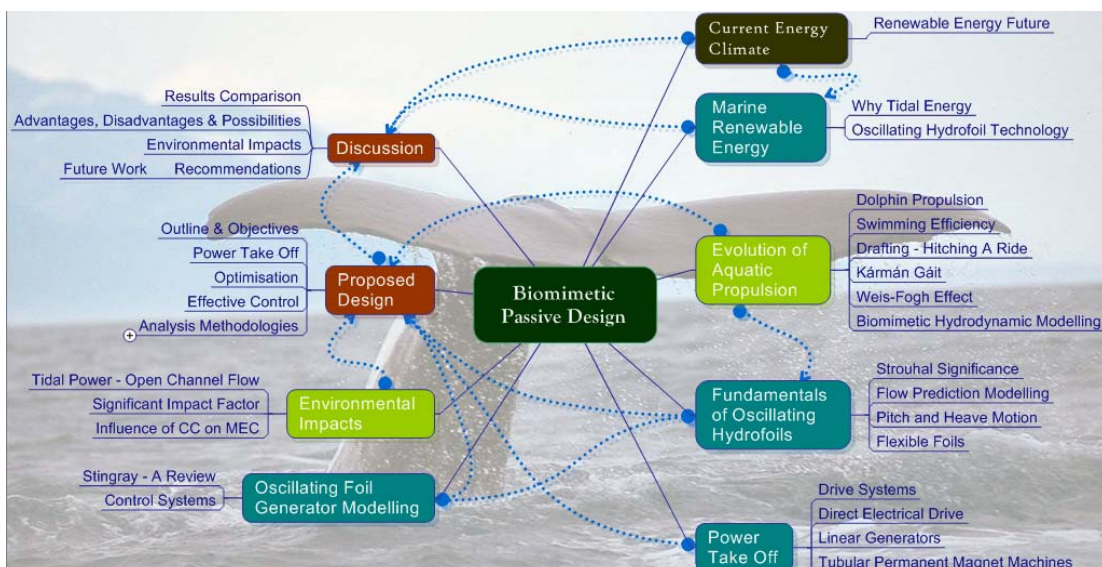
 +353 87 2251375 (Ireland)

Abstract

Since the Industrial revolution, we have been burning CO₂-emitting fossil fuels, at an ever increasing rate. This trend is set to continue for the coming decades, as our social and economic structure seems unable or unwilling to deal with immediately required changes. In addition to these stored hydrocarbon fuel reserves, albeit rapidly diminishing, the Sun and Moon also provide more variable energy resources on a continuous basis. As an alternative to the rapidly diminishing fossil fuels, work on harnessing these other sources – using PV solar cells, wind turbines, marine energy capture, and numerous alternative renewable energy technologies are broadly-based and growing in volume.

The energy reserves that are obtainable from tidal flow are substantial, and are available at high flux densities over broad areas. The constancy of the lunar cycle makes the resource secure, reliable, predictable, and suitable for a base load supply. Consequently, much academic and industrial research activity has focussed on this energy source in recent years.

In this work, an initial design is proposed for a biomimetically inspired, second generation, oscillating hydrofoil system as a tidal energy generator. The device is designed to manipulate the flow stream and contained vortical energy. It is self controlling with autonomous start-up, and demonstrates a 55% increase in cyclic lift force when compared with data from existing industrial prototypes. Thus, a heightened theoretical coefficient of power and decreased cycle times are calculated for the device, with a minimal envisaged significant impact factor.



Acknowledgments

I want to thank my mom and dad, Briege and Tom Glynn, for their never ending support, encouragement and for providing me with the opportunities in life which they have; they often don't get the praise they deserve.

I wish to thank my true friends old and new, who provide me with my sense of self worth and confidence to persevere with my work; without them life and this last year would have been a whole lot tougher.

Finally, I wish to thank the academic staff of the sustainable engineering programme in The University Strathclyde and ESRU, for creating an intriguing and interesting year. I particularly wish to thank Dr. Andy Grant, Dr. Paul Strachan and Dr. David Griersen who have each made a considerable impact throughout the course, both motivationally and inspirationally.

Sincerely, thank you all.

*“.....by “new” I do not mean “change”,
Change that can merely be quantative, inertial and physical,
I mean “new” in terms of development and process,
Rather than, “motion” and “displacement”.....”
Murray Bookchin (1921-2006)*

Terminology

AoA	Angle of Attack
AR	Aspect Ratio
CCS	Carbon capture and storage
DCMNR	Department for Communications, Marine and Natural Resources (Ireland)
DPIV	Digital particle image velocimetry
DTI	Department of Trade and Industry (UK)
EB	Engineering Business Ltd.
EU-ETS	EU Emissions trading scheme
FREDS	Forum for renewable energy development in Scotland
IPCC	Intergovernmental Panel on Climate Change
MCT	Marine Current Turbine
MEC	Marine Energy Capture
MEG	Scottish Marine Energy Group
Mtoe	Million tonne of oil equivalent
NACA	National Advisory Committee on Aeronautics (Precursor to NASA)
NASA	National Aeronautics and Space Administration
PLC	Programmable logic control
RE	Renewable Energy
ReFit	Renewable Energy Feed in Tariff
RO	Renewable obligation
ROS	Renewable obligation Scotland
TPER	Total primary energy requirement
LEV	Leading Edge Vortex
CFD	Computational Fluid Dynamics
BEM	Boundary element model
RANS	Reynolds averaged Navier-Stokes
UDF	User defined Function
AUV	Autonomous underwater vehicle
DoF	Degrees of freedom
VKS	Von Kármán street.
RGU	Robert Gordens University

Terminology

SIF	Significant Impact Factor
ESRU	Energy Systems Research Unit
PM	Permanent Magnet
EMF	Electro-motive Force
EM	Electromagnetic
RMS	Root mean square
VHM	Vernier Hybrid Machine
AWS	Archimedes Wave Swing
PMLSG	Permanent Magnet Linear Synchronous Generator
VSI	Voltage Source Inverter
CSI	Current Source Inverter
PLC	Programme Logic Control
CG	Centre of Gravity
GRP	Glass Reinforced Plastic

Nomenclature

St	Strouhal Number	v	Voltage (Volts)
f	Frequency (Hz)	i	Current (Amp)
A	Characteristic wake width Approximated as $2h_o$ (m)	$F_y(t)$	Lift Force (N)
S	Foil Plan Area (m^2)	$F_x(t)$	Drag force (N)
U	Relative Swimming Velocity ($m.s^{-1}$)	$P(t)$	Mechanical Power Output (W)
c	Chord length (m)	C_p	Power Coefficient
s	Span width (m)	L	Hydrodynamic Lift (N)
Re	Reynolds Number	D	Hydrodynamic Drag (N)
C_l	Lift Coefficient (2D)	M	Mass (kg)
C_d	Drag Coefficient (2D)	P	Power (W)
ρ	Fluid Density ($kg.m^{-3}$)	p	Pressure (Pa)
V	Velocity Vector ($m.s^{-1}$)	t	Time (s)
μ	Dynamic Viscosity	η	Dynamic efficiency
ν	Kinematic Viscosity	Γ	Circulation
Re	Reynolds Number	l	Representative length (m)
h_o	Heave Amplitude (m)		Free Stream Velocity
θ_o	Pitch Amplitude (rads)	ψ	Phase Angle
α	Angle of Attack (deg)		$h(t)$ leads $\theta(t)$
K	Reduced frequency	HC_{ratio}	Heave/chord length ratio

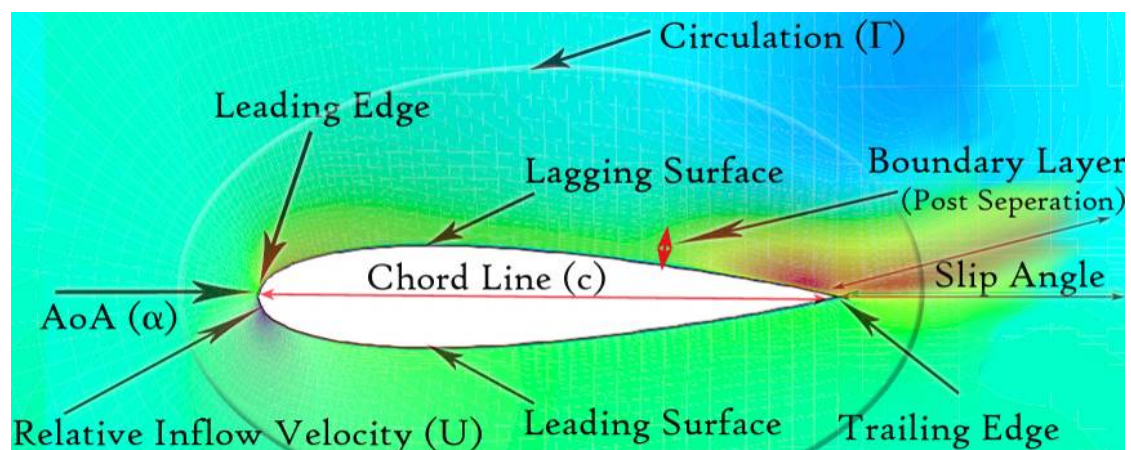


Table of Contents

<u>COPYRIGHT</u>	<u>II</u>
<u>ABSTRACT</u>	<u>III</u>
<u>ACKNOWLEDGMENTS</u>	<u>IV</u>
<u>TERMINOLOGY</u>	<u>VI</u>
<u>NOMENCLATURE</u>	<u>VIII</u>
<u>TABLE OF CONTENTS</u>	<u>IX</u>
<u>TABLE OF FIGURES</u>	<u>XIII</u>
<u>CHAPTER 1 INTRODUCTION – CURRENT ENERGY CLIMATE</u>	<u>- 1 -</u>
1.1 RENEWABLE ENERGY FUTURE	- 3 -
<u>CHAPTER 2 MARINE RENEWABLE ENERGY</u>	<u>- 5 -</u>
2.1 WHY TIDAL ENERGY?	- 7 -
2.2 OSCILLATING HYDROFOIL TECHNOLOGY	- 9 -
<u>CHAPTER 3 EVOLUTION OF AQUATIC PROPULSION</u>	<u>- 11 -</u>
3.1 DOLPHIN PROPULSION	- 12 -
3.2 SWIMMING EFFICIENCY	- 14 -
3.3 DRAFTING – HITCHING A RIDE	- 16 -
3.4 KÁRMÁN GAIT	- 17 -
3.5 UNSTEADY WEIS-FOGH EFFECT	- 18 -
3.6 BIOLOGICAL HYDRODYNAMIC MODELLING	- 19 -
<u>CHAPTER 4 FUNDAMENTALS OF OSCILLATING HYDROFOILS</u>	<u>- 20 -</u>

Table of Contents

4.1	STROUHAL SIGNIFICANCE	- 23 -
4.2	FLOW PREDICTION MODELLING	- 23 -
4.3	PITCH AND HEAVE HYDROFOIL MOTION OPTIMISATION	- 24 -
4.4	FLEXIBLE FOILS	- 26 -
4.5	HYDRODYNAMIC FUNDAMENTALS	- 27 -
4.5.1	BERNOULLI	- 27 -
4.5.2	VENTURI EFFECT	- 28 -
4.5.3	CIRCULATION	- 29 -
4.5.4	BIOT SAVART	- 29 -
4.5.5	VORTICITY	- 30 -
4.5.6	THEODORSEN'S THEORY – UNSTEADY FLOW & FLUTTER	- 31 -
4.5.7	DYNAMIC STALL	- 32 -
4.5.8	CAVITATION	- 33 -
4.5.9	NAVIER-STOKES EQUATIONS - WHY MODEL VISCOUS TURBULENCE?	- 34 -
<u>CHAPTER 5</u> <u>POWER TAKE - OFF – LINEAR GENERATORS</u>		<u>- 36 -</u>
5.1	DRIVE SYSTEMS	- 36 -
5.1.1	MECHANICAL LINKAGES	- 36 -
5.1.2	HYDRAULIC SYSTEMS	- 37 -
5.2	DIRECT ELECTRICAL DRIVE	- 37 -
5.3	LINEAR GENERATORS	- 38 -
5.3.1	PERMANENT MAGNET SYNCHRONOUS GENERATION	- 39 -
5.4	TUBULAR PM MACHINES	- 40 -
5.5	ARCHIMEDES WAVE SWING	- 41 -
<u>CHAPTER 6</u> <u>OSCILLATING FOIL GENERATOR MODELLING</u>		<u>- 43 -</u>
6.1	STINGRAY – A REVIEW OF ENGINEERING BUSINESS'S DEVICE	- 45 -
6.1.1	INTRODUCTION	- 46 -
6.1.2	PRINCIPLES OF OPERATION	- 46 -
6.1.3	TESTING OBJECTIVES	- 48 -
6.1.4	CONTROL SYSTEMS	- 48 -
6.1.5	POWER TAKE OFF	- 51 -
6.1.6	SUMMARY	- 51 -
<u>CHAPTER 7</u> <u>ENVIRONMENTAL IMPACTS</u>		<u>- 53 -</u>

Table of Contents

7.1 OPEN CHANNEL FLOW - TIDAL POWER	- 53 -
7.2 SIGNIFICANT IMPACT FACTOR	- 55 -
7.3 INFLUENCE OF CLIMATE CHANGE ON MARINE ENERGY	- 56 -
<u>CHAPTER 8 SRUTH SAOIRSE: CONCEPT DESIGN</u>	<u>- 57 -</u>
8.1 DESIGN OUTLINE & OBJECTIVES	- 60 -
8.1.1 DESIGN EVOLUTION	- 60 -
8.2 ANALYSIS METHODOLOGIES & COMPARISON	- 62 -
8.2.1 QUAZI-STATIC MODEL	- 62 -
8.2.2 CFD STEADY-STATE FIRST ORDER MODELLING	- 63 -
8.2.3 CFD UNSTEADY RANS MODEL	- 65 -
8.2.4 CFD DYNAMIC UNSTEADY RANS MODEL	- 70 -
8.3 POWER CYCLE MODELLING	- 71 -
8.3.1 SRUTH SAOIRSE POWER CYCLE	- 71 -
8.3.2 POWER TAKE OFF	- 72 -
8.3.3 COEFFICIENT OF POWER	- 74 -
8.4 EFFECTIVE CONTROL	- 75 -
8.5 DISCUSSION	- 75 -
8.5.1 OPTIMISATION OF DEVICE	- 76 -
8.5.2 STRUCTURAL CONCERNS	- 77 -
8.5.3 ENVIRONMENTAL EFFECTS	- 79 -
8.5.4 ADVANTAGES, DISADVANTAGES & POSSIBILITIES	- 81 -
8.6 RECOMMENDATIONS & FUTURE WORK	- 82 -
8.7 CONCLUSIONS	- 84 -
<u>REFERENCES</u>	<u>- 86 -</u>
<u>BIBLIOGRAPHY</u>	<u>- 93 -</u>
<u>APPENDIX A - USER DEFINED FUNCTIONS</u>	<u>- 94 -</u>
PREDEFINED PITCH HEAVE MOTION	- 94 -
CODE	- 94 -
LOOP FORCE INTEGRAL	- 95 -
CODE	- 95 -

Table of Contents

APPENDIX B - ALTERNATIVE TIDAL GENERATION SITES - 97 -

APPENDIX C - DEEP ECOLOGICAL MOTIVATION - 99 -

Table of Figures

<i>Figure 1.1 Approximate global distribution of wave power levels [kW.m^{-1}] (Thorpe, 1999).....</i>	- 4 -
<i>Figure 2.1 Approximate Distribution of Global Wave Energy by mean wave height</i>	- 6 -
<i>Figure 2.2 Mean Tidal Flow Velocities (Sustainable Energy Ireland, 2005a).....</i>	- 9 -
<i>Figure 2.3 MCT Comparison with offshore wind Turbine ©MCT ltd.....</i>	- 9 -
<i>Figure 2.4 Engineering Business's Stingray.....</i>	- 10 -
<i>Figure 2.5 Pulse Generation's Pulse Stream 100.....</i>	- 10 -
<i>Figure 3.1 Stingray Rajiform Propulsion.....</i>	- 12 -
<i>Figure 3.2 Thresher Shark - Caraniform Propulsion.....</i>	- 12 -
<i>Figure 3.3 Whale Thunniform Propulsion.....</i>	- 12 -
<i>Figure 3.4 Dolphin - Airfoil profile comparison (Fish and E., 2006).....</i>	- 13 -
<i>Figure 3.5 Caraniform Propulsion - Von Kármán Vortex Shedding © University of Washington .</i>	- 15 -
<i>Figure 3.6 NASA LandSat 7 Image of cloud Von Kármán Street off the Chilean coast</i>	- 15 -
<i>Figure 3.7 Elliptical representation of the mother dolphin and induced streamlines (Weihs, 2004) -</i>	- 16 -
<i>Figure 3.8 Vortex aided energy efficient group propulsion (McNeill, 2004)</i>	- 17 -
<i>Figure 3.9 Clap-Fling motion (Weis-Fogh, 1973)</i>	- 19 -
<i>Figure 4.1 Pressure Field & Subsequent Forces & Foil Motion [pascal].....</i>	- 21 -
<i>Figure 4.2 LEV reconnecting with the Trailing Edge Vortex [m.s^{-1}]</i>	- 24 -
<i>Figure 4.3 AoA Profile Vortical Effects (F.S. Hover, 2004).....</i>	- 25 -
<i>Figure 4.4 Parameter Comparison varying AoA and Strouhal Number (Michael S. Triantafyllou, 2003)</i>	- 26 -
<i>.....</i>	
<i>Figure 4.5 Static pressure [Pascal] 2m.s^{-1} inflow AOA 15 Deg.....</i>	- 28 -
<i>Figure 4.6 Velocity distribution [m.s^{-1}] 15 AOA 15 deg.....</i>	- 28 -
<i>Figure 4.7 Venturi Tube</i>	- 29 -
<i>Figure 4.8 Rotation, Translation & Skewing of Fluid Element ABCD.....</i>	- 31 -
<i>Figure 4.9 DSV Separation Bubble (W. Geissler, 2006).....</i>	- 33 -
<i>Figure 5.1 Rotary generator to Linear generator transformation (I. Boldea, 1999)</i>	- 38 -
<i>Figure 5.2 Vernier Hybrid Machine (VHM).....</i>	- 40 -
<i>Figure 6.1 McKinney & Delaurier Model.....</i>	- 45 -
<i>Figure 6.2 Stingray Final Assembly © 2003 Engineering Business.....</i>	- 46 -
<i>Figure 6.3 Stingray Power Cycle Comparison © Engineering Business Ltd. 2005.....</i>	- 50 -
<i>Figure 6.4 Power cycle comparison with Accumulator firing.....</i>	- 50 -
<i>Figure 6.5 Stingray Lift Generation © Engineering Business Ltd. 2005</i>	- 51 -
<i>Figure 7.1 Irish Sea - North Channel Tidal Energy ©Google 2006 ©Dti 2002</i>	- 54 -
<i>Figure 8.1 Sruth Saoirse Modular Design</i>	- 58 -
<i>Figure 8.2 AoA Axel Restrictor</i>	- 58 -
<i>Figure 8.3 Position and Butterfly Pneumatic Ram Control</i>	- 59 -
<i>Figure 8.4 Sruth Saoirse Array Plan View.....</i>	- 59 -

Table of Figures

Figure 8.5 Empirical Steady State Lift Generation	- 62 -
Figure 8.6 Cyclic Lift Generation Comparison for flow at $2m.s^{-1}$	- 63 -
Figure 8.7 Control Pressure Distribution [Pascal]	- 64 -
Figure 8.8 Control Velocity Distribution [$m.s^{-1}$].....	- 65 -
Figure 8.9 Sruth Saoirse Velocity Flow Field [$m.s^{-1}$]	- 66 -
Figure 8.10 Sruth Saoirse Static Pressure [Pascal].....	- 66 -
Figure 8.11 Inflow Phase Pressure field	- 67 -
Figure 8.12 Inflow Phase Velocity Field.....	- 68 -
Figure 8.13 Boundary Layer collapse [$m.s^{-1}$] (a, b respectively).....	- 68 -
Figure 8.14 Cycle Start Pressure Field [Pascal]	- 69 -
Figure 8.15 Cycle Start Velocity Field [$m.s^{-1}$]	- 69 -
Figure 8.16 Hydrofoil Pressure Distribution during thrust from control area	- 70 -
Figure 8.17 Hydrofoil Pressure Distribution during normal heave motion.....	- 70 -
Figure 8.18 Sruth Saoirse Power Cycle	- 72 -
Figure 8.19 Stator; 300 x 300 structural steel box section cross member (Stress & Strain).....	- 78 -
Figure 8.20 Stator; 300 x 300 structural steel I beam section (Stress & Strain)	- 78 -
Figure 8.21 Main Hydrofoil Shaft	- 79 -
Figure 8.22 Root style pivot mooring structure.....	- 81 -
Figure 0.1 The Shannon Estuary, Ireland	- 97 -
Figure 0.2 The Galway Mayo Coast, Ireland.....	- 97 -
Figure 0.3 Achill Island, Ireland.....	- 97 -
Figure 0.4 The Donegal, Derry Antrim Coast, Ireland	- 97 -
Figure 0.5 The Kerry Peninsula, Ireland	- 98 -
Figure 0.6 The Sound of Islay, Scotland.....	- 98 -
Figure 0.7 Strangford Lough, Ireland	- 98 -
Figure 0.8 The Scottish Western Isles, Scotland	- 98 -

Chapter 1 Introduction – Current Energy Climate

Total global energy generation in 2003 was 1.221×10^{11} kWh (International Energy Agency, 2003b). The incoming solar radiation of 1.75×10^{17} Watts, volcanic, hot springs, geothermal and general terrestrial energy of 3.24×10^{13} Watts, and gravitational interaction between the earth, sun and moon orbits providing 3×10^{12} Watts of tidal energy, accounts for the world's natural energy balance* (Hubbert, 1971). All these sources are renewable, sustainable and clean. This also accounts for the energy converted through biological processes of photosynthesis in generating carbon based life forms which over the preceding millennia have been the constituent ingredient for our energy source of the day; fossil fuels. Our global fossil fuel reserves have been and continue to be vastly depleted at rates far greater than their regeneration.

In 2003, over 75% of the global energy mix was produced by coal, oil and gas (International Energy Agency, 2003b). Over the period of 1971-2003 global electricity consumption has all but tripled; over 60% of which was produced again by coal, oil and gas, with Nuclear and Hydro filling in the majority of the rest of the demand (International Energy Agency, 2003a). Presently specific increases in oil prices, a revival in the consumption of coal particularly in North America and Asian Pacific ring is being seen. This is economically driven specifically by reserve to production ratios projecting at present rates of consumption, 150 years of coal, 55 years of gas and 30 years of oil to be left in reserve (BP, 2006). The global energy demand is increasing, and with it CO₂ emissions, both are expected to rise by 60% within the next 25 years. Europe imports 50% of its energy, and if trends continue will be importing up to 70% within 20-30 years, with much of these energy imports originating in just a few countries. Gas imports come mainly from Russia, Norway, and Algeria, while oil reserves come from middle-eastern countries, which are presently experiencing continual political and social unrest. Security of supply has huge political, social and economic implications. Oil and gas prices have doubled within the last two years, with the effects being passed on

* Powers quoted are approximate and subject to subsequent revision.

to the consumer. The Intergovernmental Panel on Climate Change (IPCC) report that the world is already 0.6 degrees warmer and, if this trend continues, by the end of the century global average temperatures will have risen by between 1.4 and 5.8 degrees (European Commission, 2006b, European Commission, 2006a).

Ireland and the UK are experiencing similar trends. Ireland's total primary energy requirement (TPER) grew between 1980 and 1998 by 58% and is expected to grow a further 37% by 2010. Ireland's indigenous energy supplies peaked in 1985 with peat and natural gas from Kinsale gas fields being used in electricity generation. Projections for 2010 are that, with dwindling peat and gas production, Ireland will be heavily dependant on imported gas & oil, with only 6% indigenous energy supplies (Department of Public Enterprise, 1999). Development of the controversial Corrib gas field off Erris head, Mayo is estimated to hold 1080-1980 Mtoe. This would considerably alleviate dependency on imported gas. In 2003 renewable energy, mainly hydro and wood burning, contributed 1.8% to the total energy generation but is anticipated to rise to 3% by 2010 (Martin Howley: Dr. Brian Ó Gallachóir, 2005).

In The United Kingdom coal has been reinstated as the main fuel supplying 40% of the electricity generation requirements. The Department of Trade and Industry (DTI) is aware of the UK's dwindling oil and gas reserves, energy trends, and possibility of importing 90% of it's oil and gas requirements by 2020 (Department of Trade and Industry, 2006b). Subsequently, the DTI and subsidiary specialist groups are highly active in securing their energy future through indigenous, European and International policy. The Carbon Trust provides funding for RE technology feasibility studies and development. Furthermore the UK Government are committed to: 60% of coal fired power stations being refurbished with carbon capture and storage (CCS), progression of EU emissions trading scheme (EU ETS), heightening renewable obligation (RO), CO₂ emission reduction in accordance with the Kyoto protocol, awarding record number of licences and drilling commitments in the north sea, committing to utilise remaining oil and gas reserves effectively, and developing further nuclear generation plants. (Department of Trade and Industry, 2005, Department of Trade and Industry, 2006b, Department of Trade and Industry, 2006a, European Commission, 2006b)

The 2005 Gleneagles G8 summit was the stage where world leaders declared their recognition of the fact that current energy trends are not sustainable economically, environmentally nor socially and called for a “*clean, clever and competitive energy future.*”

1.1 Renewable energy future

In 2004 the first considerable change in the Irish energy mix saw wind reported as the second largest renewable energy source after solid biomass, and the older hydro generation profile. The total contribution from renewable energy to gross electrical consumption in 2004 was 5.2%, with considerable input from wind power. Installed capacity by December 2005 stood at 495.5 MW (Leary et al., 2006).

In September 2005, the Irish Department for Communications, Marine and Natural Resources (DCMNR) announced increased renewable energy generated electricity targets at 1450MW, 13.2% of 2010 predicted energy demand. To support this, the new Renewable Energy Feed in Tariff (ReFit) programme has been established, providing €119m in support of developing at least 400MW of renewable energy projects towards 2010 targets.

The UK government plans to reduce its carbon dioxide emission by 60% by 2050, with significant inroads made in that effort by 2020. 30-40% of the UK's energy will have to be from renewable sources to achieve this goal, and hence targets of 10% energy demands being met by indigenous RE supply by 2010 has been set.

Scotland is by far leading the way in this drive, aiming for 18% RE generation by 2010 and 40% by 2020 (Astron, 2005). The forum for renewable energy development in Scotland (FREDS) is confident this target will be met and they are currently reviewing their 2020 targets. Renewable obligation Scotland (ROS) is the means of achieving this by requiring electricity suppliers to generate an increasing percentage of their power from approved renewable sources. Currently a consultation review is taking place to possibly amend ROS in favour of developing greater wave and tidal renewable energy from Scotland's plentiful marine energy supply in light of recent resource review surveys (Thomson, 2006).

The Irish 2010 RE targets are more than likely to be met by wind generation. In the long term, post 2020, Ireland should also be looking to her

enormous ocean energy resource. Europe's accessible wave energy is estimated at 320,00MW, largely concentrated off the west coasts of Ireland and Scotland [Figure 1.1, Figure 2.1](Sustainable Energy Ireland, 2005b). A considerable tidal resource flows through the Irish Sea, western Scottish isles and the UK Channel Islands (Snodin, 2001, Sustainable Energy Ireland, 2005a). The potential energy, far over supplying the relatively low indigenous demand, enables Ireland to become a net exporter of energy through an interconnected Scottish, UK and European energy grid.

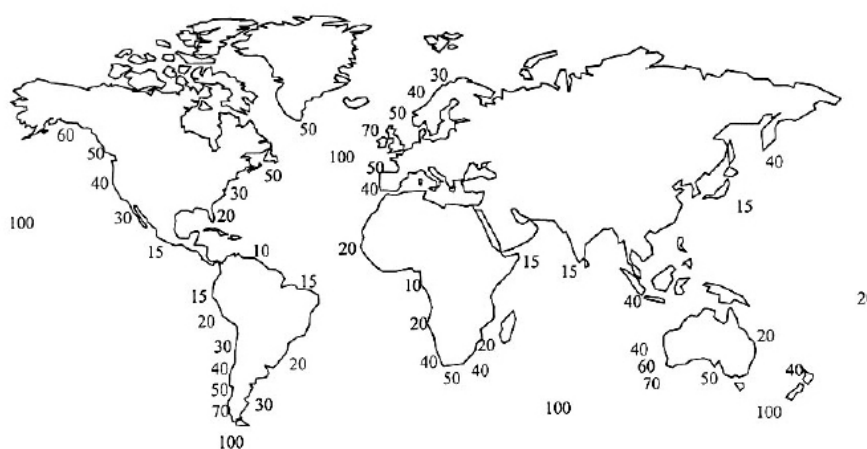


Figure 1.1 Approximate global distribution of wave power levels [kW.m^{-1}] (Thorpe, 1999)

The Scottish Marine Energy Group (MEG) was established to develop the marine energy resource, and the supporting academic and industrial infrastructure. It is believed that by 2020, 10% of Scottish power will be generated from marine sources estimated at 1300MW with the underlying infrastructure providing economic development exporting expertise and technology (Astron, 2004).

Chapter 2 Marine Renewable Energy

The earth's oceans are its circulatory system, transporting physical and thermal energy, moderating temperatures, CO₂ levels and most importantly providing a habitable planet and thus comfort for life. While wind energy currently dominates the RE industry, marine energy also holds huge potential. Water density is approximately 1000 times greater than that of air, relatively providing much higher energy flux densities, and enabling high energy extraction from smaller devices. It is clean and sustainable. As of yet there is no market leader in marine energy capture (MEC) but there is growing activity in technology research, testing and development.

Marine energy can be broken down into two main categories. *Wave energy* is created as a result of weather variations in heat and pressure, generating winds blowing across a great fetch impinging on the oceans below. Waves can gather and transfer large amounts of energy extremely efficiently. The energy is contained within the relative motion of vertically rotating particles near the water surface, causing undulations on the oceans surface, with some sites gathering power levels up to 100kW/m wave length.

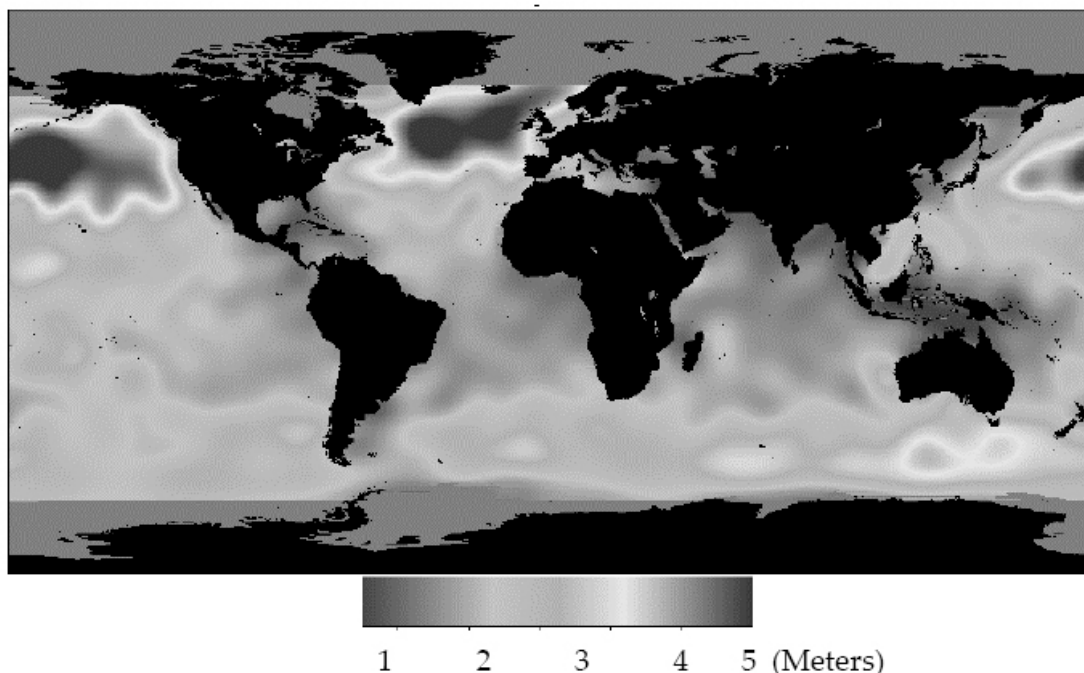


**Figure 2.1 Approximate Distribution of Global Wave Energy by mean wave height
Synthetic Aperture Radar (SAR) Imagery (Sustainable Energy Ireland, 2003)**

Tidal current energy on the other hand is generated by the gravitational pull of the sun and moon as their orbiting magnetic fields intertwine with the earth's. The moon being closer holds the greater strength over the rise and fall of our sea levels. The earth's rotation causes a (high-low-high) tidal cycle period of 12.5 hours approximately. The moon's rotation has an approximate cycle of 28 days creating spring and neap tides between every new moon. There are variations on this effect caused by the sun and seasonal weather, but the motion of the sun and moon is highly predictable, and subsequently as is tidal flow. The effect of this rise and fall would be negligible, other than the concentrating effect which landmasses have on the tidal flow. Areas of constriction between landmasses cause acceleration in the velocity of the marine tidal current. Therein these sites hold a dense energy resource, and it is this energy that tidal energy capture devices aim to harness.

MEC devices have been extensively supported through European, governmental and industry sponsored research & development initiatives. However, with the large variation in technology design, power output, economic feasibility and environmental impact variables, there is as of yet an industry leader to develop. Ocean Power Delivery's Pelamis device is the first commercial wave energy capture device to be deployed. Recent investment of €13m was announced

to aid the device development for current construction of the wave farm off the North West Portuguese coast^{*}. This farm will provide vital and much needed real world data towards the long term variables unpredictable by prototype testing. As with the wave device industry, there is a large variation in tidal energy capture devices. This may be surprising, considering the uniform and predictable nature of the resource. There has been considerable research in vertical[†], horizontal^{‡§}, Darrieus and Gorlov turbine development with lessons learnt and adapted from comparable technologies in the wind industry. In an effort to hasten further commercial development and accelerate industry leading technology, it has been recommended that specific devices of verifiable merit be supported, rather than the broader general support to the industry as a whole (Bound, 2003, Ian G. Bryden, 2005). The focus of this report is on the development of oscillating hydrofoil technology^{**} in tidal energy extraction regimes.

2.1 Why Tidal Energy?

Tidal energy is regular, predictable and at higher power densities than alternative weather dependant renewable energy sources (See Figure 2.2). There is a large resource concentrated in numerous sites globally. Tidal energy has only become of interest, as a feasible source of renewable energy, relatively recently. Resource observations, modelling and mapping have found there to be considerable tidal resource in the UK and Ireland (See Figure 1.1). Early interest was concentrated on tidal barrage systems^{††} in estuaries with a large tidal range. Renewed interest in less environmental invasive devices is currently underway in energetic coastal regimes. A tidal flow of $3\text{m}\cdot\text{s}^{-1}$ has an energy flux of approximately $14\text{kW}\cdot\text{m}^{-1}$. A case study for the Alderney Race in the English Channel estimates that annual energy of 7.4 TWhrs is available as part of a variable RE portfolio. This amasses to 2% of the UK energy demand in 2000 and shows the considerable energy available from tidal generation sites. (A.S. Bahaj, 2004) A European study of 106 European sites estimates the extractable energy to

* See press release at <http://www.oceanpd.com/LatestNews/default.html>

† http://www.pontediarchimede.com/language_us/index.mvd

‡ <http://www.e-tidevannsennergi.com/index.htm>

§ <http://www.marineturbines.com/home.htm>

** <http://www.engb.com/>

†† <http://www.edf.fr/html/en/decouvertes/voyage/usine/retour-usine.html>

be 50 TWhrs/yr (European Commission, 1996). Throughout the traditional utilities generators it is felt that renewable energy technology is not suitable for large scale base load supply. Alternatively the predictability of tidal energy guarantees security of supply with a network of phased tidal generators feeding the electrical grid throughout the tidal cycle (A.S. Bahaj, 2003). More importantly, tidal energy is clean and emits no CO₂. Devices can be designed to be environmentally benign.

Nonetheless, site specific flow analysis must be carried out to fully characterise a potential location. There can be considerable harmonic flow anomalies and even unidirectional flow, which diverge from simple lunar semi-diurnal sinusoidal modelling, as a result of land mass orientation in tidal flow streams. Furthermore, simple analysis techniques do not take into account the energy extraction and blockage effects of MEC devices. Open channel flow models driven by a static hydraulic pressure head show that device placement can lead to local flow accelerations and overall flow deceleration in the far field. (Bound, 2003, Ian G. Bryden, 2005) To fully understand and quantify a site resource specific analysis of the local tidal regime, site bathymetry and blockage effects must be carried out. Far-field effects suggest environmental ramifications are not specifically local to the device. Wake analysis and environmental impacts must be taken into account in deciding the design for device size and power rating. This is to be discussed later in Chapter 7. Further technology research & development is also required in the areas of on site access, mooring, cabling technologies, minimum maintenance, corrosion shielding, device cavitation and integration in the harsh marine environment (A.S. Bahaj, 2003).

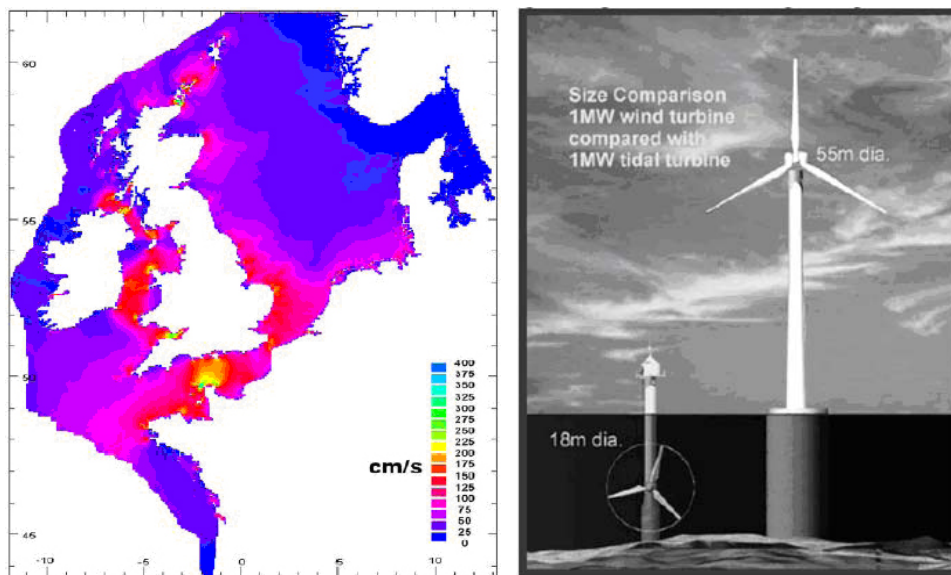


Figure 2.2 Mean Tidal Flow Velocities (Sustainable Energy Ireland, 2005a)

Figure 2.3 MCT Comparison with offshore wind Turbine ©MCT ltd

2.2 Oscillating Hydrofoil Technology

There are two main oscillating hydrofoil devices under development in the UK. [1] Engineering Business Ltd *Stingray* and [2] the newer *Pulse stream 100* designed by Pulse Generation Ltd. in conjunction with IT Power Ltd.^{*†‡} *Stingray* has undergone considerable testing and hence significantly more literature is available, providing real world test data which is reviewed in section 6.1. *Pulse stream 100* has yet to be tested and is due for deployment in Yorkshire, UK in early 2007 (IT Power Ltd, 2006).

The DTI has provided £878,000 in funding for the IT Power 100kW prototype device. It is proposed that it will extract energy from accessible near shore shallow tidal streams in river estuaries, harbours, channels and lochs that are not yet accessible by alternative devices. The projects purpose is to build further understanding of devices operation on its mathematical modelling through prototype testing. The design boasts a novel mechanical angle of attack (AOA) control system and variable height extension maximising the devices inflow area and hence also maximising its overall power output. Further benefits will be reaped by the design as near shore mooring and installation will be cheaper and

* <http://www.pulsegeneration.co.uk/>

† <http://www.itpower.co.uk/pulse.htm>

‡ <http://www.dti.gov.uk/technologyprogramme/>

more manageable. Both companies have their sights set on large scale 500kW machines for commercial deployment.



Figure 2.4 Engineering Business's Stingray

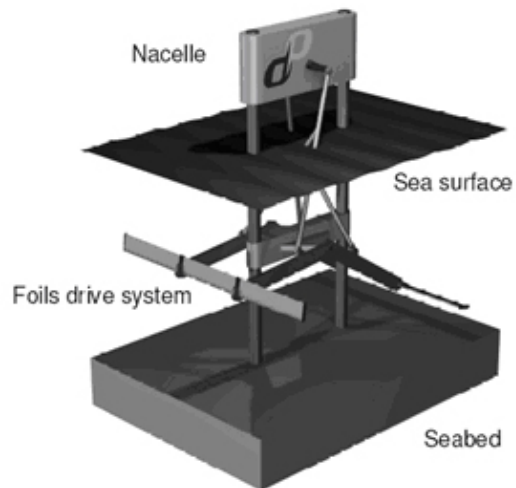


Figure 2.5 Pulse Generation's Pulse Stream 100

Chapter 3 Evolution of Aquatic Propulsion

Nature has long provided inspiration for mankind with creative design ideas & solace in development. Quite obviously an oscillating hydrofoil can be likened to the high performance caudal fin of a fish or the fluke of cetacean. They develop increased power and efficiency on lift based propulsion rather than previous paddling and undulation mechanisms (Fish, 1998). Dolphins have long been watched in awe as they swim alongside the bow of ships, breaching the ocean surface and surfing in waves. Aristotle observed them to be “.....*the fleetest of all animals, marine and terrestrial.....*” Many hydrodynamic lessons can be inferred from the decisions of evolution through biomimetic studies, as to how aquatic & avian propulsion interacts in the medium in which it thrives. This provides high thrust rates, efficient movement through fluids, reducing drag and wake effects, while alternatively utilising wake vortices and circulation where beneficial. Natural propulsion is an order of magnitude greater than any current man made underwater vehicle.

Undulating anguilliform propulsion mechanisms demonstrated by larva, tadpoles and eels are efficient at slow speeds, have reduced body and fin drag, and are highly manoeuvrable. Interestingly rays, skates and mantas use a similar Rajiform undulation mechanism through enlarged pectoral wings (See Figure 3.1). Subsequently evolution has converged on a design of caraniform and thunniform propulsion demonstrated by most sharks, dolphins and whales. The oscillatory mechanism engages less than half the body, with fastest swimmers mainly engaging only the peduncle and posterior caudal fin in motion. It is efficient at fast cruising, with minimal drag and generates greater thrust, but is less well suited for manoeuvring. (Cheryl A.D. Wilga, 2004, Wakeling, 2001)



Figure 3.1 Stingray Rajiform Propulsion

Figure 3.2 Thresher Shark - Caranigform Propulsion

Figure 3.3 Whale Thunniform Propulsion

3.1 Dolphin Propulsion

The first quantifiable technical report on fish locomotion was by J. Gray in 1935. Observations of the velocity and physiology of dolphin locomotion, estimates in dorsal and ventral muscle weight, hence power estimate and drag resistance provided the basis for his tests. He calculated the drag experienced by swimming dolphins and the power to overcome this. Relative velocity observations negating slip stream effects from the ship led him to make erroneous claims with regard to the speed at which dolphins propel themselves and the strength of dolphins red muscle tissue. The Gray paradox states that dolphins red muscle tissue would need to be 7 times as powerful as human tissue which he used as reference. In actual fact there are hydrodynamic mechanisms used by dolphins to reduce their drag by a factor of 7. His later testing laid the foundation for biomimetic foil studies.

Interestingly, evolution has given dolphins a naturally aspirated turbo charged engine; concentrations of myoglobin are found in the caudal muscles of cetaceans leading to greater oxygenation of muscle tissue and higher force output (Pollack, 1990, L. K. Polasek, 2001) but the muscle structure is not largely dissimilar to humans.

Using flexible rubber streamlined models under simple harmonic motion along the chordwise axis, Gray observed and described particle acceleration on the

leading surface at the trailing caudal edge, with the resulting thrust causing a pressure drop across the peduncle region. It was concluded that this pressure drop delayed boundary layer separation maintaining laminar flow longer and reducing drag (Gray, 1935).

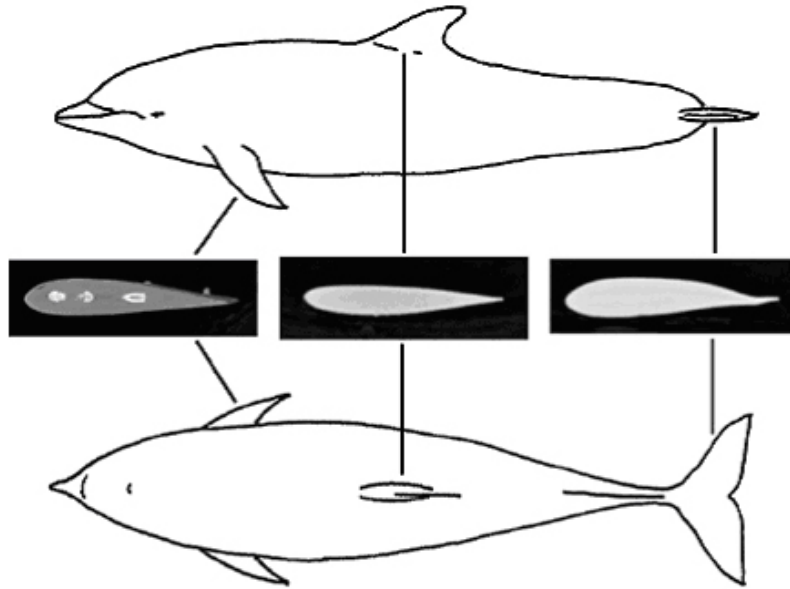


Figure 3.4 Dolphin - Airfoil profile comparison (Fish and E., 2006)

It should be noted how similar a dolphins profile is to that of streamlined aeronautical design airfoils (See Figure 3.4), with maximum thickness at the 45% chord length position. (Fish and E., 2006) Typically these foils are design to maintain optimum pressure distribution on the foil surface maintaining laminar flow, minimising pressure and induced drag. *As the medium of concern is water, airfoils will be referred to as hydrofoils from this point onward.* A caudal fluke oscillating in a laminar flow will typically generate more thrust than that of one in a turbulent flow hence dolphins can swim remarkably quickly at escape-speeds of up to 8 m.s^{-1} .

Induced drag is a component of vorticity created by a pressure gradient across a surface inclined at an angle (i.e. angle of attack) to the direction of fluid flow. The surface will experience a lifting force in reaction to the fluid flow and the pressure gradient. Energy is lost through the propagation of trailing edge vortices from high to low pressure areas and creates drag (Munson et al., 2006). Higher performance hydrofoils have high lift to drag ratios augmented by high aspect ratios (AR). This is developed by increasing the span at a greater rate than

that of the square root of increments of the foil planform area [See equation(3.1)]. Wing tip vortices can be further decreased by tapering appendages and introducing ribs to prevent cross flow on the foil surface and trailing edges. It should not be surprising, therefore, that dolphins and whales flukes are examples of this design with aspect ratios of 2.0–6.2 (Fish and E., 2006) (See Figure 3.3).

$$AR = \frac{Span^2}{Area} \quad (3.1)$$

3.2 Swimming efficiency

Swimming efficiencies of fish and cetaceans are characterised by the nondimensional Strouhal number (St). It is related to the synchronicity and frequency (f) of vortex shed by the characteristic width (l) of the jet and the mean relative swimming velocity (U). (J. M. ANDERSON, 1998)

$$St = \frac{fl}{U} \quad (3.2)$$

Initial testing in an effort to mimic a tuna in locomotion was quite disappointing leading to much awe for natures understanding and manipulation of hydrodynamics (Triantafyllou et al., 1995). Subsequent efficient models concentrated on maintaining a laminar boundary layer and vorticity control by the caudal fin (D. S. BARRETT, 1999). Tests producing a chordwise rate of oscillation (phase velocity) greater than that of the surrounding fluid are found to consistently reduce turbulence. Further optimisation is developed through appropriate caudal oscillating frequency modulation (Frank. E. Fish, 2003). Thus, maintaining St in the correct range to manipulate the vortex structure and create a propulsive reverse Kármán Street* (See Figure 3.6) (J. M. ANDERSON, 1998). AoA should be in the range of $14^\circ - 25^\circ$, fin pitching to heaving cycle should be out of phase by $70^\circ - 110^\circ$ with high AR (D. S. BARRETT, 1999). The caudal fin motion can be modelled as a pitching and heaving hydrofoil under certain equations of motion. Substantial effort has be committed to understanding and modelling the

* A Von Kármán Street is characterised by alternative contra-rotating high-low pressure vortices in the wake of a bluff body. The fluid Reynolds number needs to be in a specific range dependant on the body size for it to occur.

governing dynamics of oscillating hydrofoils in propulsive and energy extraction regimes and will be discussed further in section Chapter 4.

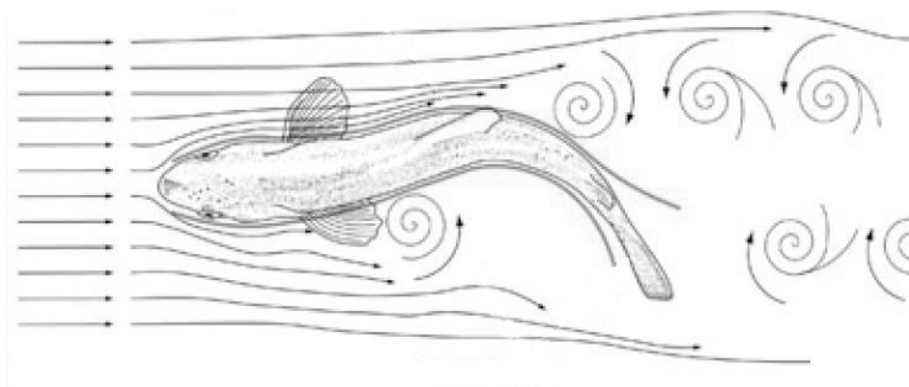


Figure 3.5 Caraniform Propulsion - Von Kármán Vortex Shedding © University of Washington*

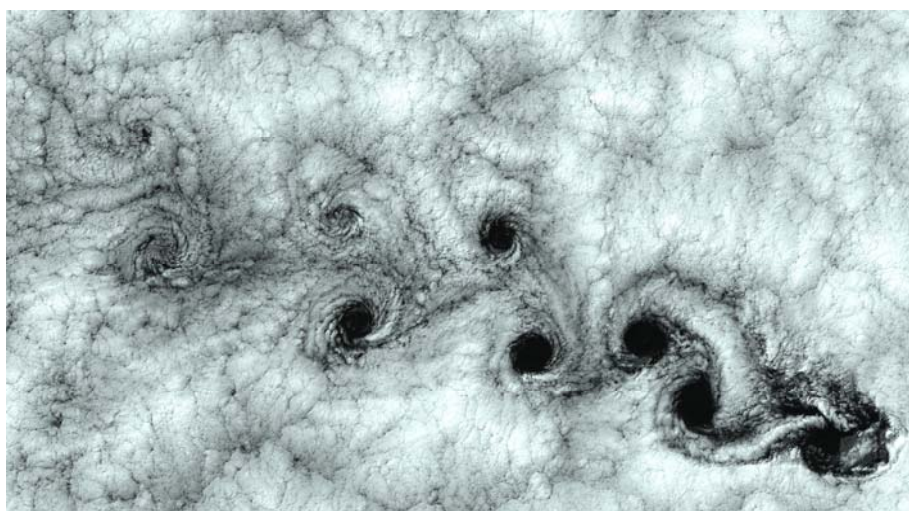


Figure 3.6 NASA LandSat 7 Image of cloud Von Kármán Street off the Chilean coast

Initial calculations indicate optimum St for propulsion to be in the range of $0.25 - 0.4$ (D. S. BARRETT, 1999, D.A. Read, 2002, Triantafyllou et al., 1995). In actual testing of trained cetaceans; dolphins, killer whales, pilot whales and beluga whales over a speed range of $2-8\text{m}\cdot\text{s}^{-1}$ considerable scatter was evident in data of 248 St s calculated between varying species. No evident concentration of St calculated suggests that there is more at play in optimum swimming. The data presented shows the natural preferred range in agreement with Triantafyllou at $0.2-0.4$, with the 74% preferred range of $0.2-0.3$ (Jim J. Rohr, 2004). It is postulated

* [University of Washington - Evolutionary Biology](#)

that while at cruising speeds in the wild of $1 - 5\text{m}\cdot\text{s}^{-1}$ swimming would be *tuned* for high propulsive efficiency, rather than the tested sprint speeds (Fish, 1998). Resonance with a characteristic propulsive reverse Kármén vortex thrust is essentially amplified (D.A. Read, 2002). These unsteady effects can induce dynamic stall producing high lift forces and delaying the onset of stall.

3.3 Drafting – Hitching a ride

Animals travelling in groups can further manipulate shed vortices to reduce the overall energy expenditure of the group. It is witnessed in observing Dolphin, mother-calf pairs or fish schooling, that they decrease drag by riding induced slip stream vortices from the leading swimmer, overall minimising propulsion energy effort. In dolphin pairs, Bernoulli suction results from attractive forces generated due to local high pressure gradients in areas of high velocity, attracting the calf towards the mother. Displacement effects due to the mothers motion pushes water radially outwards along her central axis (forwards, in other words). These effects create forward thrusts to her anterior and suction to her posterior (Weihs, 2004) (See Figure 3.7). This same effect is utilised by dolphins swimming abreast the bow of marine vessels, and was the cause of J. Gray's error mentioned previously.

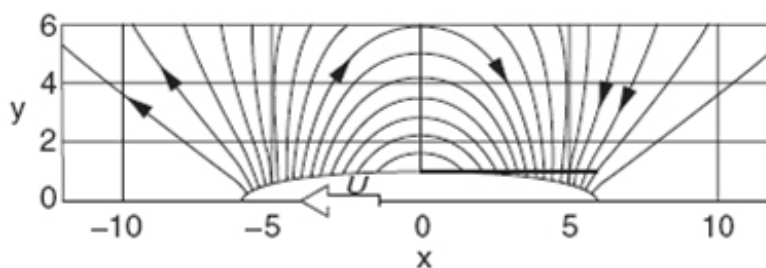


Figure 3.7 Elliptical representation of the mother dolphin and induced streamlines (Weihs, 2004)

Depending on the calf age (neonate – 2yrs) and size, in taking up correct positions (mainly laterally to the posterior) the calf can hitch a ride gaining up to 90% of the thrust required to keep up with its mother swimming at $2.4\text{m}\cdot\text{s}^{-1}$. Burst & Coast mode swimming; short bursts of thrust followed by gliding, is also used to conserve calf energy and minimise the drag penalty incurred by the mother while the calf learns to swim efficiently (Weihs, 2004, FRANK E. FISH, 1991). Trained dolphins, swimming at $3.8\text{m}\cdot\text{s}^{-1}$ in the wake of a small boat, were found using electrocardiography to have a heart rate 20% lower than when swimming at

$2.9\text{m}\cdot\text{s}^{-1}$ in free stream conditions (McNeill, 2004). Similar tests on ducklings, in linear and diamond formations following a decoy artificial mother, found a decrease in metabolic rate of 60% when compared to a single duckling, with rearward ducklings paddling 26.9% less vigorously by measurement of feet arc length of oscillation (Fish and E., 1995). Birds flying in V or linear formations also benefit from the leader's wingtip vortices. These provide lift and reducing individual energy exertion. Tests using pelicans trailing a micro-light craft observed trailing birds wing beating at decreased frequency in comparison to the leaders flight condition (See Figure 3.8).

The hydrodynamics of drafting is complicated; governed by unsteady flow conditions between deforming animals, of differing size, varying relative velocities to each other, and the free stream. In the case of dolphins periodically breaching the water surface, which momentarily changes medium the situation is aggravated even more. In aerial observations of high speed swimming, calves can be seen alternating side to side in the mothers wake. (Weihs, 2004) This may be due to yaw bias on the calf or further, the calf may be intentionally swimming in a Kármán Gait (Liao et al., 2003).

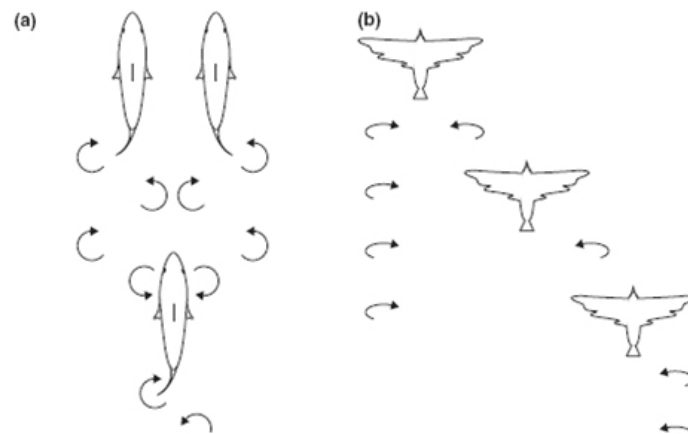


Figure 3.8 Vortex aided energy efficient group propulsion (McNeill, 2004)

3.4 Kármán Gait

In developing quantitative test data in neural control between fish and oncoming vortices using flow visualisation (digital particle image velocimetry (DPIV)) and electromyography techniques, it is demonstrated that trout will slalom the high-low pressure vortices of a Von Kármán Street with minimal musculature input. Only the anterior radial muscles are utilised to incline the head

to the localised lateral flows between high and low pressure vortices, in effect extracting further energy from the flow. This is not simply drafting described previously such as a race car or cyclist utilises, this is further levels of efficiency through synchronicity between the Kármán street frequency and the undulating fish body kinematics (Liao et al., 2003). Actuated oscillating hydrofoils generate more thrust in cutting through the vortices, although they require increased power to maintain AoA. Trout slalom to reduce their power input rather than maximise thrust output (D. S. BARRETT, 1999). Tests show fish can utilise environmental vortices in reducing locomotive efforts through Kármán gait mechanism where by the fish behaves as a self correcting hydrofoil (Liao et al., 2003).

It should be noted that drafting and Kármán Gait swimming are destructive interference methods of extracting vortical energy. This reduces energy loss increasing overall efficiency of propulsion. Crossover is apparent from the physics of wave theory.

3.5 Unsteady Weis-Fogh effect

Insect flight also exhibits interesting unsteady lift generation through a mechanism described as “*the clap, fling & flip*” (Weis-Fogh, 1973). This occurs at maximum and minimum morphological wing stroke as part of a dual steady-unsteady flight and hovering mechanism. Insects of the Hymenoptera family* generate high lift coefficients (C_l) of about 3 which, at such low Reynolds numbers (Re) (10-20) are not in line with traditional airfoil theory. As the leading edge of insects wings instantaneously *fling* open, separating in pronation rapid wing tip vortices are created bypassing the Wagner effect[†] (See Figure 3.9) (Weis-Fogh, 1973). The vortices propagate by the Helmholtz-Kelvin argument (Anderson, 1990);

- I. *The strength of vortex filament is constant along its length.*
- II. *The vortex filament cannot end in a fluid.*

Immediate lift is created by the effect and this sets up advantageous circulation in aiding sustained flight.

* Bees, wasps, ants etc

[†] Wagner effect states that circulation rises slowly due to viscous effects when a wing is accelerated from rest

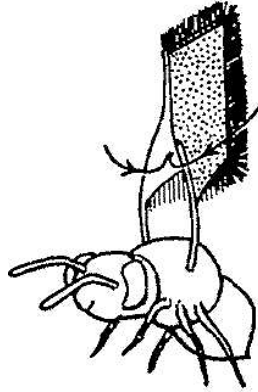


Figure 3.9 Clap-Fling motion (Weis-Fogh, 1973)

Subsequent testing using DPIV found lift enhancement with wing separation of no more than 10° - 12° with further unexpected peaks in lift and drag during the wing cycle. The most obvious lift effect was the rapid downward inflow, setting up the leading edge vortex (LEV) and overall increasing the lift generated by 17% (Fritz-Olaf Lehmann, 2005). The whole effect approximates inviscid flow with subsequent energy savings during flight.

3.6 Biological hydrodynamic modelling

There are many methods of fluid dynamic modelling of marine and avian propulsion. Slender body theory, lifting surface theories, present boundary element methods (BEM), panel methods and Navier-Stokes codes are at the computational core of modelling. They can be used to compute and quantify dynamic components of fluid surface interaction and the derived pressure & velocity distributions, turbulence and vorticity among other things (Jian-Yu Cheng, 2001).

Fluent* uses a Reynolds averaged Navier-Stokes (RANS) code in unsteady turbulence modelling, incorporating Reynolds stresses for transient effects of momentum changes in fluid flow. Fluent's RANS solver is used in developing the passive model discussed in section Chapter 8. The preceding fundamentals governing the hydrodynamics of oscillating hydrofoils, is outlined next in section Chapter 4.

* Fluent is an industry leading computational fluid dynamics (CFD) modelling software package.

Chapter 4 Fundamentals of Oscillating Hydrofoils

As outlined above in Chapter 3, it is apparent how extraordinarily adroit fish, cetaceans, birds and insects are in terms of engineering hydrodynamics. Empirical and mathematical models characterising their locomotion and manoeuvrability are based on pitching and heaving symmetrical hydrofoils, which concurrently translate (heave) and rotate during their cycle.

Their equations of motion with two degrees of freedom (DoF) are defined by:

$$h(t) = h_o \sin(\omega t) \quad (4.1)$$

$$\theta(t) = \theta_o \sin(\omega t + \psi) \quad (4.2)$$

Where, h_o is the heave amplitude, ω is the cycle frequency (rad.s^{-1}), t is time (s), θ is the pitch angle and ψ is the phase angle (rad.s^{-1}) between pitch and heave (See Figure 4.1).

The resultant angle of attack is described by;

$$\alpha(t) = -\arctan\left(\frac{h(t)}{U_\infty}\right) + \theta(t) \quad (4.3)$$

Where; α is the angle of attack (AoA) and U_∞ is the incident flow velocity.

A hydrofoil profile is characterised by its lift, drag and pitching moment at a range of Reynolds number flow, for a range of angle of attack. Most common hydrofoil profiles, especially symmetrical foils as used in oscillatory processes, are well understood for steady state flow conditions. Their characteristics are non-dimensionalised in terms of C_l & C_d ; the lift and drag coefficients respectively.

In a dynamic unsteady flow situation these non-dimensionalised coefficients cannot be used to accurately calculate lift generated by foils in motion. Hence further modelling is required to simulate the environment and flow

conditions in which the foils will operate, to gather performance coefficients for those said flow conditions.

Numerous models have been developed for the analysis of Autonomous Underwater Vehicles (AUV), biomimetic technologies and their propulsion systems which pay more attention to efficient thrust generation rather than lift generation. The difference between these two schemes is, the phase angle of the foil during the device power cycle. Generally lift generation AoA leads heaving motion, with pitching lagging. There are numerous crossovers in modelling methodologies.

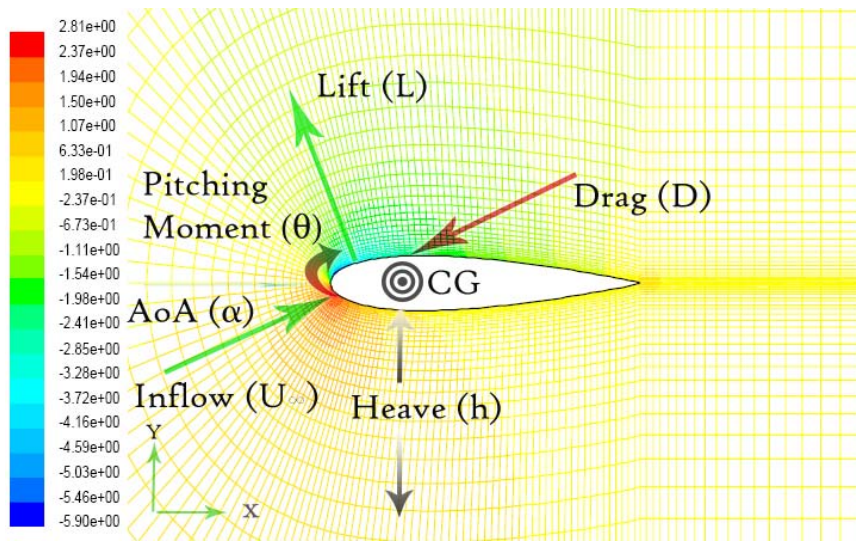


Figure 4.1 Pressure Field & Subsequent Forces & Foil Motion [pascal]

Oscillating Foils generate large vortices in their wake; the wake motion and efficiency can be characterised by the Von Kármán Street (VKS) therein. Drag is indicated by a typical VKS where as a reverse VKS is indicative of thrust (J. M. ANDERSON, 1998, Triantafyllou G.S, 1993). Unsteady vortex control can aid lift generation by inducing dynamic stall prolonging the range of AoA at which a foil can function under a given set of flow conditions. Foils can also be used to manipulate incoming vortices in the flow stream for vortical energy extraction and efficiency heightening. To quantify this some parameters need to be defined;

Strouhal Number can alternatively be defined similarly to the above equation(3.2). However, equation (4.4) is more useful using physical model characteristics.

$$St = \frac{4\pi h_o \omega}{U_\infty} \quad (4.4)$$

The reduced frequency;

$$K = \frac{\omega c}{2U_\infty} \quad (4.5)$$

The Reynolds number;

$$Re = \frac{U_\infty c}{\nu} \equiv \frac{\rho U_\infty c}{\mu} \quad (4.6)$$

The heave: chord length ratio

$$HC_{rato} = \frac{h_o}{c} \quad (4.7)$$

The mean lift force vector;

$$\bar{F}_y = \frac{1}{T} \int_0^T F_y(t) dt \quad (4.8)$$

The mechanical power output

$$P_m = \frac{1}{T} \int_0^T F_y(t) \dot{h}(t) dt \quad (4.9)$$

The non-dimensionalised force coefficient, where F can represent either the lift or drag components

$$C_F = \frac{F}{\frac{1}{2} \rho U^2 cs} \quad (4.10)$$

The non-dimensionalised lift coefficient

$$C_l = \frac{\bar{F}_y}{\frac{1}{2} \rho U^2 cs} \quad (4.11)$$

The required device structural reactance to the flow stream

$$\bar{R} = \bar{F}_x + \bar{Q}_{cg} \quad (4.12)$$

The available tidal stream power

$$P_{\infty} = \frac{1}{2} \rho c s U_{\infty}^3 \quad (4.13)$$

Finally the coefficient of power extraction

$$C_p = \frac{P_m}{P_{\infty}} \quad (4.14)$$

4.1 Strouhal Significance

There has been extensive testing of the symmetrical NACA oo series airfoils in steady state & oscillating propulsion regimes. Tests with low angles of attack (2°), incorporating increasing the frequency of oscillation causes the divergence of the VKS in its wake and a subsequent jet stream from an original inline position. At higher angles of attack, transition occurs with no inline vortices but four vortices per cycle rather than two. In terms of Strouhal number this transition to VKS regularly reveals itself in the region of $St = 0.1$ (D.A. Read, 2002). It is immediately apparent that the Strouhal number has a significant role to play in optimising efficient foil motion.

It is found that for various parametric combinations, efficiency is not concurrent with high thrust. High heave amplitudes with low mechanical frequency produce higher Strouhal numbers, but higher thrust coefficients are found at lower heave amplitudes. Efficiency at low St occurs with geometrical constraints; $HC_{ratio} = 0.75$. Optimal phase angle (ψ) is 90° with decreases in efficiency and thrust generally found for any alternative. Maintaining relative sinusoidal angle of attack pitching profiles, is seen to have considerable benefits for thrust and efficiency (D.A. Read, 2002). This is investigated for energy extraction setups in Chapter 8.

4.2 Flow Prediction Modelling

Current models typically are based on potential inviscid flow, for high Reynolds numbers; maintaining that viscosity only effects flow during boundary layer separation. Circulation calculations are then carried out to quantify the

vortices strength based on the Kutta Condition* (Guglielmini et al., 2004). Existing models neglect leading edge vortices, but, as seen in section 3.5, leading edge vortices have considerable effect in inducing lift augmentation by optimising vortices flow in insect flight utilising the Weis-Fogh effect. In Recent experimental and mathematical models, the results begin to show this effect (J. M. ANDERSON, 1998, Guglielmini et al., 2004), and sub sequentially strong thrust and high efficiency is associated with the generation of LEV's (See Figure 4.2). Dynamic modelling of trailing, and leading edge vortices is required to fully represent the foil dynamics (Guglielmini et al., 2004).

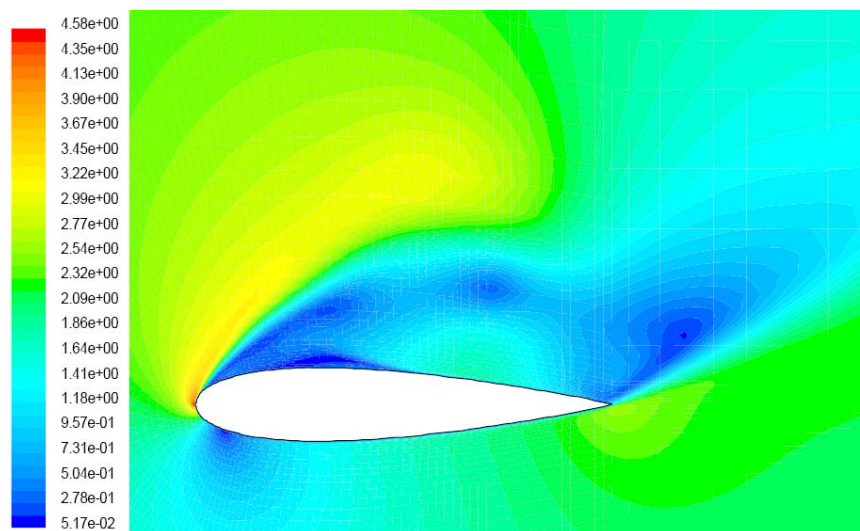


Figure 4.2 LEV reconnecting with the Trailing Edge Vortex [m.s⁻¹]

4.3 Pitch and Heave Hydrofoil Motion Optimisation

As seen above the effective control of angle of attack, pitching, and heave amplitude is of paramount importance for efficient generation; the most sensitive of those parameters being the foil AoA, its range, and rate of change (F.S. Hover, 2004). It is found that sinusoidal and square wave profiles produce two effective vortices per cycle, whereas multiple peaked motion profiles produce an increased turbulent wake with a decrease in thrust and efficiency (Michael S. Triantafyllou, 2003). For effective propulsion, therefore, the parameters of equation (4.3) should

* The Kutta condition allows the modelling of significant viscous effects in inviscid hydrodynamic theory. The velocity leaves tangentially laterally from both sides of the sharp (trailing) edge while neglecting the underlying viscous effects in the momentum equations throughout the flow. It significantly reduces computation time. It is fundamental in calculating the flow patterns in steady or unsteady flow around a hydrofoil.

be manipulated to output either a sinusoidal or square form, which can require high order harmonic inputs to create this set up. *This is an important discovery and should be noted as is further discussed in Chapter 8.* Furthermore, it should also be noted that AoA fluctuations at high St. within the cycle result in degradation of thrust by increased order of vortices and consequently increased drag.

DPIV data shows that vortices curl-up occurs at the maximum rate of change of angle of attack, and in opposite direction to the motion of the foil. Therefore, using varying AoA rate of change from harmonic, cosine and square wave forms has differing effects on the vortices roll up and subsequent thrust generated. A cosine profile has the optimum profile when comparing efficiency and thrust (See Figure 4.3); an increase of 10% is generated in some cases (F.S. Hover, 2004).

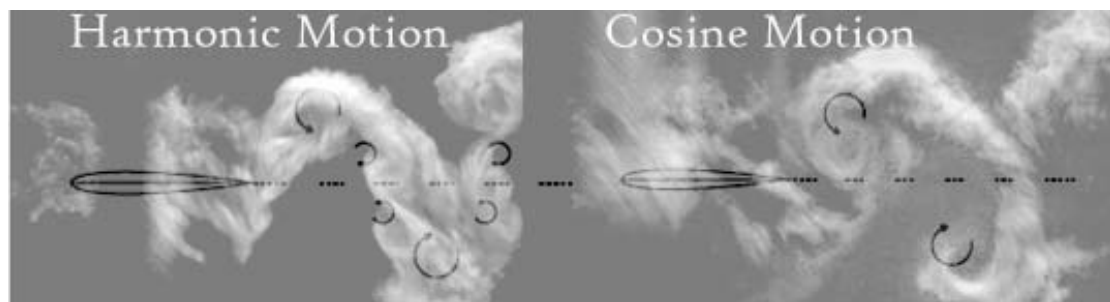


Figure 4.3 AoA Profile Vortical Effects (F.S. Hover, 2004)

This is only the beginning of truly understanding oscillating foil manipulation and motion. Biomimetic observations, as outlined above lead us from the unknown but there is much still to be learned. Generally, thus far, optimum operation is governed by relatively large AoA which develop leading edge vortices and generate two vortices per cycle.

Comparing the feathered pleated wings of avian borne animals to the streamlined caudal & pectoral fins of aquatic animals, indicates drag is of significant penalty and an evolutionary disadvantage. The aim should be to minimise drag to the same levels as a hydrofoil being towed in water, with no pitch or heave for optimal operation (Michael S. Triantafyllou, 2003). In agreement with the tow tank testing and reported testing of cetacean swimming tests the optimum regime for foil propulsion illustrated in Figure 4.4 is with an AoA and St in the range of $10\text{-}30^\circ$ and $0.2\text{-}0.5$ respectively.

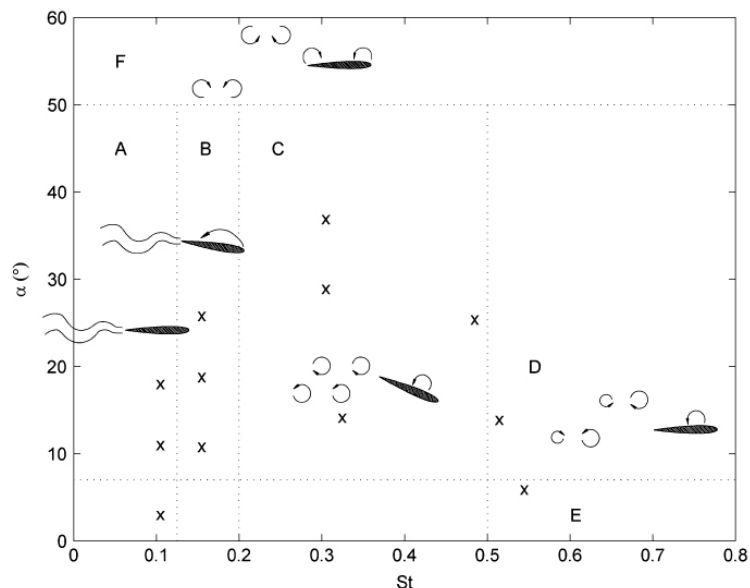


Figure 4.4 Parameter Comparison varying AoA and Strouhal Number (Michael S. Triantafyllou, 2003)

Furthermore, when two foils operate inline, they can have interaction which can have serious implications. This, however, is not necessarily detrimental, but the effects should not be ignored. Vortical energy and wave interference effects can be manipulated to have beneficial effects. Dual foils, in a similar set up to the Weis-Fogh effect operating 180° , can generate sufficient thrust to propel a ship (Michael S. Triantafyllou, 2003). However, the vortices in the wake of this set up are significantly more complicated than single VKS. If oscillating hydrofoil farms are to be deployed, this effect must be further studied and understood to be manipulated and optimised.

4.4 Flexible Foils

Correctly chosen chordwise flexibility has recently been shown to improve thrust efficiency by up to 36%, with only slight reduction in thrust generation in comparison to its rigid counterpart. Highest efficiencies reached were 0.87 at $St=0.3$; while the optimum operational range is $St=0.15-0.3$ with an AoA of 15° (Jim J. Rohr, 2004, P. Prempraneerach, 2003, J. Katz, 1978). A non-dimensional flexibility parameter has been developed while testing varying grade urethane foil models to quantify the effect of foil flexibility. Previous experiments found limited efficiencies with rigid foils at 50-60% (D.A. Read, 2002, J. M.

ANDERSON, 1998). Under properly defined spanwise and chordwise flexibility, propulsive foils closer to natural caudal fins rather than rigid foils can generate equivalent thrust at much higher efficiencies.

In comparison with conventional rotational propellers and contra-rotating propellers, the flexible foil is shown to outperform both in thrust generation and efficiency for equivalent wetted perimeters and design geometries (P. Prempraneerach, 2003).

4.5 Hydrodynamic Fundamentals

A brief introduction through classical hydromechanics is required to fully grasp the concepts discussed from here onwards. However this outline is by no means conclusive and further reference to texts (White, 2003, Anderson, 1990, Bruce R Munson, 2006, Duncan et al., 1970) is recommended for in-depth study and uncovering understanding of the underlying theory.

4.5.1 Bernoulli

The beginning of the eighteenth century brought an evolutionary leap in the understanding of fluid mechanics through the eyes of Daniel Bernoulli and Leonhard Euler. The relationship between pressure and velocity in an inviscid irrotational flow was (firstly by Euler and subsequently) described by Bernoulli's Equation;

$$P + \frac{1}{2} \rho U^2 = Const \quad (4.15)$$

Derived from Newton's Second Law;

$$\begin{aligned} F &= ma \\ \text{Or} & \\ F &= \frac{d}{dt}(mV) \end{aligned} \quad (4.16)$$

The conservation of momentum from any point to another in a flow field can thus be calculated by;

$$P_1 + \frac{1}{2}\rho V_1^2 = P_2 + \frac{1}{2}\rho V_2^2 \quad (4.17)$$

The application of Bernoulli's equations is pretty simple but highly significant. When the velocity increases the pressure decreases and vice versa. This is illustrated in flow about a NACA 0015 in Figure 4.5 and Figure 4.6.

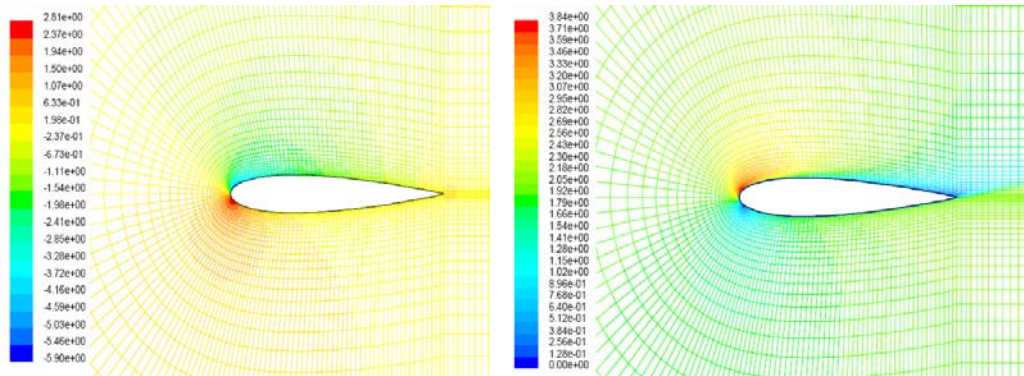


Figure 4.5 Static pressure [Pascal] 2m.s⁻¹ inflow AOA 15 Deg

Figure 4.6 Velocity distribution [m.s⁻¹] 15 AOA 15 deg

Bernoulli suction, as mentioned previously in section 3.3, is a simple application of Bernoulli's equations. Suction is observed in areas where there is high velocity flow due to the subsequent low pressures being filled by local inflow. In the case of a mother and calf dolphin, this is how a mother can swim quite rapidly and maintain an invisible hydrodynamic grip on her young calf. In actual fact the faster the better the grip prior, to boundary layer separation.

4.5.2 Venturi Effect

The venturi effect is a continuation of Bernoulli's governing equations. In special cases, where there is a constriction in the flow field, as in Figure 4.7, due to the Bernoulli principles of conservation of momentum, the velocity in the constricted area must be increased. Subsequently there is a drop in pressure head. (Note the difference pressure head h) *This is another point which should be specifically noted and will be returned to in Chapter 8.*

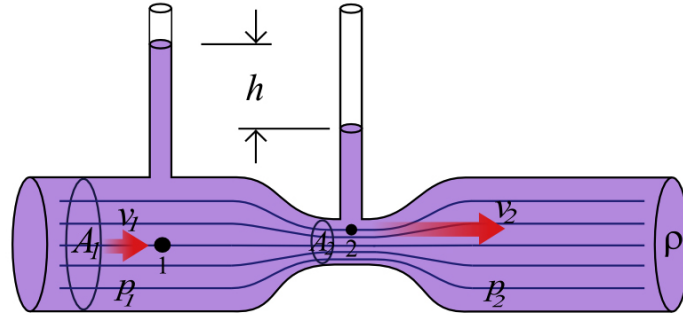


Figure 4.7 Venturi Tube*

Consider the image above, where the flow is incompressible and ρ is constant. The conditions are eloquently governed by;

$$A_1 V_1 = A_2 V_2 \quad (4.18)$$

4.5.3 Circulation

As discussed in cetacean swimming in Chapter 3, it is quite apparent that the understanding of circulation is critical to fully understanding the generation of lift. Independently the relationship between circulation and lift generation was utilised by Frederick Lanchester (England, 1878-1921), Wilhelm Kutta (Germany, 1867-1944) and Nikolai Joukowski (Russia, 1847-1921), the three of whom have developed the significant groundwork in the field.

Taking a control loop C , where ds are the local flow velocity and directed line segment respectively, circulation (Γ) is defined by;

$$\Gamma \equiv -\oint_C U \cdot ds \quad (4.19)$$

This is a simple representation of the velocity field in a predetermined control loop C . More importantly, circulation is directly proportional to vorticity (See section 4.5.5)

4.5.4 Biot savart

With reference to the Weis-Fogh effect of insect lift generation following the Helmholtz-Kelvin condition (Section 3.5) as a visual aid; if circulation

* Public domain image from <http://www.wikipedia.org/>

propagates about any filament length (the leading edge of a foil or wing for example) a constant value of Γ is arrived at. The resultant velocity at a point p, a radius r from this filament along the direction segment dr is defined by the Biot-Savart equation;

$$dV = \frac{\Gamma}{4\pi} \frac{dl \times r}{|r|^3} \quad (4.20)$$

This again has significant implications in developing and understanding farfield flow effects at a distance from the circulation generating edge or filament.

4.5.5 Vorticity

Vorticity is utilised to quantify the skewedness, rotation and translation of an elemental volume of fluid in a flow field, overall describing the velocity field in that said flow.

The angular velocity of a 2D element in the XY plane rotating about the z axis is defined by (See Figure 4.8);

$$\omega_z = \frac{1}{2} \left(\frac{d\theta_1}{dt} + \frac{d\theta_2}{dt} \right) = \frac{1}{2} \left(\frac{\partial v}{\partial x} + \frac{\partial u}{\partial y} \right) \quad (4.21)$$

In three dimensional space;

$$\omega = \frac{1}{2} \left[\left(\frac{\partial w}{\partial y} - \frac{\partial v}{\partial z} \right) i + \left(\frac{\partial u}{\partial z} - \frac{\partial w}{\partial x} \right) j + \left(\frac{\partial v}{\partial x} - \frac{\partial u}{\partial y} \right) k \right] \quad (4.22)$$

Vorticity (ξ) is simply twice the angular elemental velocity;

$$\xi = 2\omega \quad (4.23)$$

Therefore in a velocity field the curl of the velocity is equal to the vorticity;

$$\xi = \nabla \times V \quad (4.24)$$

Irrotational flow is that of a flow field with $\nabla \times V = \mathbf{0}$, i.e. the flow is purely translational moving along a straight line.

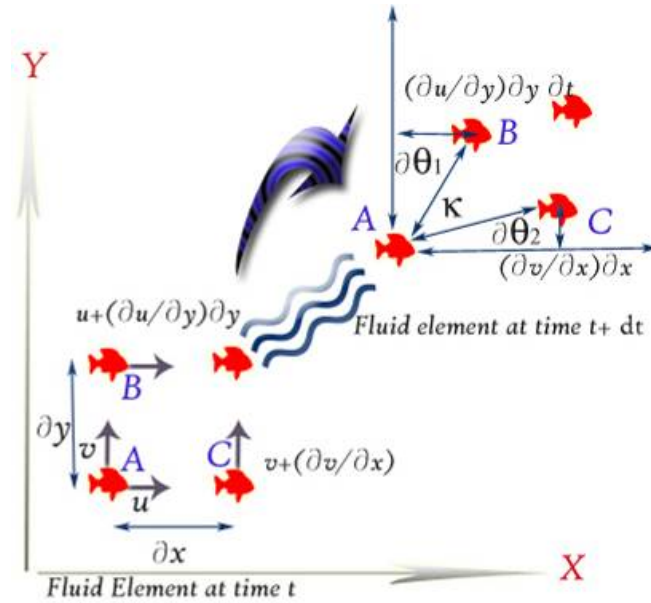


Figure 4.8 Rotation, Translation & Skewing of Fluid Element ABCD

In relation to hydrofoils, the application of this relationship is the governing factor to lift generation; through circulation and vorticity theory the pressure field potential across the foil chord is calculated, and hence the resultant forces thereupon. (Revisit; Figure 4.1 Pressure Field & Subsequent Forces & Foil Motion [pascal])

4.5.6 Theodorsen's Theory – Unsteady Flow & Flutter

In 1935, steady state airfoil theory was understood, in that above a certain AoA and above a specific velocity a foil with two DoF would stall, drastically reducing lift. This is specifically due to the separation of the flow boundary layer on the foil, causing the pressure gradient there on to drop dramatically. Theodore Theodorsen (1935) took the next step in aeronautical theory, laying down the ground work in understanding the mechanism of flutter in sinusoidally oscillating foils. Large oscillations are not of interest, where as the infinitesimally small oscillations caused by flutter are of interest. The theory developed from extended Bernoulli's equations, steady state theory and the Kutta condition*. It lead to their loop integrals and the understanding of the pressure distribution and unsteady lift forces experienced by a foil (Theodorsen, 1935).

* For unstable irrotational and circulatory flow component

Some of the assumptions regarding two dimensional regular flow* at the trailing edge made by Theodorsen meant, that at the limits of the Kutta condition, at high angles of attack, and at reduced oscillation frequencies, his theory would be inaccurate (E. Hoo, 2005). Hysteresis effects delay the onset of stall, maintaining maximum values of lift drag and pitching moment which can far exceed the static steady flow counterpart (E. Hoo, 2005). This effect can be noticed in Figure 6.5, wherein the prototype testing of the stingray machine, lift generation continued past the originally theoretically calculated AoA stall angle.

4.5.7 Dynamic Stall

Dynamic stall is the limiting factor of foil motion. The capabilities of foils from helicopter rotors to wind and marine current turbines are limited by this effect. Numerous studies are being conducted into the understanding of dynamic stall but, as of yet, it is not fully mathematically understood.

It has already been shown that optimum operating AoA for NACA 0012 and NACA0014 foils is approximately 20°. Typically, steady flow theory based on empirical testing specifies a maximum AoA for these foils between 12° and 15°, so it is apparent that in naturally occurring motion there is more at play. The vorticity created by dynamic motion in swimming and weis-fogh motion is referred to as the Dynamic Stall Vortex (DSV). At low Reynolds numbers, the transition from laminar to turbulent flow at the leading edge is important in the development of DSVs. Analytical solutions have shown that the Spalart-Allmaras turbulence model to yield the most accurate modelling results with only one equation (W. Geissler, 2006).

Lab testing manipulating turbulent flow over a hydrofoil, using a rough turbulence tripping layer along the upper surface near the leading edge has shown, that prior to the development of DSV and dynamic stall, a low pressure bubble is generated in the laminar boundary layer at the leading edge. As the AoA is increased the pressure gradient across the bubble (See Figure 4.9) increases and propagates further along the chord length away from the leading edge. The flow is deflected about the bubble causing clockwise flow acceleration and anti-clockwise deceleration in the flow field causing additional local vorticity. This additional

* Kutta Condition

vorticity can increase and detach from the boundary layer and reattach further along the chord length, locally stabilising the vorticity and prolonging lift generation. This essentially provides an extra enclosed low pressure field and when calculating the surface loop integrals influence on lift, drag and hysteresis pitching moment is observed. *This is an important point to note. If the leading edge can be mixed with localised vorticity, particularly anticlockwise to counteract the prevailing flow regime, stall can be controlled, and lift range can be prolonged* (W. Geissler, 2006). It was further found in tests of flapping foils that LEV also augmented propulsive efficiency, but performance deteriorated when the vortex grew to large generating prohibitive drag effects (Michael S. Triantafyllou, 2003).

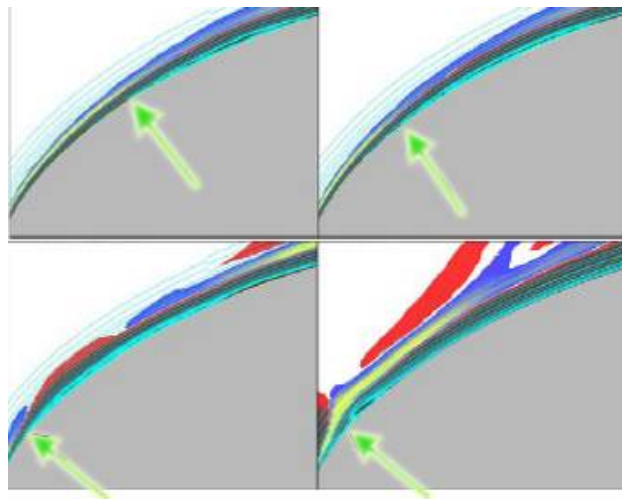


Figure 4.9 DSV Separation Bubble (W. Geissler, 2006)

AoA =16.95°, 17.16°, 17.36° & 17.56° respectively from top left, clockwise

4.5.8 Cavitation

When local pressure in a liquid falls below its vaporisation pressure, cavitation bubbles are formed. This change of state typically occurs due to high speed disturbances in fluid flow, such as turbine and propeller wing tips or the trailing edges of rapidly moving hydrofoils. This vaporisation pressure is affected by many local variables but temperature is the main one. Essentially (high velocity - low pressure) energy transfer from the hydrofoil trailing edge boils the water locally where the pressure is sufficiently low. Adapting Bernoulli's equation, one

can predict the critical relative flow velocity for onset of cavitation. (See equation(4.25))

$$U_c = \sqrt{\frac{p_o - p'}{\frac{1}{2}\rho}} \quad (4.25)$$

Where p_o is the free stream pressure and p' is local vapourisation pressure (Duncan et al., 1970).

The bubbles formed later collapse or more so implode giving off energy to local flow and surfaces. It can have serious corrosive and stress effects to devices in their near stream and should be avoided at all cost to minimise maintenance, erosion and possible device failure. Due to the length of the foil trailing edge in comparison to turbine and propeller wing tips, high speed hydrofoils generate cloud cavitation as opposed to local streams of cavitation. These clouds can collapse with some violence and significant noise (G. E. Reisman, 1994). Considerable information is available for marine propellers and knowledge transfer to hydrofoil motion is applicable. Research into the cavitation performance of laminate polymers, glass reinforced plastics (GRP) and urethane moulds is required to establish foil performance in regards limitations due to cavitation (Batten et al., 2006). Some limited work has been carried out on oscillating foils and it specifies that water quality, reduced frequency, amplitude of oscillation and vortical structure about the foil are the main contributing factors (Michael S. Triantafyllou, 2003).

It is suspected, due to the low relative velocities of tidal hydrofoil devices, that cavitation shall not be a degenerative problem to power take off, but further work is recommended for applications to smaller device models

4.5.9 Navier-Stokes Equations - Why model viscous turbulence?

It has been shown that Dynamic stall, DSV, LEV, the Weis-Fogh effects all have interaction with viscous turbulent flow to varying degrees. While potential flow models produce accurate local and farfield simulations, they assume inviscid irrotational flow substituting the Kutta condition for vortex generation at

the trailing edge. This neglects viscous boundary layer effects and the influence of leading edge vortices (LEV) in lift generation.

Simulation using a Reynolds Averaged Navier-Stokes (RANS) model, using viscous momentum equations, taking into account time step transient effects, does not require illegitimate assumptions to be made. Furthermore it takes into account viscous shear stresses experienced in the hydrofoil boundary layer (Anderson, 1990). It is in this boundary layer and the leading & trailing edge near field (within viscous turbulent flow) where the interesting small scale hydrodynamics take place that are responsible for the generation of the non linear lift effects seen in prototype testing. There are various viscous models available to run concurrently with the Navier-Stokes equations, but the Reynolds stress model is the most complete and physically accurate. Flow history, transport and anisotropy of turbulent stresses are all accounted for, however it requires 2-4 times more computing time to run these models (Srinivasans et al., 1995).

Numerous Models have been developed using RANS codes to model biomimetic propulsion, (Cheng et al., 2001), dynamic stall, (Akbari et al., 2003), hydrofoil cloud cavitation, (Wang et al., 2005), and initial oscillating hydrofoils in energy extracting regimes (Jones et al., 2003). Further definition and development of the Navier-Stokes momentum equations is given in (Anderson, 1990) chapter 15.

Chapter 5 Power Take - Off – Linear Generators

It is not imperative to delve deeply into the inner workings of linear generators. A basic understanding, however, of their design and construction will provide an insight into the simplicity of manipulating power output by either power electronics or PLC feed back to control the phase of generation and if proved useful, the foil phase position. It will also give the reader an appreciation of the simplicity of the design outlined in Chapter 8.

5.1 Drive Systems

Electrical generation machines have traditionally been designed to be driven at high rotational speeds. These are energised by a fossil fuel combustion process of some description, coal, oil, gas or nuclear cycles generating high pressure steam. This corresponds to an air gap rotational speed in the range of 60m.s^{-1} which generate rapid changing flux field ideal for electricity generation.

To date it has become the standard that renewable devices, operating at low linear or rotational speeds, have their output speeds rectified and stepped up through mechanical gearing, pneumatic or hydraulic systems. Wind turbines can be expected to operate within a 10-20 RPM range relating to a $5\text{-}6\text{ m.s}^{-1}$ generator air gap speed. Similarly low speeds are typical with wave point absorbers reaching oscillatory speeds of $0.5\text{-}2\text{ m.s}^{-1}$ (Baker, 2003).

5.1.1 Mechanical Linkages

Gearboxes are the industry convention to convert low speed high thrusts to more generator-friendly, low thrust high speeds. Rectifying an MEC device to a particularly desirable speed range adds mechanical complexity and with it systems inefficiency, increased possibility of failure, oil change and maintenance requirements. Systems failure has already been experienced in the wind turbine industry, with whole product range recalls required for gearbox replacement. Consider the Stingray device introduced in section 2.2. Stingray outputs a high torque low speed sinusoidal varying power. Even at high speed cycles, to utilise a

traditional generator set up the gearing linkage ratio would be in the order of a factor of 30 (Baker, 2003, Joseph E. Shigley, 2003). This places considerable stress on the gearing mechanism itself.

5.1.2 Hydraulic Systems

The heavy steel, maritime and oil rig industry have been leaders in adapting their manufacturing processes to developing MEC devices. Technology and knowledge transfer is apparent in the design choices and preferences towards hydraulic power take off systems. These systems are well understood, and give flexibility in complex devices structures undergoing motion. There are, however, some inherent weaknesses in their use.

Hydraulic power take off systems utilise high pressure oscillating rams, pressurising and transferring high pressure oil to drive a variable speed hydraulic motor which in turn drives an electrical generator. Secondary systems with many moving parts are required to actuate and smooth high pressure thrusts. This is a 3 phase energy transfer, with inherent losses in efficiency due to seal friction limiting translational velocity to $0.5\text{m}\cdot\text{s}^{-1}$, internal viscous friction, mechanical friction, thermal losses and finally electrical losses (Baker, 2003). These devices can be costly and add considerable weight to any device where deployed. The working medium of oil in a marine environment is also cause for concern. It can be problematic transmitting pressurised oil over distances and requires regular maintenance and systems checks.

5.2 Direct Electrical Drive

Direct drive systems are those where the prime mover in the device is, or is directly connected to, the prime mover of the generator. This removes the inherent inefficiencies and complexities of previously discussed energy phase conversion and design criterion. It does, however, require design of generators to the specific low speed, variable high thrust and speed range of any specific device utilising direct drive systems. Consequently, large area air gaps are required to electromagnetically react against the low speed high energy thrusts (Baker, 2003).

The stator coils will experience a change in flux linkage in coherence with faradays law (5.1) inducing an electro-motive force (EMF) by the oscillating permanent magnets (PM) within the generator housing (Cutnell et al., 2001).

$$E = -N \left(\frac{\Phi - \Phi_0}{t - t_0} \right) = -N \frac{\Delta\Phi}{\Delta t} \quad (5.1)$$

Where N is the number of coil loops, $\Delta\Phi$ is the change in magnetic flux through one coil loop and Δt is the time interval over which the change takes place.

The Root mean square (RMS) voltage (V) and current (I) are both $\sqrt{2}$ times smaller in sinusoidal motion when compared with a linear motion range, hence a decrease in generated power is inherent in sinusoidal generation devices.

Direct drive systems are simple, and removing moving parts are potentially highly efficient with a long life span. Until recently the costs of PM's have made it prohibitive to look at these designs but research in the area is on going with varying high power topologies suggested with reduced magnetic material required. This reduces cost and weight (Baker, 2003, E Spooner, 2001).

5.3 Linear generators

Linear generators can theoretically and visually be represented as simply its rotational counterpart split, rolled out and flattened, turning the device radial symmetry to axial symmetry (See Figure 5.1).

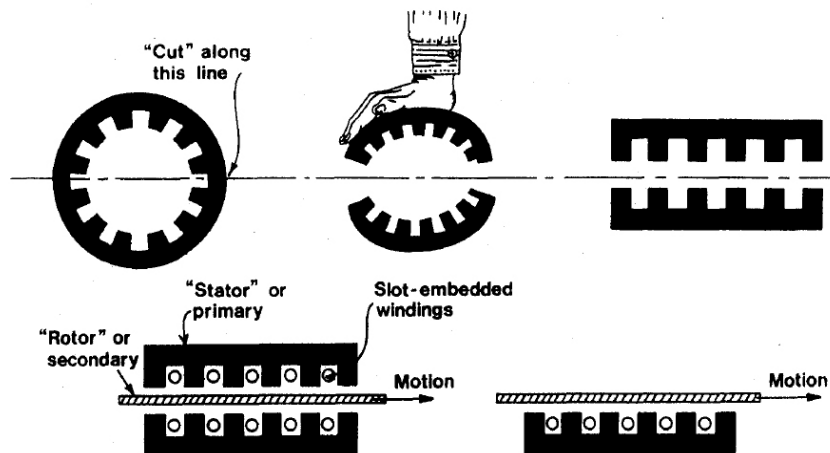


Figure 5.1 Rotary generator to Linear generator transformation (I. Boldea, 1999)

Induction generators are by far the industry standard with regard to traditional electricity generation. An electrical current is required to excite the induction coils in beginning the power device power cycle. This requires a two way gird connection. Also a linear induction machine is likely to have a larger air gap in comparison to its rotary counterpart, causing low inductance and reactance and low overall efficiencies. Typically it is useful, to manipulate the excitation current as a means to control the generator. In a passive device this is obviously not the case, nor a feasible choice of generator set up.

Linear synchronous devices have been shown to be more favourable and reliable, with efficiencies of 90% compared with 82% of comparable induction device (Baker, 2003, Jiabin Wang, 1999).

5.3.1 Permanent Magnet Synchronous Generation

Alternatively in regard to excitation requirements of induction generation, PMs can be used to cause field excitation supplying pole flux rather than current carrying coils. As the translator moves, the flux linkage generated by the magnets is cut, inducing an emf.

$$B_g = B_r \left(\frac{t_m}{t_m + u_r g} \right) \quad (5.2)$$

Where B_g is the air gap flux density, B_r is the Magnet remnant flux density, t_m is the thickness of the magnet, g is the length of the air gap, u_r is the relative permeability.

Using Lorenz's law the mechanical-electrical force relationship is defined by;

$$F = B_g i L \quad (5.3)$$

Where F is the force, i the current and L is the length of interaction.

Rare earth PM machines are capable of shear stresses unmatched by other electrical machines, providing high power density in restricted device sizes (Baker, 2003).

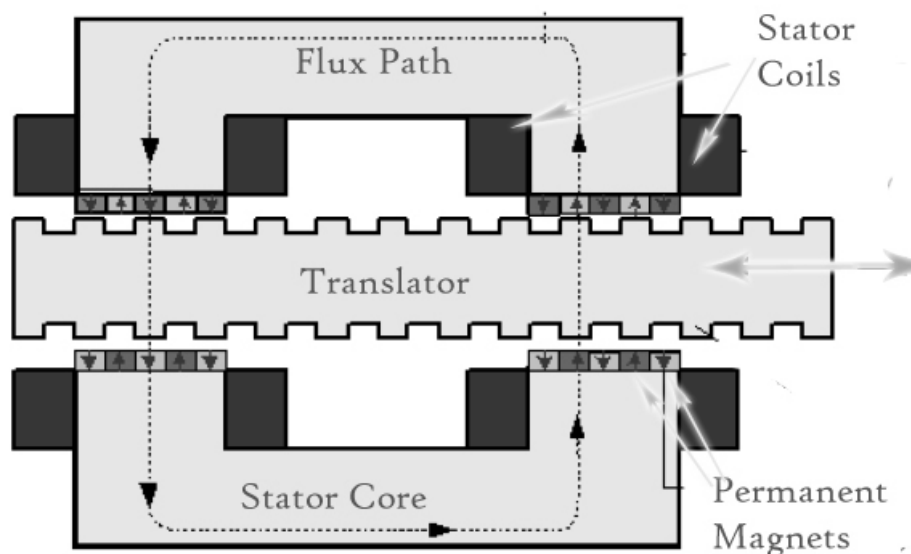


Figure 5.2 Vernier Hybrid Machine (VHM)

Topologies, similar to Figure 5.2 vernier hybrid machines utilising multiple air gaps and coils interacting in flux linkage through an iron core translator, have been suggested in minimising rare earth PM material required while maintaining high shear stresses and flux linkage density. Further suggestions have been to mount the PMs on the translator with similar effect. The small pitched teeth, designed in the iron core, provide a rapid rate of change in flux linkage, generating higher power outputs as a result (Baker, 2003, E. Spooner, 2003).

Linear generator designs can utilise both flat plate cross sections and tubular generators sections. PMs can be sealed within a ceramic coating to prevent corrosion and mechanical shear. This reduces overall mechanical friction, providing purely EM shear resistance. In Oscillating wave point absorbers, linear generators have been found to be the superior power take off choice (E Spooner, 2001).

5.4 Tubular PM machines

The topologies, discussed above have been designed in flat cross sections. However, this is not a requirement of linear generators and in some cases tubular designs can be useful. Tubular design refers to a circular cross section of the device along the stator longitudinal axis.

They are beneficial, as they have high flux linkage density extracting high power thrusts. They have high relative efficiencies, no end windings and a null attractive force between the stator and translator (Jiabin Wang, 2004). The translator can be air or iron cored providing flux insulation or linkage where desired.

On the downside, in many cases, tubular design is found to be wasteful with PM material require up to 25 times more material, due to radial magnetic effects (Baker, 2003). This adds weight to the generator and to the structure supporting it. Flux leakage across the axially mounted PMs is also identified as a significant problem within the complicated flux paths (Jiabin Wang, 2004).

5.5 Archimedes Wave Swing

The wave point absorbing prototype, Archimedes Wave Swing (AWS) device utilises a PM linear synchronous generator (PMLSG) with a current source inverter as its power take off system. Point absorbers have specifically simplistic vertical motion at varying harmonic rates. Their one DoF motion is conducive to the use of linear generators.

A iMN generator was designed and built specifically for the prototype. The PM material was translator mounted to give the following advantages;

- High force density
- Efficient at low speeds
- Reduce PM material cost
- No electrical contacts required to the translator

The generator was double sided to balance system loads and reduce loading on the linear bearings. The translator & PM material is not required to be of the same dimensions, as long as common cross sectional areas and linkage occurs during high thrust power cycle phases.

The input force from wave front varies sinusoidally. However, the rms current value does not, as it must reach a rated force prior to generation. At low speed the PMSLG limits the system efficiency, while at high speeds copper cable losses are found to limit device efficiency with losses ranging from 2.5% - 10%. It was found that increases in systems efficiency to the tune of 18% are gained when

using voltage sources inverter (VSI) rather than current source inverter (CSI) as originally used (Henk Polinder, 2004, H. Polinder, 2002).

Chapter 6 Oscillating foil generator modelling

McKinney & DeLaurier of the University of Toronto, the main pioneers of oscillating hydrofoil technology, described the use of oscillating hydrofoils for wind, ocean or river energy extraction in 1981 (See Figure 6.1). They tested and described similar foil equations of motion as already introduced and defined the power available from a foil in sinusoidal pitching motion, while rotating on the end of a boom (William McKinney, 1981) (Similar to the Stingray design. (See Figure 6.2))*

Other than some of DeLaurier's Students (Moores, 2003), and the United States Naval Postgraduate School, little interest in oscillating hydrofoils has been developed since this with only a rare few alternative institutes developing linear theory knowledge in the field. Much more detailed unsteady dynamic theory is required for full understanding for extraction power cycles.

Panel method codes are available with the progression of codes from original Hess and Smith methods to current developmental codes specifically for oscillating hydrofoils (Katz et al., 2001), and are used in developing mathematical models for oscillating hydrofoils. They are useful as they are open source codes, which can be executed in most mathematical software packages and enable the researcher to implement empirical data and up to date research with minimal cost. In resolving the hydrofoil geometry to linear panels, normal and tangential flow forces can be discretely modelled over the geometry and flow field.

Numerical panel methods have been used thus far to simulate unsteady flow about a hydrofoil in motion in prescribed pitch and heaving motion. It is found that, similar to propulsion regimes, that maximum efficiencies are generated with pitch and heave motions cycles out of phase by 90° . Furthermore, the deforming vortex wake is non linear as one would expect (Kevin D. Jones, 1999).

* Interestingly Professor DeLaurier in the summer of his retiring year saw the flight of his designed ornithopter; "flapper" used as a design project over the past 20 years by 50-60 undergraduate and postgraduate students for the application of their theoretical classes and flew in self sustained flight for 14 seconds on the 8th of July 2006 at an average speed of 88 kmph in Downsview park Toronto.

More recently, testing has begun on developing physical models, highlighting the tendency of the Hess & Smith panel method code to over predict measured values at low AoA and is suspected to be due to low boundary layer separation effects at those angles and mechanical losses in the experiment. It was also found, that due to the panel method being essentially a linear method, it predicts a linear rise in coefficient of power. This causes it to under predicted measured values at higher AoA, unable to predict flow separation (Kevin D. Jones, 1999). It is suspected that this is due to hysteresis effects, dynamic stall and DSV effects, previously discussed in section 4.5.

Reduced frequencies in the range of $0.5 < k < 0.8$, with non dimensional heave velocities in the range of $0.15 < h_0 k < 0.25$ were tested. It became apparent that maximum power occurs, as the reduced frequency tends to zero ($k \rightarrow 0$); thus the heave amplitude tending to infinity ($h_0 \rightarrow \infty$). However, large heave amplitudes have a negative effect on the device efficiency and wake structure, as seen earlier in propulsion testing. Modelling using a 15° AoA found an efficiency of 0.26 a power coefficient of 0.58 at a reduce frequency of 1.6 and heave amplitude of 0.95 (Kevin D. Jones, 1999, K.D. Jones, 2003).

Feasibility studies into oscillating hydrofoil devices have called for better non-forced models (i.e. driven by external locomotion), allowing effective simulation and modelling of free flow energy extraction (Lindsey, 2002). Their results compared favourably to existing models with predefined equations of motion. In Chapter 8 a CFD method incorporating a UDF to integrate the surface forces experienced on the hydrofoil to naturally drive the foil motion is outlined.

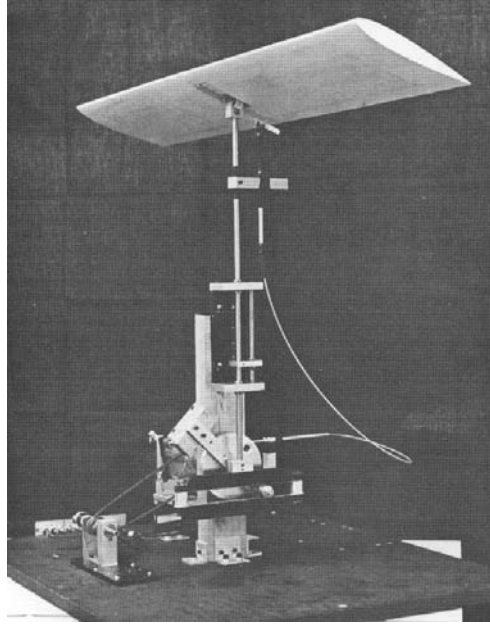


Figure 6.1 McKinney & Delaurier Model

6.1 Stingray – a review of Engineering Business’s Device

Stingray is a 150kW prototype device that was developed by Engineering Business Ltd. with governmental funding from the DTI. It was developed to prove the robustness and economic feasibility of oscillating hydrofoil technology for tidal energy extraction. They accomplished this objective quite successfully in two testing seasons in the summers of 2002 and 2003 in the Shetland Islands off the Northern Scottish Coast line; the test site near Yell Sound. Their full technical reports are published online* (The.Engineering.Business, 2003, Department.of.Trade.and.Industry, 2005)

The economic feasibility is not of concern in this study, but, it is noted that due to machine complexity and inability to take advantage of economies of scale in production, the device prototype and subsequent unit cost of energy was inflated, thus causing the suspension of the project. It is the opinion of the author that huge reductions in unit energy cost to the consumer would be reaped by design simplification and optimisation outlined in Chapter 8. Analysis of stingray’s test data has enabled EB Ltd. to design a second generation 500kW mechanical (rather than hydraulic) model which was initially to be built and

* <http://www.engb.com>

tested at a later date (post 2005). The current public status of the project is that it has been suspended.

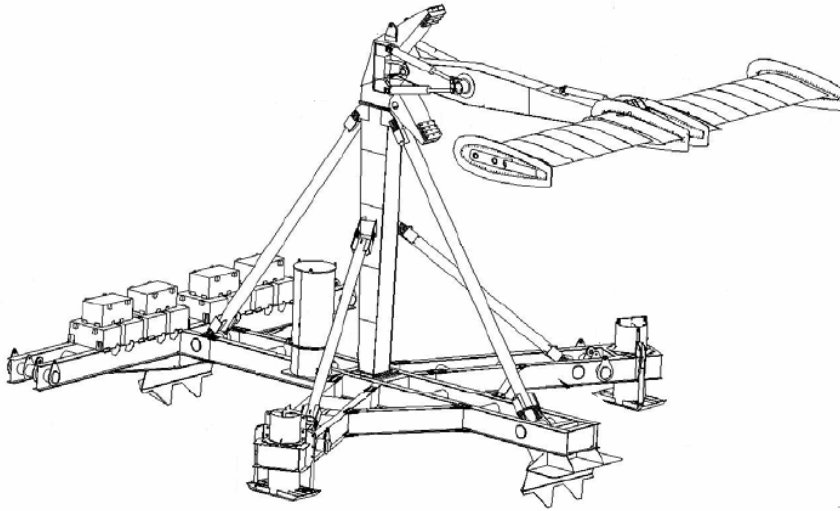


Figure 6.2 Stingray Final Assembly © 2003 Engineering Business

6.1.1 Introduction

It has been shown that oscillating hydrofoil technology varies considerably in comparison to rotary MEC devices. Hydrodynamic forces due to flow stream over the hydrofoil induce a pressure gradient across the hydrofoil chord and generate lift and drag forces in a single plane of motion. These forces can be controlled and manipulated to efficiently harness the stream energy and generate useful power- mechanical, pneumatic, hydraulic or electrical.

In the Stingray design, the incident forces are captured by hydraulic rams by means of a structural arm which creates a high torque reacted about the coincidental centre of rotation about the ram's centre of oscillation. The Rams pump high pressure hydraulic fluid to a variable speed hydraulic motor, which in turn drives the device generator and outputs electrical power. It should be realised that each of these power phase changes have maximum efficiencies of approximately 0.9. This means that immediately, just in transforming power through the drive-train, at least 20-25% of the original energy captured is lost.

6.1.2 Principles of operation

The main principle of operation is quite eloquent. Given a specific AoA, the foil will want to rise or fall in an oscillating motion at varying rates, which are dependant on previously discussed hydrodynamic and control phenomena. One of

the downfalls in Stingrays complexity is in the use of an oscillating arm in the power take off system. This causes a sinusoidal decay in power take off as the only useful force in power generation is that tangential to the arm arc of oscillation, being generated by the vertical lift forces. Thus the range of oscillation was limited to $\pm 35^\circ$ to limit this loss. Secondly, due to this sinusoidal variation, the AoA must be continually actuated, which increases device complexity, as it is much simpler to hold the AoA at a steady angle.

The lift force that drives the foil motion is dependant on the AoA, free stream velocity, the foil surface area and smoothness, the foil aspect ratio, and the foil profile characteristics; namely the foils lift and drag coefficients. Lift is defined as;

$$L = \frac{1}{2} \rho S C_l U_\infty^2 \quad (5.4)$$

Where, ρ is the flow density, S the foil planer area, C_l the empirical coefficient of lift, and U_∞ is the free stream velocity. Unlike conventional rotary devices, Stingray does not reach a constant speed. Due to the non linear lift and loss of momentum in its oscillation cycle extremities, the device is constantly in a state of dynamic control actuation. The complex nature of the device, as will be seen, makes this no easy task.

Stingray's foils oscillate in the vertical plane which further complicates the power cycle by inducing cyclic loading by the arm structure and GRP hydrofoils combined weight and buoyancy.

Depending on the phase of the power cycle, the foil induced drag can have beneficial effects aiding acceleration from extremities of oscillation, but it also adds a varying force changing every 90° phase during the power cycle. It is postulated that increasing the hydrofoil AoA at maximum arm oscillation angles, induces increased levels of drag. These would be useful to accelerate the foil and regenerate momentum lost in changing direction. However, this would add another degree of complexity to the device cycle and is more so an *after the fact thought* rather than an inclusive design idea.

6.1.3 Testing Objectives

The phase three testing objectives were defined to encourage improvement in areas where the device had previously been identified as performing below expected or desired values. Most importantly the mean power output was to be increased by control optimisation and automation based on data logging at 10Hz (10 data packets logged every second). This was to be achieved by reducing cycle times over particular tidal flow ranges.

Further identification and modelling of optimising sufficient instantaneous percentage power extraction needed to be balanced with lift forces, allowing the device to efficiently accelerate the foil and cycle speeds.

The effect of the introduction of a variable speed hydraulic motor was also to be quantified in regards to the power cycle, cycle time, and power quality output.

6.1.4 Control Systems

Hydrofoil control was mainly regulated by predefined programme logic control (PLC). The PLC digitally samples the device parameters at a frequency of 15Hz. Due to the complexity of the design, there are a considerable number of system variables to be sampled, logged, analysed and output, determining the control output signal to actuate the foil by means of a hydraulic ram. The main variables are as follows:

- *Angle of attack*
- *Arm relative angle*
- *Flow velocity*
- *Cycle phase*
- *System pressure*
- *Actuator pressure*
- *Accumulator pressure*

A high sample rate is required due to the devices AoA sensitivity to flutter. It is seen in Figure 6.3 that the hydraulic system is unable to react quickly enough to the PLC output. This is due to the viscous lag inherent within hydraulic systems and difficulties in combining varying pressure inputs (Department of Trade and Industry, 2003).

There is considerable scatter seen in the AoA profile. In an effort to overcome power actuation effects high pressure accumulators were added to the hydraulic circuit. This increased system pressure, but the result is even poorer control (See Figure 6.4). This highlights the lag between control and actuation further. The device's ability to hold the hydrofoil stably at its optimum AoA is critical to efficient and powerful operation. Otherwise, unsteady lift forces are generated having an accumulative degenerative effect, which makes it increasingly difficult to control the device. Further increased drag is generated and the device will be severely hindered, which increases the cycle time and decreases the overall power output.

The crux of the device lies in actuating the foil to change its AoA from positive to negative (and vice versa) reversing the oscillation direction. In doing this, the control and actuation system needs to overcome the device inertia, and the foil pitching moment. Considering the size of the device, these are formidable forces. (*Stingrays foil chord is approximately 3 metres with a total span of 15.1 metres*). High pressure accumulators firing to rapidly actuate the hydrofoil AoA spends 15-20% of the cyclic captured power. If the accumulators are not used the device cycle time suffers greatly. (See Figure 6.4)

It is well known in submerged hydrofoil craft that hydraulic control systems are sluggish due to the orbital motion of the waves over which the craft is in motion (Sang-Hyun Kim, 2004). It is postulated that DSV would have the same effect on Stingray. It is seen in Figure 6.5 that increased levels of lift (red dotted scatter) were measured on the device, rather than steady state theory calculated in the device mathematical model. This indicates the presence of DSV and inconsistency in the design mathematical modelling, and presumably control logic employed. It was also found during testing that, when stall condition occurred, the device is not self-correcting nor self-starting and considerable effort is required to restart the device.

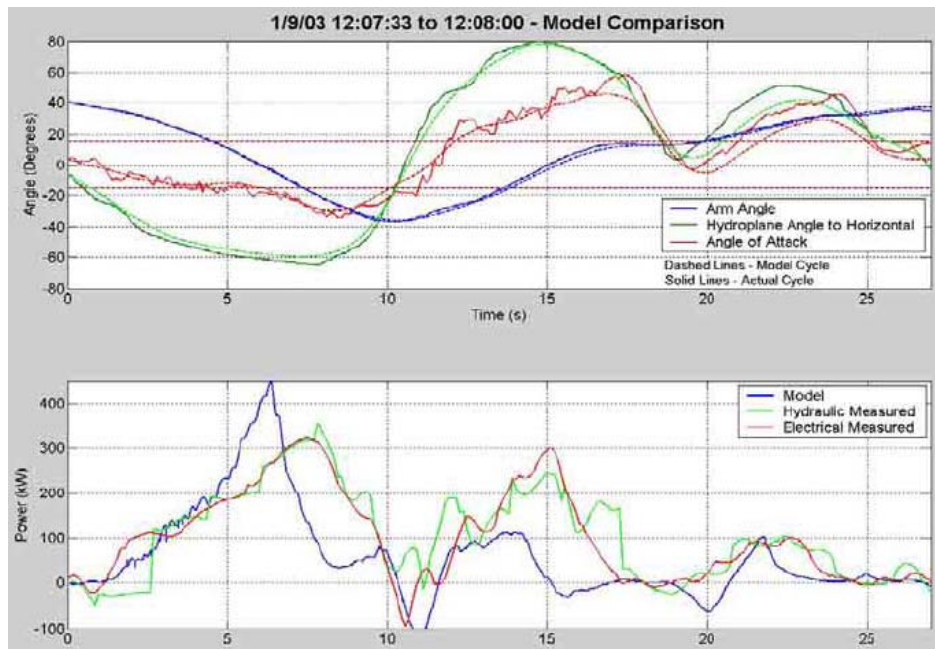


Figure 6.3 Stingray Power Cycle Comparison © Engineering Business Ltd. 2005

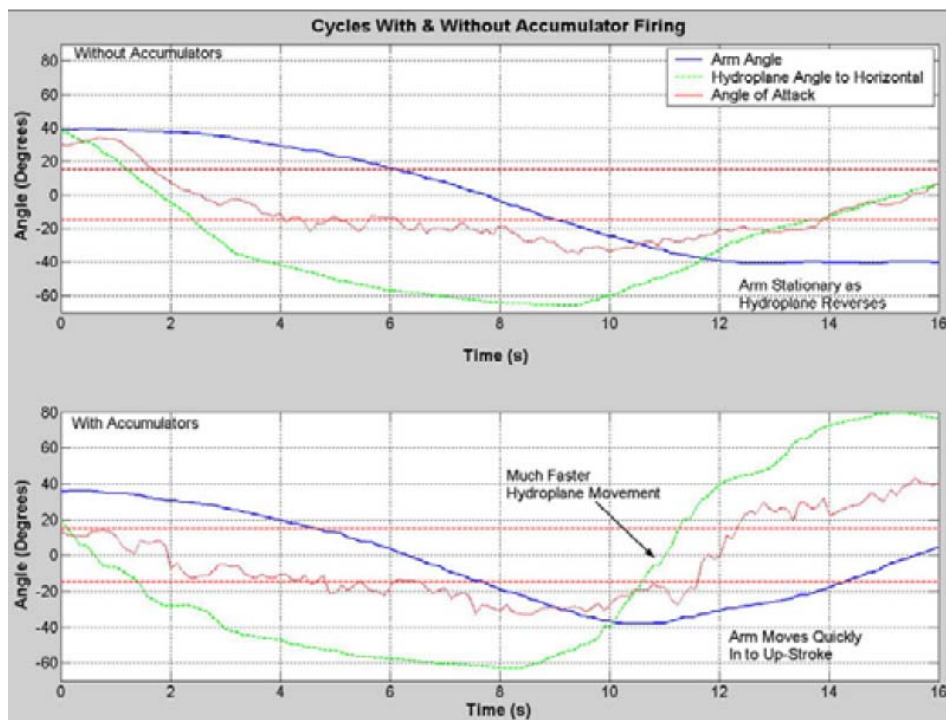


Figure 6.4 Power cycle comparison with Accumulator firing

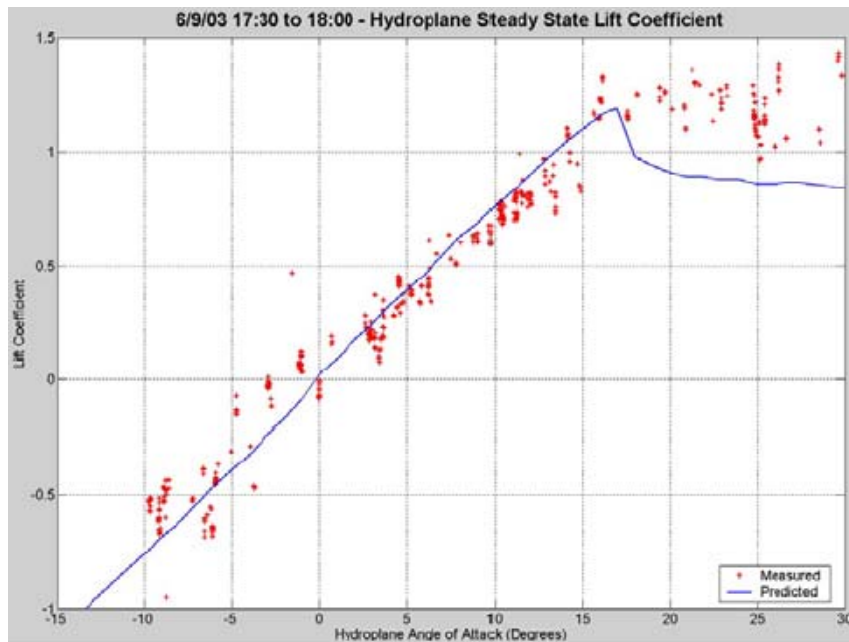


Figure 6.5 Stingray Lift Generation © Engineering Business Ltd. 2005

6.1.5 Power take off

As the lift and resultant power cycle is sinusoidal, monitoring and optimisation of power take off is required. In this vain, power take off is not constant, nor sinusoidal, but is tuned to extract a varying percentage of the calculated power depending on flow conditions and cycle phase. None of the available power is extracted at the beginning of a cycle to allow device acceleration. When the device has reached sufficient velocity, subsequent power output is increasingly extracted. When 100% is taken, the device oscillation reverses to the opposite direction. This allows the device average speed to be heightened and the cycle time to be minimised. The output power quality, however, is impulsive and requires smoothing either electronically or via hydraulic or mechanical means.

6.1.6 Summary

It is seen that the Stingray provides much invaluable test data and practical knowledge and experience. There is, however, much device complexity, system variability, and debugging needed before optimum generation is achieved.

Efficient AoA control is critical to reduce cycle time and generate optimal power outputs. The power loss, due to accumulator firing, could be minimised by increasing the hydrofoil AR and decreasing the pitching moment, while

maintaining overall lift. This would require increased flexural rigidity and mass of the foil steel spine.

Furthermore, the device generation could be simplified and increase the power-take off system efficiency by utilising PM's in an onboard direct drive generator. Increased understanding of the hydrodynamics about the hydrofoil is required, in aiding the development of a better control algorithm to efficiently control all the device parameters. Power cycle mathematical modelling, and comparison with the developed passive design is outlined in Chapter 8.

Chapter 7 Environmental Impacts

In this section concepts and development of present models into open channel tidal flow and environmental issues which need to be addressed are presented.

7.1 Open channel flow - Tidal Power

Analysis based upon open channel flow theory demonstrates that energy extraction in a simple channel driven by static head differences can have a significant upstream and downstream effect. This suggests that the environmental impact of energy extraction is not necessarily restricted to the immediate area around the extraction site. It also suggests that there is potential for the process of energy extraction to either diminish or even enhance the available resource at a particular site. Further research is required and is ongoing in this area. The limits to exploitation are shown to be inexact. A useful approximate guideline for resource analysis is that 10% of the raw energy flux, produced by the tide, can be extracted without causing undue modification to the flow characteristics. (Ian G. Bryden, 2005)

Tidal flow for the most part is simply driven by the interaction with oceans and the moon's magnetic pull, causing tidal height ranges. The pressure head, as a result of the height range, is the driving force. Model adjustments for varying bathymetry & roughness using manning coefficients can be used to generate a more accurate tidal model, rather than the idealised sinusoidal model assumptions.

Wake effects of wind turbines are well understood and aid in placement when developing wind farms. Tidal flows, however, differ from atmospheric flows in that their energy flux is constricted by the surrounding sea bed, ocean surface and potentially the bathymetry in which it is placed. This leads to differing flow patterns and potentially detrimental effects on those constricting areas.

Device design should take into account the localised flow phenomenon that the device will experience to minimise impact of those effects and maximise the

extraction efficiencies (I.G. Bryden, 2004). See (Hamilton et al., 2006) for a detailed tidal model outline & site selection criterion. Tidal atlases have been developed in Ireland & the UK identifying ideal site criterion and potential sites Figure 7.1.

- **Channels** or constrictions between islands
 - Focuses the tidal energy in a geological venturi tube
- **Headlands** in the path of moderate flows
 - *Best when the headlands are large and do not protrude too sharply into the flow, minimising macroscopic turbulence & vorticity*
- **Estuaries** or other resonant water volumes
- **Narrow entrances** to enclosed tidal lakes
 - *High currents but only through a small channel cross section area*

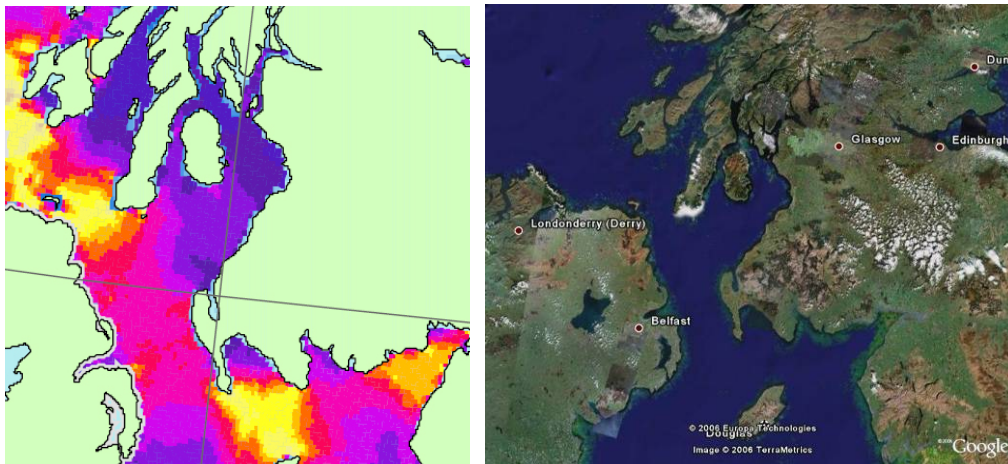


Figure 7.1 Irish Sea - North Channel Tidal Energy ©Google 2006 ©Dti 2002

However, due to computational limitations and relatively coarse grid calculations, excellent sites can be omitted. Tidal modelling has been, so far, initialised utilising surface flow data, while considerable depthwise decrease in flow velocities by the 7th power law is experienced. The empirical manning equation is useful in taking into account site specific bathymetry and surface roughness in generating an accurate site velocity profile.

Some potential sites are also illustrated in Appendix B - Alternative Tidal Generation Sites, which have been unrealised until more recent modelling and some of which continue to be ignored. Conversation with local weathered

mariners, fishermen, surfers and divers often highlight local fables of high energy sites.

7.2 Significant Impact Factor

The environmental engineering and sustainable energy group of Robert Gordon's University (RGU) has led the way under the auspices of Professor Ian Bryden* in understanding the environmental impact of tidal energy extraction. They have identified, prioritised and begun quantifying these effects and generating a guideline extraction system; The Significant Impact Factor (SIF). The summary of potential impacts are outlined below:

1. Disturbance to the seabed and benthic ecology during installation, operation and decommissioning of a tidal energy capture device.
2. Auditory and visual disturbance to seabirds, pinnipeds and cetaceans
3. Potential changes in tidal & wave dynamics in the device locality, due to vortices and blockage effects
4. Seabed disturbance due to sediment transport in disturbed flow
5. Changes in water quality chemically and turbidity
6. Potential risk of collision with diving birds and marine life.

(Bryden, 2002)

Further study into the area is ongoing. It should be noted that water turbidity, EM noise, auditory noise and sediment transport are of major concern. All of these will be further addressed in Chapter 8.

In designing tidal energy extraction devices, the blockage effects and the decrease in tidal velocity due to the energy extraction must be taken into account. If they are ignored the device will not be running at optimum efficiency and giving falsely augmented coefficients of power under the illusion of higher local flow velocities than those actually present in physicality. Dynamic feedback to develop accurate measurements and modelling of actual local and farfield flow velocities is suggested (Scott J. Couch, 2004, Bound, 2003). The blockage of marine current turbines is found to be considerable (Scott J. Couch, 2004). This indicates that potentially underwater windmills are not the ideal tidal energy extraction

* Recently (Summer 2006) moved to the University of Edinburgh as part of the Sustainable Energy Group

device to be developed as it is not only energy extraction but large blockage effects and wake turbidity that cause environmental problems. *A streamlined device with minimal drag and wake turbidity would address this problem.*

7.3 Influence of climate change on marine energy

As outlined in Chapter 2, tidal energy has a major part to play in offsetting & decreasing carbon emissions and in developing a long term renewable and sustainable energy infrastructure. This system is inherently dependant on natural varying power sources. These natural resources have recently been reported to be changing due to global warming, or climate change depending on ones point of view. Increased incoming solar thermal radiation, heightened average temperatures, melting ice caps and redirection of prevailing ocean currents are all contributing to the general augmentation of wave height, wind speeds and tidal ranges. Naively, from a renewable energy developer's point of view, this would portray a picture of more energy to be captured, and more opportunity. This is not an ethical, nor a sustainable point of view. The Earth's energy balance is a precarious one, which is currently destabilising.

Charles Darwin said, "It is neither the strongest of the species that survive, nor the most intelligent. It is the one that is the most adaptable to change." Society at large have ignored the warnings during the 1960's and '70's of peak oil, limits to growth and our tendency towards a mechanistic anthropocentric fossil fueled society. We are now reaping the effects of those seeds we sowed.

Renewable energy systems can be used in an effort with other alternative management contingencies to control and help correct this destabilisation.

Increased wave heights of 2% per year, have been suggested, that indicate a 30-50% increase over the next 3 decades. Recent reports have indicated that UK wind speeds have risen between 15-20% over the past 40 years (Gareth P. Harrison, 2004). There are calls for further in depth research to quantify the effect that global warming will have on renewable energy sources. Quite possibly, tidal regimes will alter with heightened tidal ranges, and possibly generating higher flow rates. Harmonic tidal flow anomalies could also be generated, to the detriment of tidal farm schemes.

Chapter 8 SRUTH SAOIRSE: Concept Design

In the observation of natural hydrodynamic phenomena, an alternative passive approach is decided upon. An approach of flow & vortex manipulation, rather than forced PLC hydraulic control systems, is utilised to optimise and maintain autonomous start-up and self control of a tidal energy capture device. As a result, the conceptual device illustrated below, “**SRUTH SAOIRSE***” is conceived (Figure 8.1).

There is no control mechanism in the traditional sense used in controlling the hydrofoil AoA. The NACA 0015 hydrofoil is restricted to pitching between its maximum and minimum AoA by means of an internal rib attached to the foils axel, rotating about its quarter chord length, the centre of hydrodynamic pressure and pitching moment. (See Figure 8.2) Unsteady flow effects will cause the foil to flip from either positive or negative AoA; which way is initially unimportant. The subsequent lateral lift will cause EM shear friction on the linear generator to which the foil is attached, inducing an electrical current. The modular design allows multiple device arrays to be deployed, wired out of phase, ensuring correct operation, maximum power output and higher multi-phase power and power quality (See Figure 8.4 for visual aid).

The novel aspect of the device is in manipulating the flow field and reversing the pitching moment the foil experiences. The control mechanism, entailing a spoiler and a butterfly valve of sorts utilises drag and venturi effects, sets up a low pressure field on the leading surface of the foil, reducing the driving lift. As the foil motions towards the control wing, opposite flow through the butterfly valve creates a high pressure field in the lagging surface of the foil, reversing the pitching moment and consequently the lift direction, and foil heave direction. This motion is controlled by the flow, so that is, it is autonomously controlled with the instantaneous flow input. During excessive tidal flows the butterfly valve will close due to the leading surface pressure overcoming the normally open pneumatic rams holding the valve in position. The resulting effect

* Sruth Saoirse – Translates from Irish to Free Stream. Pronounced “*Sh-ruh Seer-sha*”

reduces the inflow velocity and slows the power cycle. Similarly, if the position control hydrofoil experiences excessive lift, its normally open pneumatic ram will shorten, causing the foil to pitch and stall. This action allows the device to drop out of high velocity flow profile of its own accord. The ram pressures regulating this action must be tuned to individual device size and the local flow velocities which the device experiences. These effects *turn off* the device thus protecting it from excessive forces and potential damage. This therefore increases the device life term and reduces its life cycle cost in maintenance and repairs.

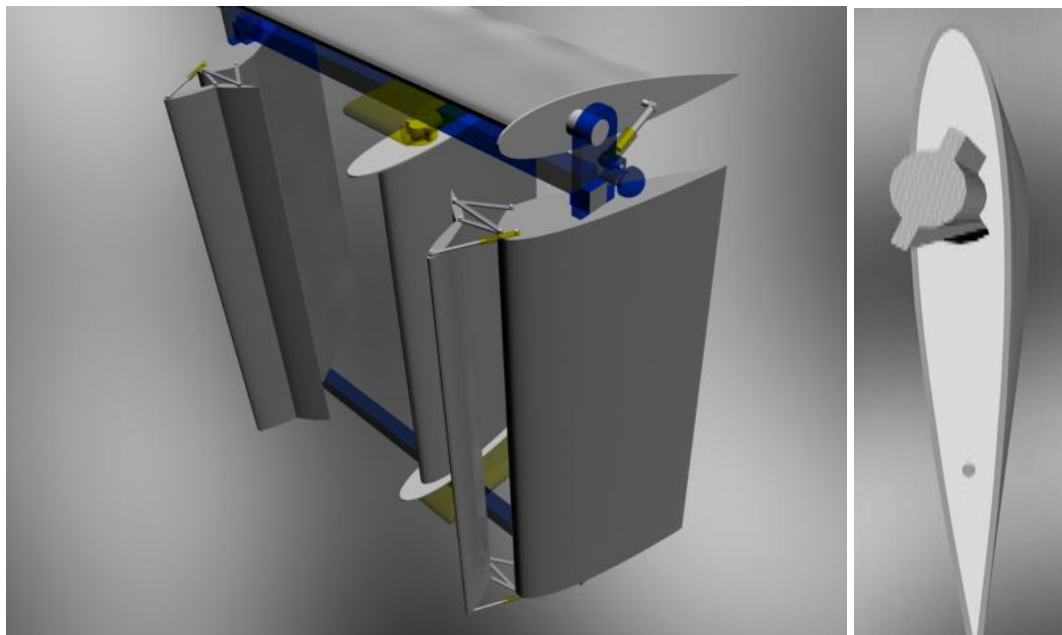


Figure 8.1 Sruth Saoirse Modular Design

Figure 8.2 AoA Axial Restrictor

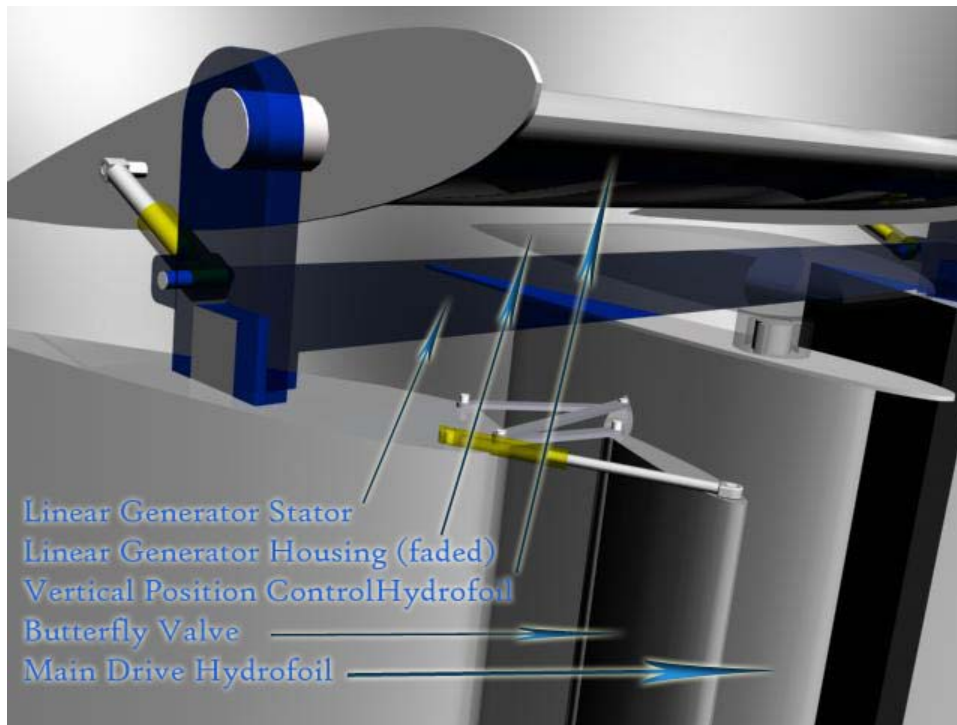


Figure 8.3 Position and Butterfly Pneumatic Ram Control

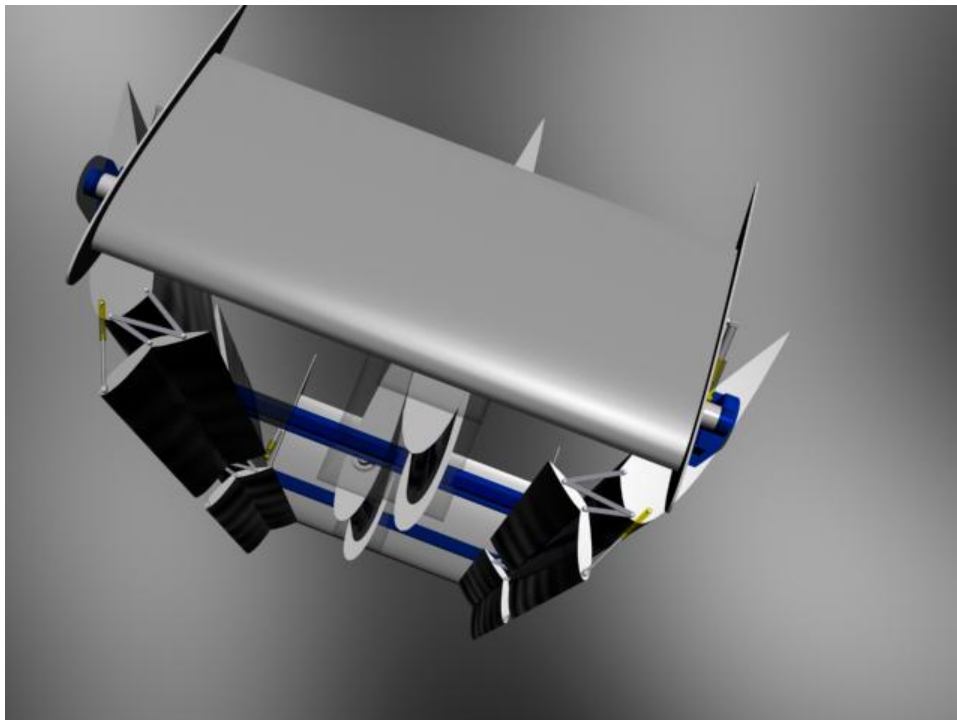


Figure 8.4 Sruth Saoirse Array Plan View

8.1 Design Outline & Objectives

The main objective to be accomplished is to efficiently generate more power while having minimal impact to the environment. This is accomplished in a number of ways as outlined below.

The cycle time is an easily visualised measure of the power cycle improvement. As the power output is not just dependant on the lift force reacted upon the hydrofoil, but also the rate at which the foil heaves, imparting its energy to the linear generator. As discussed in section 6.1, huge efforts were made in decreasing cycle time which resulted in Stingrays increased power losses and inefficiency.

It is apparent that developing a passive control system using environmental energy rather than captured energy enables a tidal MEC device to firstly save up to 20% on actuation cyclic power cost and, in doing so, this power is further added to the power output, increasing device efficiency. Further design simplification and passive control enables the device to have autonomous start-up & recovery from stall conditions. In prototype testing, reinstating power cycle operation and generation took considerable time and effort.

It is apparent that energy lost through drive train and transmission accounts for huge loss and inefficiency in any device power cycle. The Sruth Saoirse concept uses a direct drive linear generator (outlined in section 5.3) to overcome these multiphase energy conversion inefficiencies.

8.1.1 Design Evolution

The concept evolved from hydrofoil fundamentals, existing prototypes and biomimetic observations in an effort to create an idealised flow environment while holding to the belief that a simple design is often the best design. The following ideas were sketched and modelled during the process, but were ruled out due to varying mechanical and hydrodynamic complexities.

- i. The instantaneous relative angle of attack to the boom crank angle is simply calculable for an oscillating foil generating torque by means of a boom (See Figure 6.2). Its AoA profile can be simply calculated and can be mechanically controlled by means of a CAM mounted on the boom rotating over the power cycle period. The hydrofoil would need to have

its AoA tensioned by means of a spring or ram, so that it does not separate from the CAM during the power cycle. The number of moving parts, cyclic loading, potential for corrosion, and failure ruled this initial design out

- ii. The secondary design was simplified from the above using a spring and ratchet mechanism. This design provided excellent AoA control and system tension. Unfortunately due to the ratchet mechanism, the device was only useful in one direction of oscillation.
- iii. The third generation design overcame the limitation of the unidirectional ratchet mechanism by use of a hydrofoil section which was symmetrical about its vertical axis. This allowed the ratchet tension to be released at the maximum and minimum range of oscillation and the pitching moment would carry the foil to the opposite AoA. At this point, the ratchet would relock and the device would oscillate in the opposite direction. This device showed promise, but the existence of test data of such hydrofoil profiles has not been found to date. The device still maintained considerable mechanical complexity and potential for failure. Furthermore, at the extremities of oscillation the flipping of the foil would create large drag effects, useful in accelerating the foil in this slow section of its cycle, but detrimental to the environment within the locality of the device.
- iv. The fourth generation design was a combination of the above which incorporated a direct mechanical linkage to control the hydrofoil AoA. This concept used dual foils oscillating at 180° out of phase so that their relative characteristics would be constant. A linkage inspired by that used in old steam train locomotion was sketched maintaining relative AoA. Each foil pulled on each other at the extremities of oscillating, pitching the foils and reversing the cycle. This device was again overly complex and hydrodynamically ridiculous, as the drag caused by the linkages would be prohibitive. However it did inspire the device concept presented here, by simplifying the structure, finding cyclic constants that can be designed for, and applying the correct relative external forces at the correct instant in the device power cycle (See section 8.3).

8.2 Analysis Methodologies & Comparison

Prior to understanding the device power cycle the forces driving the cycle must first be quantified. This is outlined below through increasing degrees of accuracy, complexity, and completeness. First order analysis uses steady state empirical data (Sheldahl et al., 1981) to give an indication of power generation and the effects of differing cycle setups, particularly square wave velocity profiles as opposed to harmonic wave forms. Stingray’s operation is compared to that of the proposed Sruth Saoirse device.

8.2.1 Quazi-Static model

Lift generation is proportional to the square of the free stream velocity and the foil AoA as seen in equation(5.4). Empirical test data of symmetrical NACA 00 series hydrofoil profiles is used to quantify lift generation in line with linear theory and calculate first order power estimates (See Figure 8.5). A NACA 0015 hydrofoil with chord length of 3m a span of 7m (21m^2 planer area) fixed at an optimum angle of attack of 15° (according to linear theory) in a free stream of $3.5\text{m}\cdot\text{s}^{-1}$ experiences a lift force of 180kN.

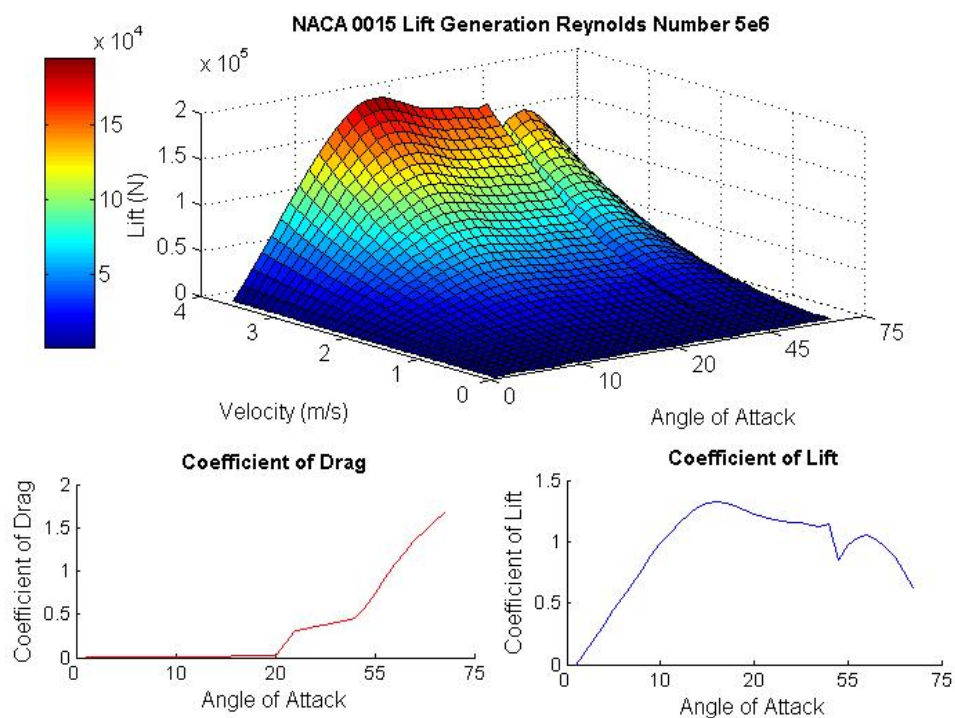


Figure 8.5 Empirical Steady State Lift Generation

These lift forces induced, however, are dependant on the foil orientation to the incident flow. Therefore varying mechanical cycles and foil control have an effect on the lift forces. As seen in Figure 8.6, the previously described Stingray AoA control cycle varies harmonically, therefore so too does its lift generation. The Sruth Saoirse concept, however, maintains an optimum AoA for longer periods during its cycle, as it holds its AoA constant rather than when pitching and changing cycle directions. It can be initially seen that there is a considerable difference in the mean lift forces experienced during the device cycles, with Sruth Saoirse maintaining on average 55% higher cyclic lift force. Depending on the period of time spent pitching AoA, this effect can be increased or decreased. *It should be noted at this stage that this difference in lift is directly proportional to power output.*

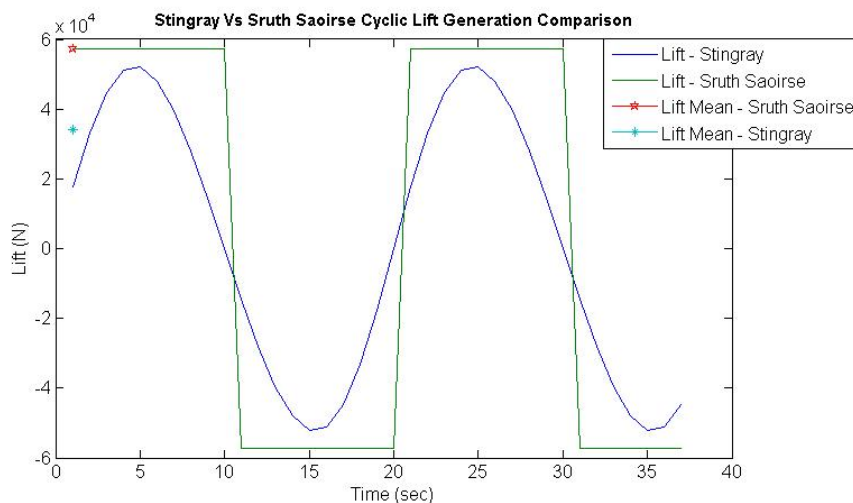


Figure 8.6 Cyclic Lift Generation Comparison for flow at 2m.s^{-1}

The analysis is taken a step further in modelling the control system used in Sruth Saoirse, initially using a steady state, inviscid CFD model to calculate flow conditions. Unsteady flow conditions require constant parameterisation of lift, drag, pressure, and pitching moment coefficients and their cyclic variations to correctly model device power cycle; hence CFD is used in this effort.

8.2.2 CFD Steady-State First Order Modelling

All CFD models developed use a design velocity of 2m.s^{-1} . Sites exist with increased flow velocities of up to 3.5m.s^{-1} but on average 2m.s^{-1} is a more realistic

expected velocity. For a NACA 0015 hydrofoil, with chord length of 3m, this velocity corresponds to a Reynolds number in the range of 5×10^6 . The model is further geometrically rescaled for a foil chord of unit length (1 metre) of which other design parameters and calculations can be scaled. A simulated depth of 15 metres in sea water of density 1025kg.m^{-3} is used as the ambient pressure within the free stream which flows from left to right on all illustrations below.

It is seen in Figure 8.7 and Figure 8.8 that initially the control mechanism will create the desired pressure and velocity flow conditions. A low pressure field downstream from the butterfly valve is seen. This is utilised to balance and remove the driving high pressure on the leading* surface of the hydrofoil, slowing the hydrofoil as it reaches its extremity of heave, preventing collision and damage to the control wing and the hydrofoil.

Secondly, within the flow stream, between the butterfly valve and the control wing, a high velocity flow of up to 200% of the free steam is observed. During the cycle as the hydrofoil heaves into position, it will block this high velocity flow. This in turn causes a high pressure to react upon the hydrofoil lagging surface, causing it to rapidly pitch. This is illustrated in greater detail in section 8.2.3.

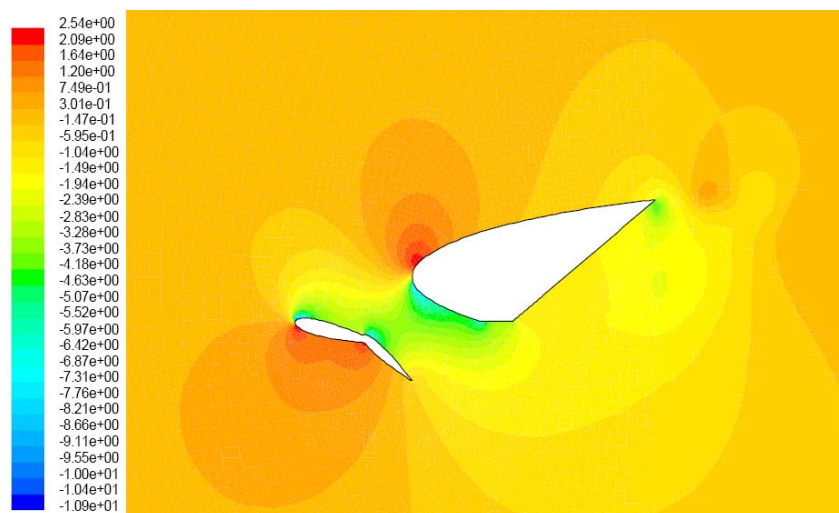


Figure 8.7 Control Pressure Distribution [Pascal]

* It should be noted that throughout analysis, the terms, *leading* and *lagging*, refer to the driving high pressure experienced upon the hydrofoil surface, and not the direction of motion

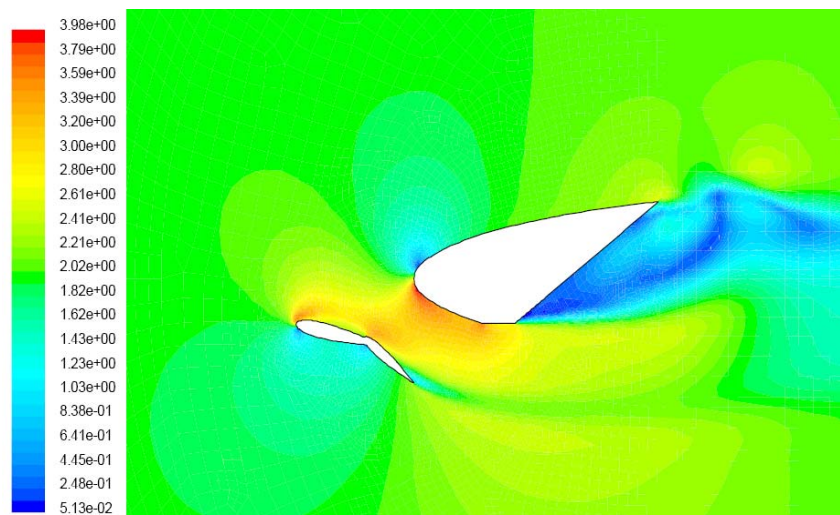


Figure 8.8 Control Velocity Distribution [m.s⁻¹]

8.2.3 CFD Unsteady RANS* Model

RANS is the new standard turbulence model in fluent which utilises Reynolds stresses with the Navier-Stokes equations to compute transient turbulent effects on a model[†]. The RANS model has higher accuracy than panel methods. Assumptions of inviscid, irrotational flow and utilising the Kutta condition are not required to complete the model to convergence.

Alternative to the previous steady state model, in the RANS model, the whole device system is modelled (See Figure 8.9 & Figure 8.10). Viscous effects allowing boundary layer interaction are taken into account presenting some interesting findings.

The most pertinent effect is the Venturi effect which the dual butterfly valves create; together accelerating the inflow velocity by 30% compared with the free stream. *Remember that the power extractable from a tidal stream is proportional to the cube of the velocity (Equation (4.13) See Figure 8.9).* This translates to a 69% increase in lift upon the hydrofoil. As the model is only conducted in 2D thus far, the venturi effects of the vertical control hydrofoil have not been taken into account. It can be assumed that when the control hydrofoil AoA is positive, this will further accelerated the flow onto the main drive hydrofoil.

It is also observed that a low pressure field is created between the low pressure wake of the control wing and the lagging surface of the hydrofoil. This

* Reynolds Averaged Navier-Stokes
[†] [Fluent e-Learning](#)

reduces pressure and viscous resistance on the lagging surface, increasing the pressure gradient. The subsequent lift force accelerates the device further, lowering its cycle time. This effect varies throughout the cycle and at this stage of analysis is not directly quantifiable.

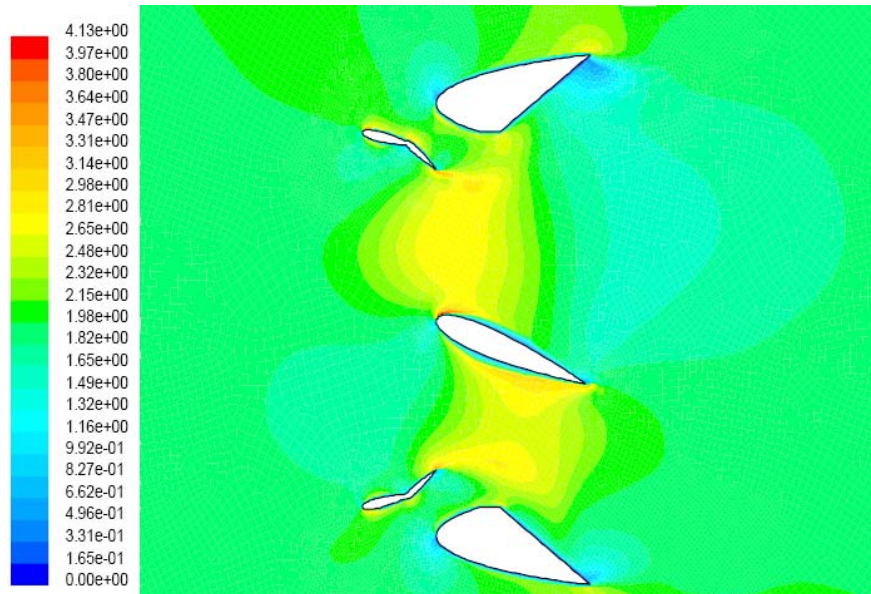


Figure 8.9 Sruth Saoirse Velocity Flow Field [m.s⁻¹]

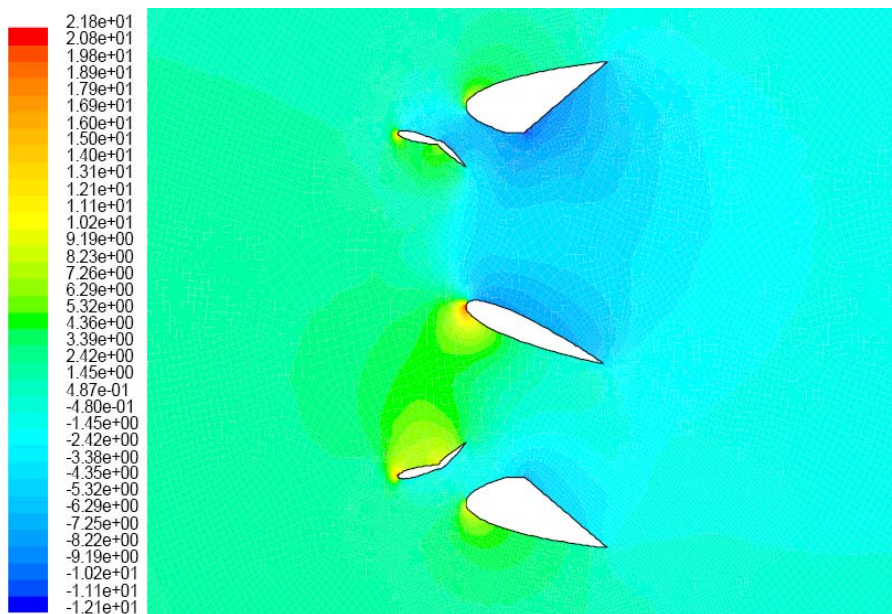


Figure 8.10 Sruth Saoirse Static Pressure [Pascal]

Upon closer inspection, looking at the device in its pitching phases of its cycle, some further interesting effects were discovered and areas of improvement identified (See Figure 8.11 & Figure 8.12).

Initial worries regarding the lack of high pressure reacting to hydrofoil at the low pressure zone downstream of the butterfly valve is shown in Figure 8.13a. However, as the control wing and hydrofoil approach contact, their boundary layers collapse together, restricting the fluid flow between them (Figure 8.13b). This causes a high pressure and the desired pitching moment to build up on the leading surface of the hydrofoil and react upon it to pitch and heave in the opposite direction. Optimisation of the control wing geometry can optimise this flow; this is discussed in section 8.5.1.

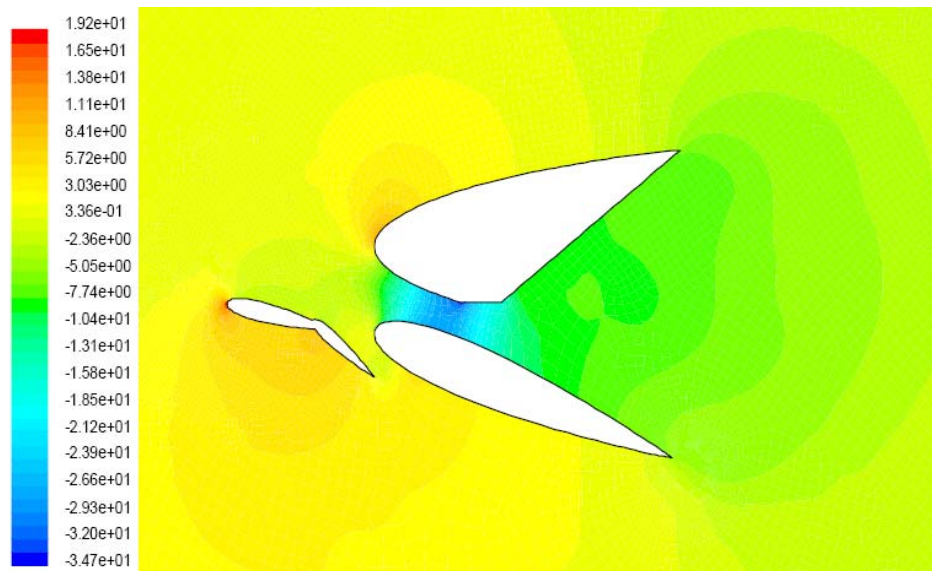


Figure 8.11 Inflow Phase Pressure field

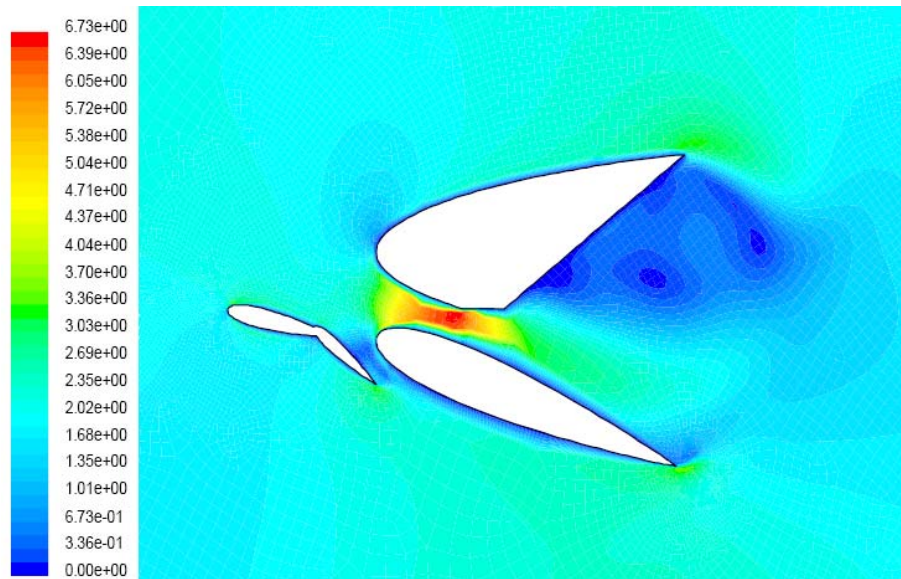


Figure 8.12 Inflow Phase Velocity Field

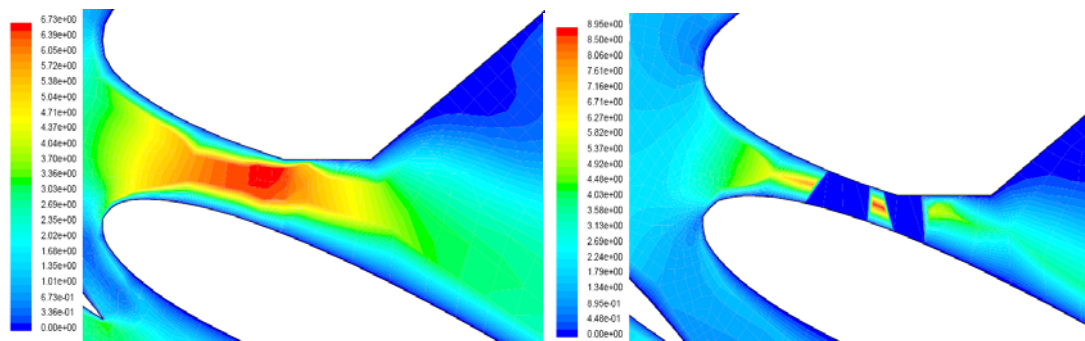


Figure 8.13 Boundary Layer collapse [m.s^{-1}] (a, b respectively)

Later, in the pitching phase of the cycle, beneficial effects take place. The hydrofoil is rapidly thrust clear of the control mechanism due to two effects. *It should be noted that the maximum pressures experienced in this phase are lower than previous operations, but due to effects outlined, lift is greater (See Figure 8.14 & Figure 8.15).* The hydrofoil is now at a negative AoA causing a constriction between it and the control wing. According to the venturi effect, the flow must accelerate through this constriction and subsequently causes a low pressure field posterior to the foil centre of gravity (0.25 of the chord length). Secondly, the low velocity-high pressure flow over the leading edge of the hydrofoil joins the similarly high pressure flow from the butterfly valve trailing edge. This creates a high pressure field upon the leading edge of the hydrofoil.

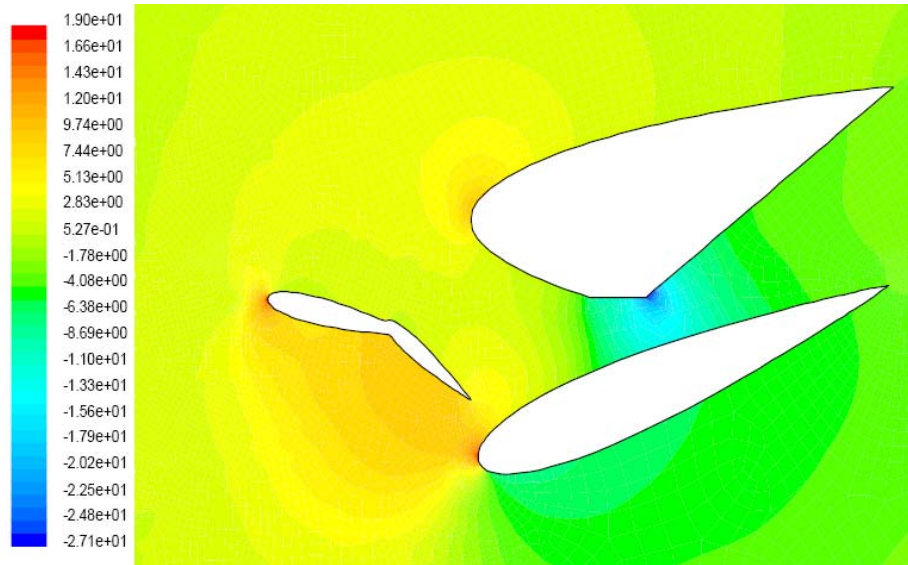


Figure 8.14 Cycle Start Pressure Field [Pascal]

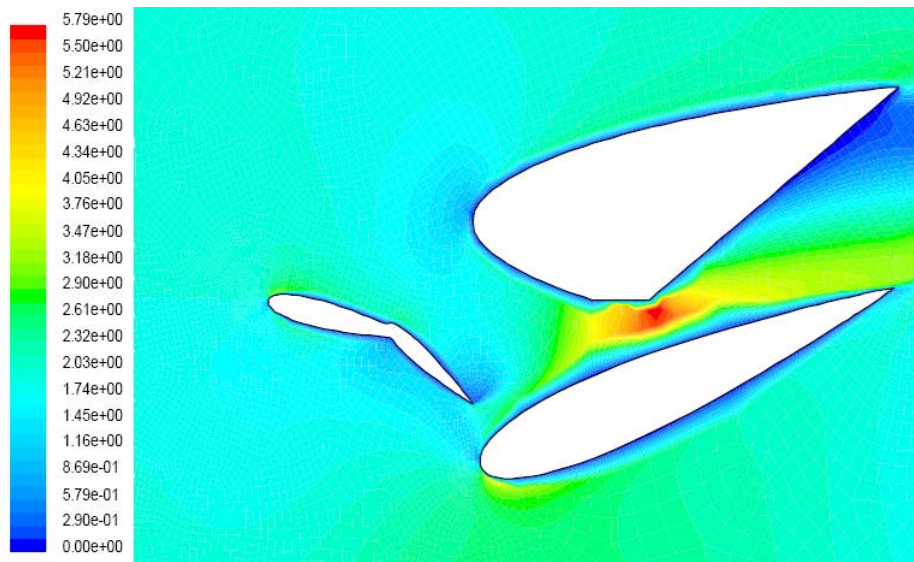


Figure 8.15 Cycle Start Velocity Field [m.s⁻¹]

This sharp pressure gradient along the leading surface of the hydrofoil increases the rate of pitching as it pivots about the hydrofoil centre of gravity (CG). This is highlighted in Figure 8.16 when compared with normal pressure gradients during heave motion in Figure 8.17. The overall effect of this is to increase the C_l to 1.39, rapidly thrusting the hydrofoil into the heave and power generation period of the cycle.

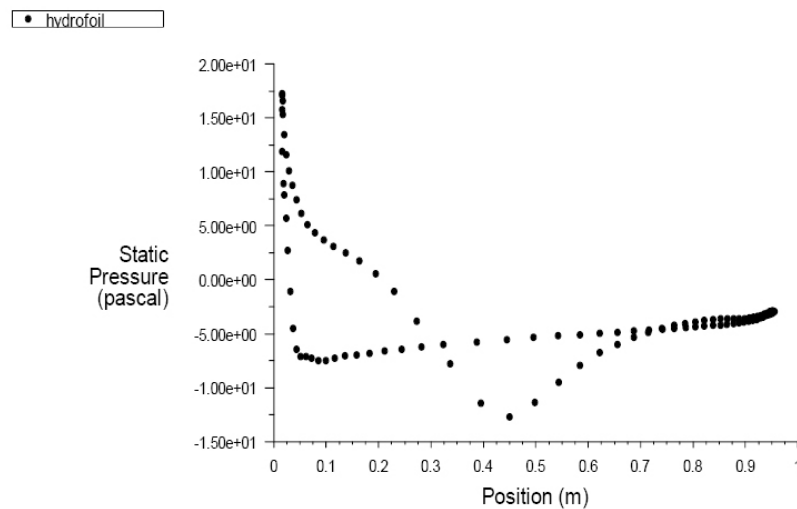


Figure 8.16 Hydrofoil Pressure Distribution during thrust from control area

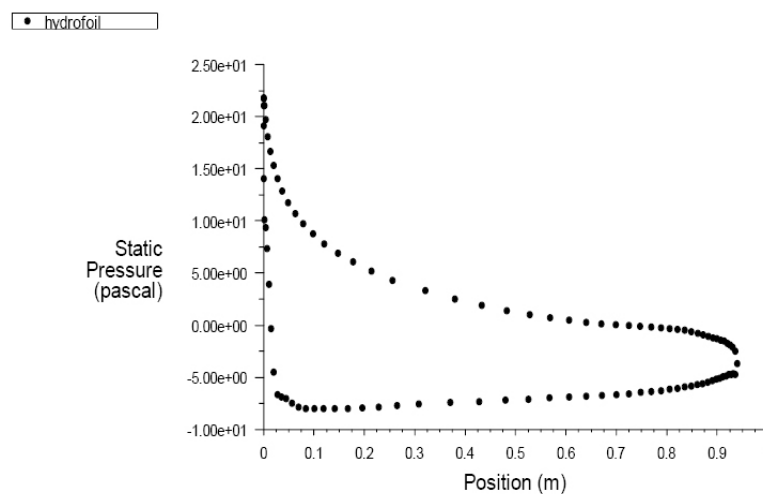


Figure 8.17 Hydrofoil Pressure Distribution during normal heave motion

8.2.4 CFD Dynamic Unsteady RANS* Model

It is possible to incorporate a UDF with the CFD model, to calculate the influence of the pressure on the hydrofoil through an integral path along its surface. This in turn can calculate the free force, velocity, and position of the hydrofoil during its cycle. Developing this code will enable free analysis of energy extraction, rather than using forced predefined motion and inferring the energy that may be extracted. The code is neither required nor part of the remit of this project. The present code is presented in Appendix A - User defined functions. It

* Reynolds Averaged Navier-Stokes

is still required to be debugged and compiled to be used within the model. This code is not currently operational.

8.3 Power cycle modelling

The Betz limit, developed in mind for wind generation relates the maximum extractable, to the conservation of momentum through an energy extraction device. The pressure drop across the device limits the amount of *power* extraction to 0.59 of the total available inflow energy. This limit is suggested as also relevant to tidal energy extraction (William McKinney, 1981). However, it has been previously discussed in studies into SIF's that a lower) limit of 10% of the total site power should not be attempted to be overcome by a tidal farm (*which is also dependant on number of devices within the farm*). This is required as a precautionary measure until more is understood about the environmental effects of energy extraction from a tidal flow. The Sruth Saoirse device is considerably less invasive to the tidal environment and its power cycle is clarified below.

8.3.1 Sruth Saoirse power cycle

At this point it is important that the hydrodynamic effects which the device experiences are understood. These are outlined and clarified below (See Figure 8.18);

1. During the heave motion the hydrofoil AoA is held constant. The device experiences a constant lift force proportional to the square of the velocity and causes a lateral heave motion. The Venturi effect accelerates the inflow velocity field, which in turn further increases the attainable lift the device experiences.
2. As with the dolphin mother and calf, described earlier, drag effects from the butterfly valve and control wing create a low pressure field. This creates suction, pulling the hydrofoil from heave motion to pitching motion. This effect reduces the proportion of the cycle time wasted controlling the pitch of the hydrofoil AoA.
3. Pitching motion, somewhat similar to the Weis-fogh effect, is experienced. Blockage caused by the hydrofoil creates a high pressure build on the hydrofoil surface. The hydrofoil pitches away from the high pressure,

generating LEVs and lift, to alleviate this pressure, which can no longer escape between the hydrofoil and control wing,.

4. The released high pressure blockage, flows through the low pressure field downstream of the butterfly valve, and joins the coinciding high pressure flow at the trailing edge of the butterfly valve. This in turn rapidly thrusts the hydrofoil out of its pitching phase back to venturi effect heave motion.

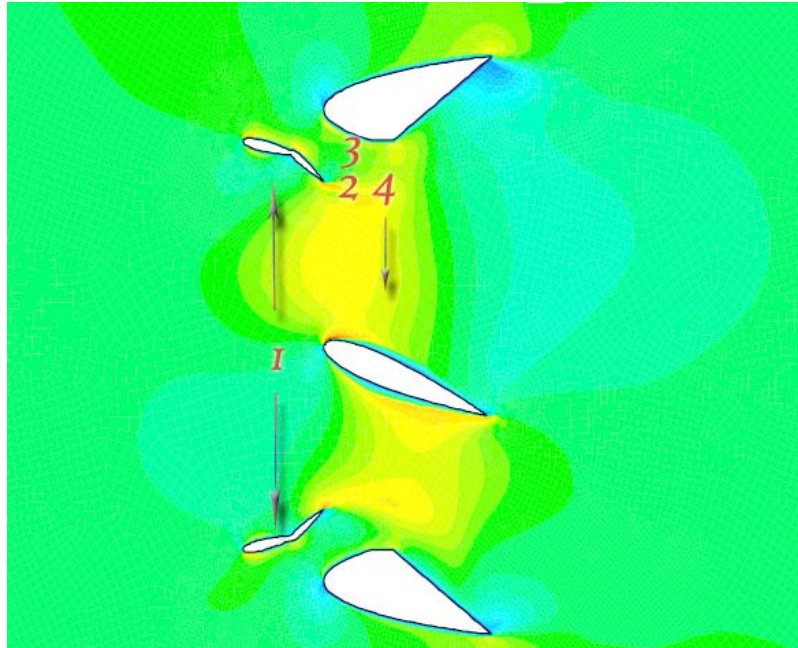


Figure 8.18 Sruth Saoirse Power Cycle

8.3.2 Power take off

Power contained within a tidal stream is directly proportional to the cube of the velocity, so even a slight increase in average velocity can have a large increase in overall device power output (See equation(4.13)).

However, power take off is not so easily defined. The extractable power and the subsequent coefficient of power the device has is dependant on the incident lift forces and how the power cycle manipulates those forces. Newton's second law simply describes the acceleration the hydrofoil will undergo during its cycle.

$$\sum F = ma \quad (8.1)$$

Where, $\sum F$ (N) is the sum of all the incident forces, m is the (hydrofoil) mass (kg) to be moved, and a is the rate of acceleration ($\text{m}\cdot\text{s}^{-2}$).

Due to the lateral heave motion of Sruth Saoirse, the hydrofoil weight does not come into play as a resistive force, only a mass to be moved. As stated previously, *alternative devices with vertical oscillations have cyclic loading due to the varying effects of the weight and buoyancy of their structure and hydrofoil.*

Typically airfoils are constructed using a rib skeleton structure wrapped in a lightweight material. However, the hydrofoil consists of a steel spine axis of rotation/pitching, which, is shrouded with a glass reinforced plastic (GRP) outer shell. Depending on the materials and design chosen, the mass of this structure varies considerably.

So as not to generate inaccurate power estimations, a comparative indication of the power will be presented together with an approximate calculation of actual power. This calculation is based on the NACA 0015 profile used in Sruth Saoirse. It is made of GRP ($\rho \approx 2100 \text{ kg}\cdot\text{m}^{-3}$), with dimensions $c=3\text{m}$, $s=7$, and a high tensile strength steel axel ($\rho \approx 7850\text{kg}\cdot\text{m}^{-3}$). The total estimated mass being 19,050kg (Calister, 2003). Greater structural analysis of the hydrofoil is needed to be carried out to calculate its mass and inertia accurately.

Needless to say, due to a varying number of factors, the mass of the prime mover of Sruth Saoirse is considerably less than that of Stingray. The GRP hydrofoil section is supported via the two rail linear generator stators, which at their core have structural steel supports. Due to their being 2 supports, rather than a central pivot, the hydrofoil does not need to be as flexurally rigid and hence the structural steel spine can afford to loose mass. Secondly, there is no large structural steel boom, which removes a varying resistive tonnage from the power cycle as the boom oscillates with the hydrofoil.

As seen previously in Figure 8.6, the mean cyclic lift generated is 57.257kN and 34.169kN for Sruth Saoirse and Stingray respectively. Ignoring power take-off for the moment, the total heave time accelerating from stationary over a distance of $2h_0\text{m}$ (6m) is 2 seconds. This may seem excessively quick, but this is calculated under no-load conditions. The theoretical power the device can output for half a cycle (i.e. 1 heave motion) is:

$$\bar{P} = \sum F \cdot \bar{V} = 171.75 \text{ kW / heave} \quad (8.2)$$

The total cycle power is less than the heave power due to time lost during pitching. Dynamic modelling is required to calculate this time loss, and hence the total cycle time.

Stingray's rated design power output is 150kW although at a flow of $2\text{m}\cdot\text{s}^{-1}$ best test results showed a hydraulic pressure relating to power collection of 117kW. *It should be noted that Stingray has twice the hydrofoil surface area of Sruth Saoirse* (Department.of.Trade.and.Industry, 2005). As stated previously, the weight of the steel boom and the sinusoidal lift generation are the limiting factors in stingrays design.

This is the point, at which the simplicity of the design becomes apparent. The use of a direct drive PMLSG means that this power can be directly converted to electricity with mechanical-electrical efficiencies of up to 0.87 as seen in section 5.3. As the lift generated is a constant throughout the heave-generation period of the cycle, power take off can be optimised. This is achieved simply by varying the number of coil windings on the linear generator stator, depending on the lateral position. This varies the EM shear resistance to motion and subsequent electricity generation in phase with the motion of the hydrofoil. Having an increased number of coil windings in the central position of the stator, enables the hydrofoil to accelerate more rapidly at the beginning of the heave motion, decreasing cycle time and increasing overall power output (See equation(5.1) & equation(5.3)). As the hydrofoil accelerates, a back emf will be induced to resist the translator motion. The decreasing number of coil windings past the central stator position minimises this effect as the hydrofoil reaches higher speeds.

8.3.3 Coefficient of Power

The coefficient of power is an overall description of the device efficiency in extracting power from a moving fluid. It is the ratio of the available tidal power with the extracted mechanical power:

$$C_p = \frac{P_m}{P_\infty} = \frac{P_m}{0.5\rho A_{in} U_\infty^3} \quad (8.3)$$

Where A is the inflow area of the device; $A = 2h_o \times s$.

Increasing the cycle time by 50%, to take into account power loss during pitching, the device maintains a $C_p=0.67$. This seems potentially quite high and is above the Betz limit, but is an indication of the device effectiveness. The C_p will further decrease as the resistive force of the generator is taken into account in slowing the power cycle time. Even with a considerable increase in cycle time and drop in C_p , the device is predicted to output considerable power. In a similar flow regime Stingray is estimated to hold a C_p of 0.144, based on reported hydraulic power prior to energy conversion. Further modelling into the legitimacy of the Betz limit for streamlined hydrodynamic designs should be carried out. The inclusion of mechanical friction within the generator also needs to be taken into account, but is not likely to be a limiting factor with effective linear bearings installed.

8.4 Effective Control

Discussed in section 4.3, effective control and stable manipulation of the AoA is seen as critical in efficient biomimetic hydrofoil motion. In the event of further modelling, it is possible that harmonic wave forms may be advantageous in manipulating DSVs and augmenting lift and power.

It is proposed that rather than actively actuating the AoA, wasting captured power, the AoA could be resisted and controlled using PM's. A curved setup within the hydrofoil, similar to a MagLev track, resisting the AoA pitching in a controlled fashion could be installed. PM material mounted to the outer surface of the pitching restrictor rib could create an EM shear force with a toothed partially curved linear generator (See Figure 8.2).

Introducing this mechanism would further increase power output, as power would be generated when heave motion is nil and the device is in pitching motion control, phases two and three in Figure 8.18.

8.5 Discussion

There are many areas to be discussed which are particular to Sruth Saoirse, general tidal devices and potential future work.

The main point to be made is that Sruth Saoirse is a biomimetic, hydrodynamically-streamlined, and environmentally benign design, rather than a rotational turbine device. There are great advantages in having a structured VKS wake, as opposed to a circulating vortical wake (MCT). It is postulated that energy recapture is more readily viable with VKS wave form wakes, rather than rotational wakes. This is due to the complexity of the hydrodynamics of MCT vortical wakes and the relative simplicity of recapturing wave form wakes through destructive interference and in phase device motion.

8.5.1 Optimisation of device

Detailed structural and hydrodynamic modelling will reveal further areas for optimisation. The analysis thus far identifies the following areas of device optimisation.

It is seen in Figure 8.13, that boundary layer collapse and high pressure build up on the hydrofoil leading surface occurs relatively late in its pitching motion. Initially all parts have been designed to create minimal drag and maintain laminar flow. Altering the control wing geometry will, however, correct this initial design flaw. Increasing the width of the control wing, creating a steeper inflow incident angle, will create two effects.

Firstly, it will increase the venturi effect experienced between the control wing and the butterfly valve, increasing the flow velocity utilised during pitching. Again this will reduce cycle time spent pitching the hydrofoil AoA.

Secondly, it will increase the probability of earlier boundary layer separation from the control wing. This will cause the BL collapse between the hydrofoil and the control wing sooner, and subsequently pitching the hydrofoil sooner in the cycle. It is important to balance this adjustment with the initial Bernoulli suction into the pitching phase. If this is not designed correctly, the effect could be to slow the pitching period of the power cycle.

Further biomimetic study, device modelling and design, incorporating foil flexibility is desirable. It is suspected that the device will operate at higher efficiencies, in line with existing research outlined previously in section 4.4. Increases of 37% were found in device testing. It is not unreasonable to assume similar efficiencies would be reached with Sruth Saoirse. Drag and energy loss in

the trailing edge would be further reduced, heightening overall rate of pitching, efficiency, and energy extraction. The addition of ribs and a rippled trailing edge, as seen in Figure 3.3, will deviate from 2 dimensional theory but, it will reduce spanwise propagation of vortical energy. This increases efficiency and resultant VKS sharpness for further downstream recapture.

Similar to ongoing work in biomimetic propulsion (seen in Chapter 3), it is suggested that a mathematical function for optimum power extraction can be devised. This would take into account device geometry, heave ranges, and cycle frequency for a given flow condition and desired energy extraction.

8.5.2 Structural Concerns

Initial concerns with regard to the structural rigidity of load bearing supports is put to rest with the bending moment and shear torsion analysis below.

Tests conducted for the design geometry, previously described, uses high tensile strength steel as the material with material properties; density of 7840kg.m^{-3} , modulus of elasticity 200GPa , and tensile yield strength of 275.8MPa .

Two potential stator options are presented and are chosen for differing advantages. The structural box section (See Figure 8.19) was chosen as an initial option for its proven structural rigidity and benefits, as it provides a large surface area for PM material to be mounted, as part of the linear generator. The I-Beam structure was secondly modelled, as it provides similar flow wise structural rigidity. It does not provide the same surface area for PM mounting. It does, however, provide ease of mounting, thicker PM material, increasing EM flux linkage and subsequent power output. Optimisation of the ratio of PM material thickness to surface area is required. It is furthermore imagined that the Stator structure would be easier to construct, using an accessible I-beam rather than a Box section.

The models assume that the mooring structure will absorb the drag induced load from the control wings, butterfly valves, and vertical position control hydrofoil. The hydrofoil drag force is the only contributing force to the bending moment upon both structures. The models were tested for an incident force of 2.5kN with a factor of safety of two. As seen in Figure 8.5, the drag generated at an optimum AoA of 15° is negligible and, as a consequence, so to is the bending

moment reacted upon the cross member. Results show that the designed stator cross members are able to withstand the design speed force with a factor of safety of 15 resulting in no deformation. Therefore they can afford to loose some mass.

The second concern is the ability of the central AoA restrictor axel to withstand shearing torsion. The same material as above was used in testing. The pitching moment experienced by the CFD model was tested and the results are illustrated in Figure 8.21. The axel does unfortunately experience some deformation so redesign is required. Higher strength materials or hardening processes on the axel can be carried out. The deformation is not prohibitive and is less than 1cm at its largest deformation. At this design flow speed of $2m.s^{-2}$, the axel has a range of factor of safety from 15 to 0.3 along its axis. This is obviously not allowable and modification is required.

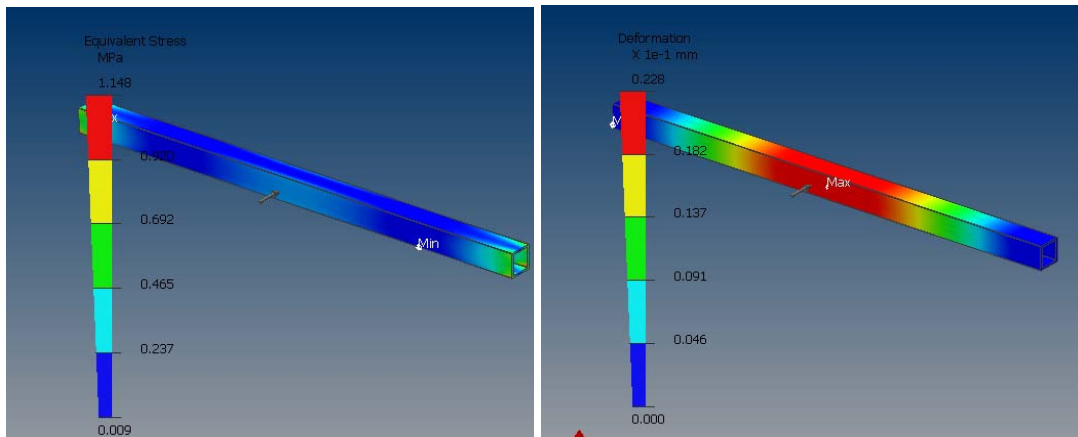


Figure 8.19 Stator; 300 x 300 structural steel box section cross member (Stress & Strain)

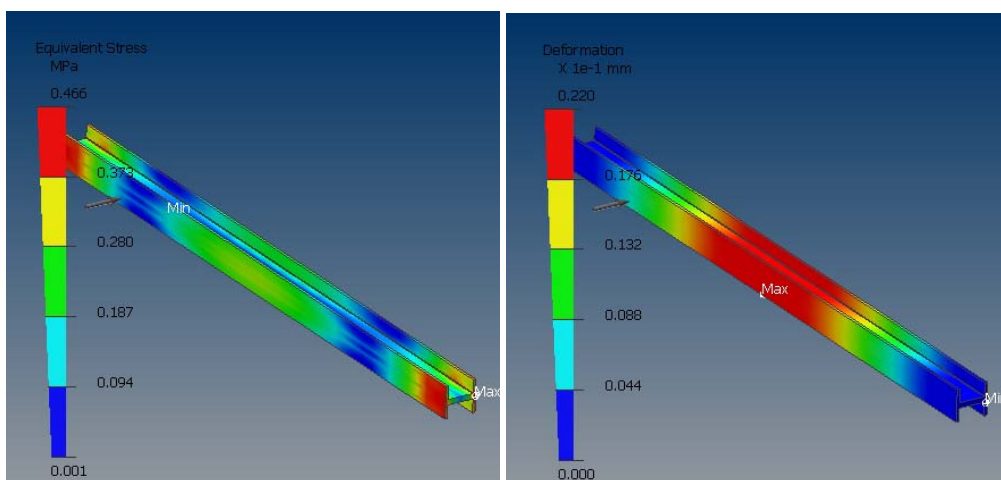


Figure 8.20 Stator; 300 x 300 structural steel I beam section (Stress & Strain)

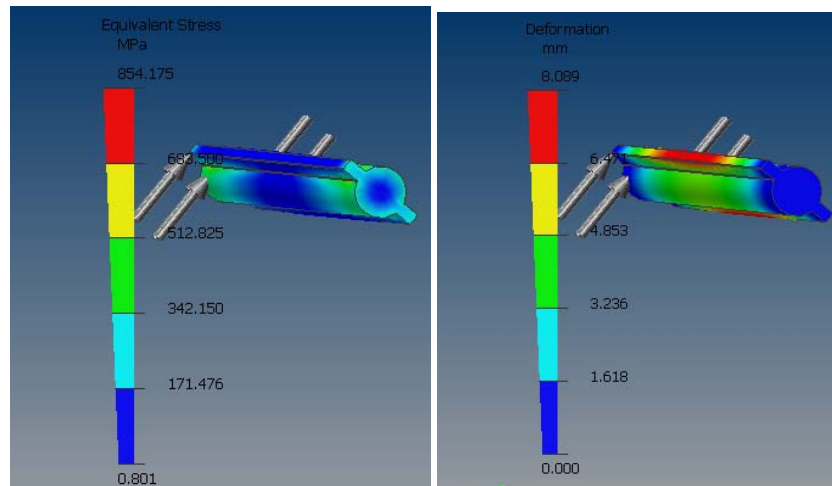


Figure 8.21 Main Hydrofoil Shaft

Another area of concern which deserves attention is the required width of the generator housing to prevent torsional binding between the stator and translator. It is expected that linear bearings need to be installed to seal the housing, and reduce friction in lateral heave motion.

The inclusion of endplates regulates hydrodynamic forces closer to two-dimensional flow. They restrict the propagation of wing-tip vortices and energy loss. As a result they experience considerable loads and require further structural analysis. In practice, it has been found that endplates are only useful for hydrofoils over a lift coefficient above 0.3 (Triantafyllou et al., 2003). Therefore, the applicability of endplates is under question in this design. Alternatively, modelling of DSV effects may prove otherwise.

8.5.3 Environmental effects

One of the main benefits of Sruth Saoirse is that it produces a structured VKS wake. A VKS is easily manipulated, recaptured, and characteristically has less wake turbidity when compared to a rotational MCT wake. The result of this minimises environmental impact to the benthic ecology, reducing scour, and sediment transport in the locality of the device. Aquatic life is more likely to be swept past the foil in the high velocity low pressure field as seen in section 3.4, rather than to be severed by a rotational turbine, thus satisfying conservation requirements. Furthermore, the relatively low oscillatory speeds will reduce EM and auditory pollution.

It is proposed that a farm of Sruth Saoirsáí would be deployed in a diamond formation similar to that taken up by ducklings, migratory birds and schooling fish as seen in 3.3. The spacing would be dependant on module size, cycle frequency and the wavelength of the VKS. Destructive interference and shed wake energy recapture can be utilised to heighten the overall efficiency in a similar fashion to the biomimetic observations.

As seen in Chapter 2, installation costs of off-shore MEC devices are currently prohibitive. The rental and modification cost to retro fit available strand jack barges or drilling rigs is of considerable cost, and has large run off costs to the kW/h unit cost. Further more this limits the depth of deployment and severely limits the number of suitable offshore sites. It is proposed that environmentally, minimally invasive, mooring structures can be developed taking inspiration from the root ball structure of large trees. Robotic coil drill bits are currently used in oil exploration and geotechnical research. It is suggested that similar technology can be developed negating large scale installation costs, to bore an array of small scale root holes rather than one enormous central monopile hole. The holes do not need to be straight or overly designed. Radial scatter along the holes central axis will provide greater surface friction and mooring stability. This mooring has a minimal effect on the geotechnical substrata, while distributing the tension from the device and mooring structure over a large seabed surface area. This structure would save considerable CO₂ emission from saved concrete production. Knowledge transfer from the medical device industry could utilise high tension guide wires (the roots), inserted and anchored in position with large scale inflatable spiked stents holding the root in position. The array of roots would be gathered to a central mooring plate (See Figure 8.22) to which the MEC device would in turn be attached by further high tension cables. As seen, the mooring structure allows full rotation and vertical motion to allow the device to yaw, and capture energy from both cyclic tidal flows. Lastly, this mooring structure can be decommissioned at much less cost to the environment and device developer.

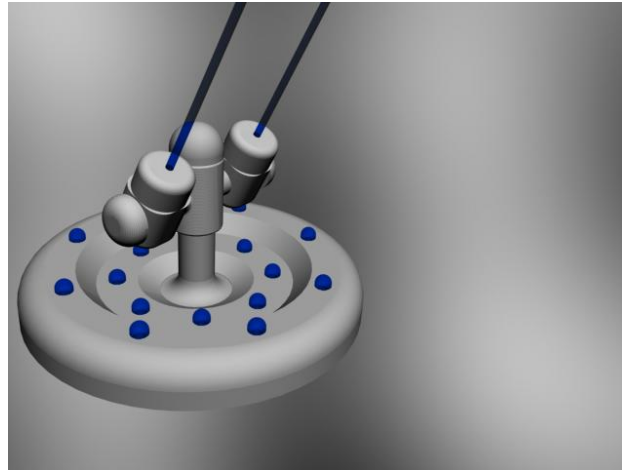


Figure 8.22 Root style pivot mooring structure

8.5.4 Advantages, Disadvantages & Possibilities

It is believed that in the light of the previous discussion and analysis, the dual foil, Sruth Saoirse holds many advantages (See Figure 8.4). These are briefly discussed below in comparison with some identified disadvantages.

The device is a tidal generation device, which produces a near constant power output at a given flow velocity. Subsequently this power is secure, predictable, and reliable. The notions of varying power supply destabilising distribution grids, which, traditional power generators use to denounce renewable power generation is no longer a viable argument.

The device has a higher power coefficient than existing tested prototypes, it is suspected to have a lower cycle time, as a virtue of being a considerably smaller and lighter device.

The device has a significantly less environmental impact, as a virtue of a compact device scale, minimal wake turbidity and an environmentally benign mooring structure.

Modular design and design simplicity enables small scale deployment in rivers, to large scale tidal array deployment. Construction techniques are not envisaged to be overly complicated, thus reducing construction and unit energy cost. Furthermore, the simple design reduces required maintenance and downtime. Failure is also less likely with a simple design. The device utilises a direct drive linear generator with conversion efficiencies up to 0.87, meaning drive train efficiencies are considerably higher than existing designs.

The device is self controlling, self starting, self-yawing and automatically shuts down during excessive tidal flows. *Tidal flow is extremely predictable and this aspect of the design is included purely as a precautionary measure.* The device rises and falls to the highest appropriate velocity flow field in conjunction with the 7th power law.

The use of a dual foil model oscillating 180° out of phase, gives better power quality, minimises lateral forces, vibrations, and any potential cyclic loading. Further phased wiring of each modules generator can insure this out of phase generation and control. Furthermore, the device wake will be reduced due to constructive interference between each foil VKS wake.

The device can, when correctly positioned, recapture vortical energy lost from upstream device wakes. This can be thought of as regeneration utilised in other device power cycles, like that in Stirling engines.

Lastly, the overall optimal device conversion efficiency from tidal energy to electrical energy in the range of 55-60% is calculated. This is not expected to decrease considerably with further analysis into mechanical, electrical and frictional losses.

On the downside, the linear generator is a newly developed device and requires effective sealing from the saltwater. It is shown that salt water can have a considerable corrosive effect on untreated PM material.

The device, once built, is none adjustable and so must be tuned to a specific tidal regime. The device efficiency and the total farm efficiency will vary over the range of velocities experienced throughout the spring neap tidal cycle.

Further, like all MEC devices placed in the most hostile environment on the planet, the device will be subject to damage due to debris floating in the water. Small scale particles and debris will pass unharmed, directed by the pressure fields within the device. However, large fish, mammals and debris must be shielded from colliding with the device. A novel means to do this is suggested in section 8.6.

8.6 Recommendations & Future Work

Dual foils in a similar setup to the Weis-Fogh effect operating 180° can generate sufficient thrust to propel a ship (Michael S. Triantafyllou, 2003).

However, the vortices in the wake of these devices are significantly more complicated than single VKS. If Oscillating Hydrofoil Farms are to be deployed, this effect must be further studied and understood. Further dynamic real world and mathematical modelling is required. In this modelling, vortical energy recapture, wake recapture and wake cancelling through destructive interference should be carried out.

The relationship between energy extraction efficiency and St needs to be modelled and quantified. Large tidal devices, due to the size of their generators, have low frequencies with higher heave amplitudes. The possibility of many smaller devices operating in a farm, having greater energy extraction efficiency, needs to be investigated.

The effect that climate change is having on renewable energy resources will have a huge impact in designing for the future. Further study will enable accurate power output estimates, with increased resource magnitude, and may reduce unit power cost making previously unviable devices, viable.

Structural analysis of the hydrofoil materials needs to be conducted, in turn developing construction methodologies and reducing hydrofoil mass. The less the hydrofoil weighs, the more power can be output from a device with the same hydrofoil surface area. Increased material analysis into the effects of cavitation on those said materials needs also to be carried out. Smaller device modules with higher operational frequencies will be susceptible to cavitation at the hydrofoil trailing edge.

There is ongoing work into the protection of submerged MEC devices from inflow, animals and debris. It is suggested along the same vane of the Sruth Saoirse design that, rather than using a metal grid filter and diffusers to protect device from debris, a passive approach could be taken. It has been seen, that a bluff body, with the correct characteristic length, in a given flow, will propagate a VKS. Research into utilising these VKS's, surrounding the device farm in a high pressure deflective barrier is recommended. Formation (probably a diamond) of the bluff bodies will depend on the wavelength and frequency of propagated VKS. Destructive interference in the internal flow should minimise turbulence and create steady flow conditions. Exterior to the VKS, floating debris and marine life would be deflected and pushed past the device by high pressure vortices within the

flow stream. D section geometry, used in testing outlined in section 3.4, were effective towards this purpose. Further flexible flags at the bluff body trailing edge will aid propagation radially, rather than axially, behind the bluff body.

Unforced Wake Vortices Modelling using physical tow tank testing and further development of the force integral mathematical code (Appendix A - User defined functions) will generate considerably more accurate power output models and validation. The development of DSVs and subsequent percentage lift increase is of particular interest.

Addition of foil flexibility is seen to increase efficiency in propulsion technologies, with insignificant decrease in thrust generation. It is suspected that similar models can be used in increasing Sruth Saoirse's efficiency.

CFD modelling showed a slight pressure drop across the device. However, the resultant C_p is in conflict with the Betz limit. The validity of the Betz limit is under question for an oscillating hydrofoil. The hydrofoil creates less blockage and drag than is experienced through a porous disc or MCT. Further modelling is required to validate the Sruth Saoirse C_p calculated.

Finally, nothing beats real world modelling and, for conclusive results, it is recommended that a scaled model be tested in a tow tank to validate the above results.

8.7 Conclusions

The project objectives are completed. A novel, self controlling passive device is presented, inspired from biomimetic observations. The device has an increased power coefficient relative to existing oscillating hydrofoil prototypes. Thus an increase in power output is achieved.

The benefits to the device locality and environment have been shown to be significant. The device produces a structured Von Kármán Street vortex wake. The benefits of this are seen in energy efficiency and minimal environmental impact. Reduced wake turbidity and heightened farm efficiency through wake recapture play their part in reducing sediment transport and scour. Power unit cost (kW/hr) is subsequently reduced by heightened farming efficiency.

The Sruth Saoirse design is modular, simple, and minimally invasive to the environment. The applications of these facts are that, it can be downscaled for

various sites and river applications. Expected installation, operation, maintenance and decommissioning costs are considerably reduced.

References

- A.S. BAHAJ, L. E. M. (2003) Fundamentals applicable to the utilisation of marine current turbines for energy production. *Renewable Energy*, 2205–2211.
- A.S. BAHAJ, L. M. (2004) Analytical estimates of the energy yield potential from the Alderney Race (Channel Islands) using marine current energy converters. *Renewable Energy*, 1931–1945.
- AKBARI, M.H, PRICE & S.J (2003) Simulation of dynamic stall for a NACA 0012 airfoil using a vortex method. *Journal of Fluids & Structures*, 2003, 855–874.
- ANDERSON, J. D. (1990) *Fundamentals of Aerodynamics*, New York, McGraw Hill.
- ASTRON (2004) Harnessing Scotlands Marine Energy Potential: Marine Energy Group (MEG) Report 2004. Edinburgh, Scottish Executive.
- ASTRON (2005) Scotlands Renewable Energy Potential: realising the 2020 target. Edinburgh, Scottish Executive.
- BAKER, N. J. (2003) Linear Generators for Direct Drive Marine Renewable Energy Converters. *School of Engineering*. Durham, University of Durham.
- BATTEN, W. M. J., BAHAJ, A. S., MOLLAND, A. F. & CHAPLIN, J. R. (2006) Hydrodynamics of marine current turbines. *Renewable Energy*, 249–256.
- BOUND, R. (2003) Status and research and development priorities | 2003: Wave & Marine Current Energy. London, Future Energy Solutions, Department of Trade and Industry.
- BP (2006) Statistical Review of World Energy.
- BRUCE R MUNSON, D. F. Y., THEODORE H OKIISHI (2006) *Fundamentals of Fluid Mechanics*, New York, John Wiley & Sons.
- BRYDEN, I. G. (2002) A scoping study for an environmental impact field program for tidal current energy. Aberdeen, Robert Gordens University, Centre for environmental engineering and sustainable energy, Future Energy Systems (Formally ETSU), Department of Trade and Industry (DTi).
- CALISTER, W. D. (2003) *Materials Science and Engineering: An Introduction*, New York, John Wiley & Sons.

References

- CHENG, JIAN-YU, CHAHINE & L, G. (2001) Computational hydrodynamics of animal swimming: boundary element method and three-dimensional vortex wake structure. *Comparative Biochemistry and Physiology, Part A* 2001, 51 - 60.
- CHERYL A.D. WILGA, G. V. L. (2004) *Biology of sharks and their relatives*, CRC Press.
- CUTNELL, D, J., JOHNSON & W, K. (2001) *Physics*, New York, John Wiley and Sons Inc.
- D. S. BARRETT, M. S. T., D. K. P. YUE, M. A. GROSENBAUGH, M. J. WOLFGANG, (1999) Drag reduction in fish-like locomotion. *Journal of Fluid Mechanics*, 392, 183-212.
- D.A. READ, F. S. H., M.S. TRIANTAFYLLOU (2002) Forces on oscillating foils for propulsion and maneuvering. *Journal of Fluids and Structures*, 163-183.
- DEPARTMENT OF PUBLIC ENTERPRISE (1999) Green Paper On Sustainable Energy. Dublin, Department of Public Enterprise.
- DEPARTMENT OF TRADE AND INDUSTRY, D. (2003) Status of Research and Development Priorities: Wave and Marine Current Energy. DTI.
- DEPARTMENT OF TRADE AND INDUSTRY, D. (2005) Long Term Trends; Energy. Crown Copyright.
- DEPARTMENT OF TRADE AND INDUSTRY, D. (2006a) Creating a low carbon economy. *Third Annual Report on the implementation of the Energy White Paper*. Sustainable Energy Policy Network.
- DEPARTMENT OF TRADE AND INDUSTRY, D. (2006b) Energy Review Report 2006. *The Energy Challenge*. DTI.
- DEPARTMENT.OF.TRADE.AND.INDUSTRY (2005) Stingray tidal stream energy device - Phase 3. London, The Engineering Business.
- DUNCAN, THOM, W. J., YOUNG, A. S. & A.D. (1970) *Mechanics of Fluids*, London, Edward Arnold.
- E SPOONER, M. A. M. (2001) COMPARATIVE STUDY OF LINEAR GENERATORS AND HYDRAULIC SYSTEMS FOR WAVE ENERGY CONVERSION. University of Durham School of Engineering, Department of Trade and Industry, ETSU.
- E. HOO, K. D. D., J. PAN (2005) An investigation on the lift force of a wing pitching in dynamic stall for a control vessel. *Journal of Fluids and Structures* 707-730.
- E. SPOONER, L. H. (2003) Vernier hybrid machines. *IEE Proceedings-Electrical Power Applications*, 150, 655-662.

References

- EUROPEAN COMMISSION, E. E., EUROSTAT. (2006a) *Energy Statistics*, Luxemburg: Office for Publications of the European Communities, 2006, European Commission.
- EUROPEAN COMMISSION, E. E., EUROSTAT. (2006b) Green Paper: A European Strategy for Sustainable, Competitive and Secure Energy. Brussels, European Commission, Environment & Energy, Eurostat.
- EUROPEAN.COMMISSION (1996) The Exploitation of tidal marine currents. Brussels, EU Commission.
- F.S. HOVER, Ø. H., M.S. TRIANTAFYLLOU (2004) Effect of angle of attack profiles in flapping foil propulsion. *Journal of Fluids and Structures* 37-47.
- FISH & E., F. (1995) Kinematics of Ducklings Swimming in Formation: Consequences of Position. *THE JOURNAL OF EXPERIMENTAL ZOOLOGY* 1-II.
- FISH & E., F. (2006) The myth and reality of Gray's paradox: implication of dolphin drag reduction for technology. *Bioinspiration & Biomimetics*, 1, 17-25.
- FISH, F. E. (1998) *Biomechanical perspective on the origin of cetacean flukes*. In *The Emergence of Whales*, New York, Plenum Press.
- FRANK E. FISH, J. F. F. C. J. X. (1991) BURST-ANC-COAST SWIMMING IN SCHOOLING FISH (NOTEMIGONUS CR YSOLEUCAS) WITH IMPLICATIONS FOR ENERGY ECONOMY. *Comparative Biochemistry and Physiology*, 100A, 633-637.
- FRANK. E. FISH, J. E. P. (2003) Stabilization mechanism in swimming odontocete cetaceans by phased movements. *Marine Mammal Science*, 9, 5-528
- FRITZ-OLAF LEHMANN, S. P. S., MICHAEL DICKINSON, (2005) The aerodynamic effects of wing-wing interaction in flapping insect wings. *The Journal of Experimental Biology*, 3075-3092.
- G. E. REISMAN, E. A. M., AND C. E. BRENNEN (1994) Cloud cavitation on an oscillating hydrofoil. *The Twentieth Symposium on Naval Hydrodynamics, Office of Naval Research, National Research Council*. Santa Barbera, California.
- GARETH P. HARRISON, A. R. W. (2004) Climate sensitivity of marine energy. *Renewable Energy* 1801-1817.
- GRAY, J. (1935) Studies in animal locomotion VI. The propulsive powers of the dolphin. *Journal of Experimental Biology*, 192-199.
- GUGLIELMINI, L., BLONDEAUX, P. & VITTORI, G. (2004) A simple model of propulsive oscillating foils. *Ocean Engineering*, 883-899.

References

- H. POLINDER, M. E. C. D., F. GARDNER (2002) Modelling and test results of the AWS linear PM generator system. Zijdewind, The Netherlands, Delft University of Technology, AWS. B.V.
- HAMILTON, K., MACDONALD, M., MCCOMBES, T. & GLYNN, J. (2006) Marine Current Resource and Technology Methodology. IN JOHNSTONE, D. C. (Ed.), Energy Systems Research Unit.
- HENK POLINDER, M. E. C. D., FRED GARDNER (2004) Linear PM Generator System for Wave Energy Conversion in the AWS. *IEEE TRANSACTIONS ON ENERGY CONVERSION*, 19, 583-589.
- HUBBERT, M. K. (1971) The Energy Resources of the Earth. *Scientific American*, 60-70.
- I. BOLDEA, S. A. N. (1999) Linear Electric Actuators & Generators. *IEEE TRANSACTIONS ON ENERGY CONVERSION* 14, 712-717.
- I.G. BRYDEN, T. G., G.T. MELVILLE (2004) Assessing the potential of a simple tidal channel to deliver useful energy. *Applied Ocean Research*, 2004, 198-204.
- IAN G. BRYDEN, S. J. C. (2005) Marine Energy Extraction: Tidal Resource Analysis. *Renewable Energy*, 2006, 133-139.
- INTERNATIONAL ENERGY AGENCY, I. (2003a) Evolution of Electricity Generation by Fuel: 1971 - 2003.
- INTERNATIONAL ENERGY AGENCY, I. (2003b) Evolution of Total Production of Energy 1971 - 2003.
- IT POWER LTD (2006) Pulse Stream 100 - Press release.
- J. KATZ, D. W. (1978) Hydrodynamic propulsion by large amplitude oscillation of an airfoil with chordwise flexibility. *Journal of Fluid Mechanics*, 88, 485-497.
- J. M. ANDERSON, K. S., D. S. BARRETT, M. S. TRIANTAFYLLOU (1998) Oscillating foils of high propulsive efficiency. *Journal of Fluid Mechanics*, 360, 41-72.
- JIABIN WANG, D. H., GERAINT W. JEWELL (2004) Analysis and Design Optimization of an Improved Axially Magnetized Tubular Permanent-Magnet Machine. *IEEE TRANSACTIONS ON ENERGY CONVERSION*, 19, 289-295.
- JIABIN WANG, G. W. J., DAVID HOWE (1999) A General Framework for the Analysis and Design of Tubular Linear Permanent Magnet Machines. *IEEE TRANSACTIONS ON MAGNETICS*, 35, 1986-2000.

- JIAN-YU CHENG, G. L. C. (2001) Computational hydrodynamics of animal swimming: boundary element method and three-dimensional vortex wake structure. *Comparative Biochemistry and Physiology, Part A* 2001, .51 - 60.
- JIM J. ROHR, F. E. F. (2004) Strouhal numbers and optimization of swimming by odontocete cetaceans. *The Journal of Experimental Biology* 1633-1642.
- JONES, K.D, LINDSEY, K, PLATZER & M.F (2003) An investigation of the fluid-structure interaction in an oscillating-wing micro-hydropower generator. Monterey, CA 93943, Department of Aeronautics & Astronautics, Naval Postgraduate School, USA.
- JOSEPH E. SHIGLEY, C. R. M. (2003) *Mechanical Engineering Design*, New York, McGraw Hill.
- K.D. JONES, K. L., M.F. PLATZER (2003) An investigation of the fluid-structure interaction in an oscillating-wing micro-hydropower generator. Monterey, CA 93943, Department of Aeronautics & Astronautics, Naval Postgraduate School, USA.
- KATZ, JOSEPH, PLOTKIN & ALLEN (2001) *Low Speed Aerodynamics*, Cambridge, UK, Cambridge University Press.
- KEVIN D. JONES, S. D., MAX F. PLATZER (1999) Oscillating-wing power generation. *Proceedings of the 3rd ASME/JSME Joint Fluids Engineering Conference*. San Francisco, California, USA, American Society for Mechanical Engineers.
- L. K. POLASEK, R. W. D. (2001) Heterogeneity of myoglobin distribution in the locomotory muscles of five cetacean species. *The Journal of Experimental Biology*, 209-215.
- LEARY, F. O., HOWLEY, M., GALLACHÓIR, D. B. Ó. & WAUGH, T. (2006) *Renewable Energy in Ireland: 2005 Update*. Cork, Sustainable Energy Ireland.
- LIAO, J. C., BEAL, D. N., LAUDER, G. V. & TRIANTAFYLLOU, M. S. (2003) Fish Exploiting Vortices Decrease Muscle Activity. *Science*, 302, 1566-1569.
- LINDSEY, K. (2002) A feasibility study of oscillating-wing power generators. *Department of Aeronautics and Astronautics*. Monterey, Naval Postgraduate School, Monterey, CA 93943-5000, USA.
- MARTIN HOWLEY: DR. BRIAN Ó GALLACHÓIR (2005) *Energy in Ireland 1990-2003: Trends Issues and Indicators*. Cork, Sustainable Energy Ireland: Energy Policy and Statistical Support Unit.
- MCNEILL, A. R. (2004) minireview: Hitching a lift hydrodynamically - in swimming, flying and cycling. *Journal of Biology*, 3, Article 7.

References

- MICHAEL S. TRIANTAFYLLOU, A. H. T., FRANZ S. HOVER. (2003) Review of Experimental Work in Biomimetic Foils. *OCEANIC ENGINEERING*, 29, 585-594.
- MOORES, J. (2003) Potential Flow 2-Dimensional Vortex Panel Model: Applications to Wingmills. *Mechanical Engineering*. Toronto, Ontario, Canada, University Of Toronto.
- MUNSON, R., B., YOUNG, F., D., OKIISHI & H, T. (2006) *Fundamentals of Fluid Mechanics*, New York, John Wiley & Sons.
- P. PREMPRANEERACH, F. S. H., M.S. TRIANTAFYLLOU (2003) The effect of chordwise flexibility on the thrust and efficiency of a flapping foil. Cambridge, Department of Ocean Engineering, Massachusetts Institute of Technology.
- POLLACK, G. H. (1990) *Muscles & Molecules, Uncovering the principles of biological motion*, Seattle, Ebner & Sons.
- SANG-HYUN KIM, H. Y. (2004) An experimental study of the longitudinal motion control of a fully submerged hydrofoil model in following seas. *Ocean Engineering*, 523-537.
- SCOTT J. COUCH, I. G. B. (2004) The impact of energy extraction on tidal flow development. Aberdeen, Centre for Research in Energy and the Environment, The Robert Gordon University, Scotland.
- SHELDAHL, E, R., KLIMAS & C, P. (1981) Aerodynamic Characteristics of Seven Symmetrical Airfoil Sections Through 180-Degree Angle of Attack for Use in Aerodynamic Analysis of Vertical Axis Wind Turbines. Albuquerque, NM 87185, Aerothermodynamics Division 5633, Advanced Energy Projects Division 4715, Sandia National Laboratories.
- SNODIN, H. (2001) Scotlands Renewable Resource. Garrad Hassan and Partners Ltd, Scottish Executive.
- SRINIVASANS, R, G., EKATERINARISG, A, J., MCCROSKEY & J, W. (1995) Evaluation of turbulence models for unsteady flows of an oscillating airfoil. *Computers and Fluids*, 24, 833-861.
- SUSTAINABLE ENERGY IRELAND (2005a) Tidal and Current Energy Resources in Ireland. Dublin, Sustainable Energy Ireland.
- SUSTAINABLE ENERGY IRELAND, M. I. (2003) Options for the development of wave energy in Ireland. Dublin, Sustainable Energy Ireland, Marine Institute.
- SUSTAINABLE ENERGY IRELAND, M. I. (2005b) Ocean Energy In Ireland. Department of Communications, Marine and Natural Resources, (Ireland).

- THE.ENGINEERING.BUSINESS (2003) Stingray tidal stream energy device - Phase 2. Department of Trade and Industry.
- THEODORSEN, T. (1935) General theory of aerodynamic instability and mechanism of flutter. National advisory committee for aeronautics.
- THOMSON, J. P. (2006) Consultation on Review of ROS (Support for Wave and Tidal Power) 2006. Glasgow, Scottish Executive: Renewables and Consents Policy Unit.
- THORPE, T. W. (1999) An Overview of Wave Energy Technologies: Status, Performance and Costs. London, Future Energy Solutions (previously ETSU).
- TRIANATFYLLOU, M.S, TRIANATFYLLOU & G.S (1995) An efficient swimming machine. *Scientific American*, 272, 64-74.
- TRIANATFYLLOU, S, M., TECHET, H, A., HOVER & S, F. (2003) Review of Experimental Work in Biomimetic Foils. *OCEANIC ENGINEERING*, 29, 585-594.
- TRIANATFYLLOU G.S, T. M. S., GROSENBAUGH M.A (1993) Thrust development in oscillating foils with application to fish propulsion. *Journal of Fluids & Structure*, 7, 205-224.
- W. GEISLER, H. H. (2006) Investigation of dynamic stall onset. *Aerospace Science and Technology*, Article In Press.
- WAKELING, J. W. (2001) Biomechanics of fast start swimming fish. *Comparative Biochemistry and Physiology*, Part A, 31- 40.
- WANG, G, OSTOJA-STARZEWSKI & M (2005) Large eddy simulation of a sheet/cloud cavitation on a NACA0015 hydrofoil. *Applied Mathematical Modelling*, Article in Press.
- WEIHS, D. (2004) The hydrodynamics of dolphin drafting. *The Journal of Biology*, 3, Article 8.
- WEIS-FOGH, T. (1973) Quick estimates of flightedness in hovering animals, including novel mechanisms for lift production. *Journal of Experimental Biology*, 169-230.
- WHITE, F. M. (2003) *Fluid mechanics* Boston, McGraw-Hill.
- WILLIAM MCKINNEY, J. D. (1981) The Wingmill; An Oscillating-Wing Windmill. *The Journal of Energy*, 5, 109-115.

Bibliography

1. Boyle, Godfrey. (2004) *Renewable Energy: Power for a Sustainable Future*. ISBN: 0-19-926178-4 © Oxford University Press in conjunction with The Open University www.ouw.co.uk
2. Drury, W. (2001) *The Control Techniques Drives and Controls Handbook*. ISBN: 0 85296 793 4 © the Institution of Electrical Engineers: Power and Energy Series 35. www.controltechniques.com
3. Higham, Desmond. J., Higham, Nicholas. J. (2005) *MATLAB guide*. Second edition. ISBN: 0-89871-578-4 © Society for Industrial and Applied Mathematics
4. Magrab, Edward B., Azarm, Shapour., Balachandran, Balakumar., Duncan, James H., Herold, Keith E., Walsh, Gregory C. (2005) *an Engineers Guide to MATLAB*. ISBN: 0-13-145499-4 © Pearson Education Inc.
5. Norvelle, F. Don. (1994) *Fluid Power Technology* ISBN: 0-31-401218-4 © Delmar Thomson Learning
6. Reddy, J.N., Gartling, J.K. (1994) *the Finite Element Method in Heat Transfer and Fluid Dynamics* ISBN: 0849394104 © CRC Press Inc.
7. Schilt, Herbet. (2002) *C++ the Complete Reference*. Fourth Edition. ISBN: 0072226803 © McGraw Hill Osborne Media
8. Warsi, Z.U.A. (1993) *Fluid Dynamics: Theoretical and Computational Approaches*. ISBN: 0-8493-4436-0 © CRC Press Inc.
9. www.esru.strath.ac.uk Energy Systems Research Unit, University Of Strathclyde. (Last viewed 18/09/06)
10. www.ukho.co.uk The United Kingdom Hydrographic Office © Crown Copyright 2006 (Last viewed 18/09/06)

Appendix A - User defined functions

Predefined Pitch Heave Motion

Using the equations of motion (4.1) and (4.2) while tuning the frequency and heave amplitude to optimum values discussed in Chapter 4, the fluent macro DEFINE_CG_MOTION, can be used in a user defined function (UDF) to predefine the hydrofoil motion. This UDF can be input into the fluent model to simulate natural motion of the hydrofoil and dynamic flow calculations, and visualisations can be thus carried out. Dynamic flow calculations are specifically required to replicate DSV and LEV, alternatively the calculations are simply turbulent flow models. In themselves they are useful, however, dynamic modelling provides considerably more information in regard to the vortex structure and dynamic system forces.

Code

For an oscillating hydrofoil with heave amplitude of 3m, a period of 20 seconds, a phase angle of $\frac{\pi}{2}$, giving an angular velocity omega of $0.31416 \text{ rad.s}^{-1}$; the UDF code required to drive sinusoidal pitch heave motion is as follows.

Note [0 1 2] correspond to the x y and z axes respectively.

```
#INCLUDE "UDF.H"

DEFINE_CG_MOTION(FOILMOTION, DT, VEL, OMEGA, TIME, DTIME)
{
VEL[1]=(3)*(SIN(0.31416*TIME));
OMEGA[2]=(0.6109)*(SIN((0.31416*TIME)+1.5707))
}
```

Foilmotion is the name assigned to the UDF, There are six variables to be defined when using DEFINE_CG_MOTION; Name, DT, Vel, Omega, Time, and Dtime. The user chooses the name of the UDF. DT, Vel, Omega, Time and Dtime are all system variables that are automatically communicated between

fluent and the UDF code. At each time step the UDF updates Fluent's Vel and Omega arrays with the velocities for this next time step.

Dt is a pointer to the matrix that stores the dynamic mesh characteristics that have been specified when generating the model mesh, or those automatically calculated subsequently by fluent during dynamic modelling. The current time and time step are given by fluent as Time and Dtime, respectively.

Loop Force Integral

One can use the DEFINE_CG_MOTION macros in fluent to specify the motion of a particular dynamic zone. This is done by providing fluent with the linear and angular velocities at every time step of the calculation. This can alternatively be achieved by reading a surface loop integral taking into account the surface forces the foil experiences within the flow. Using these forces and the UDF, the subsequent foil velocity can be calculated, and input into the model for the next time step. Fluent then in turn uses these velocities to update the mesh node positions on dynamic zones based on solid-body motion. Unfortunately an added degree of complexity in using this method is seen. The UDF source code is required to be run with fluent as a compiled UDF. The C code has to be written externally to fluent compiled and hooked up to the model. The variables are the same as those defined above.

Please note the code presented is not currently debugged or operational; human error is likely to exist in the code written below.

Code

```
#INCLUDE "UDF.H"

STATIC REAL V_PREV=0.0

DEFINE_CG_MOTION(FREEMOTION, DT, VEL, OMEGA, TIME, DTIME)
{
  THREAD *T;
  FACE_T F;
  REAL NV_VEC (A)
  REAL FORCE, DV;
```

Appendix A - User defined functions

```
NV_S(VEL,=,0.0);
NV_S(OMEGA,=,0.0);

IF(!DATA_VALID_P())
RETURN;
T=DT_THREAD(DT);
FORCE=0.0;
BEGIN_F_LOOP(F,T)
{
F_AREA(A, F, T);
FORCE+=F_P(F, T)*NV_MAG(A);
}
END_F_LOOP (F, T)

DV=DTIME*FORCE/650
V_PREV+=DV;
VEL[I]=V_PREV;
}
```

Appendix B - Alternative Tidal Generation Sites

Alternative high energy, tidal generation sites are everywhere and are waiting to be investigated. Simply because a site is not presented in a computational model does not necessarily mean there is insignificant extractable energy. Some potential sites which deserve further exploration are illustrated below.



Figure 0.1 The Shannon Estuary, Ireland



Figure 0.2 The Galway Mayo Coast, Ireland



Figure 0.3 Achill Island, Ireland



Figure 0.4 The Donegal, Derry Antrim Coast, Ireland



Figure 0.5 The Kerry Peninsula, Ireland



Figure 0.6 The Sound of Islay, Scotland

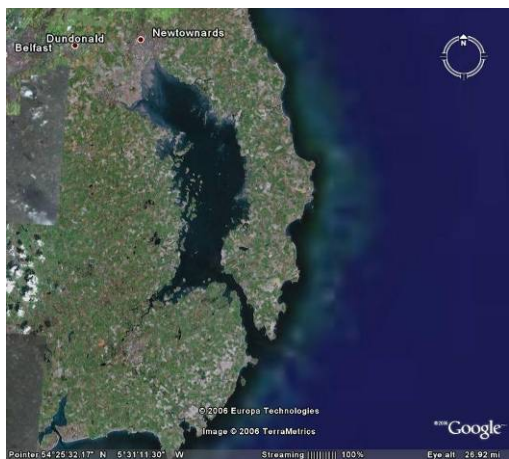


Figure 0.7 Strangford Lough, Ireland



Figure 0.8 The Scottish Western Isles, Scotland

Appendix C - Deep Ecological Motivation

The effects politicians, policy makers, economists, scientists and engineers have on the planet are profound in the social structures, economies and devices we design, develop and build. We are the summation of our past experiences and the path of our existence is our defining character, individually or for the whole of mankind.

An equation, a design, a society, and economic setup must exist to which we can adapt, evolve, oppose, and tend towards the same fluctuating goal of appreciation of our potential, purpose, and, our existence; Our purpose to better our existence, and the existence of future generations.

Environmental and social sustainability requires a tendency towards a diverse interlinked harmony of simplicity and life, rather than singular, mechanistic, anthropocentric, convoluted, and slow fluctuating societal breakdown, seeking terminating balance. A change in mindset, living and design for an environmental-human balance with minimal impact and conservation can yield increased benefit and optimisation for a design, the person using the design and the designs surrounding environment. Deep ecological lateral thinking and design for the environment is required to develop throughout the scientific and engineering professions, taking more interest in the broader life-cycle effects of our designs.

Arne Naess, a Norwegian professor of Philosophy and Ecology and the University of Oslo poignantly states his outline for an ecosophy in the following points;

- 1. The well-being and flourishing of human and nonhuman Life on Earth have value in themselves (synonyms: intrinsic value, inherent value). These values are independent of the usefulness of the nonhuman world for human purposes.*
- 2. Richness and diversity of life forms contribute to the realizations of these values & are also values in themselves.*
- 3. Humans have no right to reduce this richness and diversity except to satisfy **vital** human needs.*

4. *The flourishing of human life and cultures is compatible with a substantial decrease of human population. The flourishing of nonhuman life requires such a decrease.*
5. *Present human interference with the nonhuman world is excessive, and the situation is rapidly worsening.*
6. *Policies must therefore be changed. These policies affect basic economic, technological, and ideological structures. The resulting state of affairs will be deeply different from the present.*
7. *The ideological change is mainly that of appreciating life quality (dwelling in situations of inherent value) rather than adhering to an increasingly higher standard of living. There will be a profound awareness of the difference between big and great.*
8. *Those who subscribe to the foregoing points have an obligation to directly or indirectly try to implement the necessary changes.*

*Arne Naess – 1972,
Budapest*

Thank you for your attention in reading this far.

I hope it was beneficial?

Please feel free to email me for a chat about any insights or queries.

james.glynn@gmail.com